NAD LIMITATION AND ITS IMPACT ON *C. GLABRATA* SURVIVAL AND VIRULENCE

By

Basil Hussain

A dissertation submitted to The Johns Hopkins University in conformity with the requirements of the degree of Doctor of Philosophy

Baltimore, Maryland

October 2016

ABSTRACT

This work describes what happens in cells that are starved for NAD^+. *Candida glabrata* is an opportunistic yeast pathogen that is an NAD^+ auxotroph and limitation of NAD^+ in media leads to transcriptional activation of key adhesin genes encoded in *C. glabrata*. Additionally, starvation for NAD^+ leads to a dramatic increase in the virulence of *C. glabrata* in a mouse model of infection. Interestingly, NAD^+ depletion does not result in cell death. Although intracellular NAD^+ levels diminish dramatically, the cell somehow is able to maintain its viability over the course of weeks. The work in this thesis sheds light on both cellular survival in response to NAD^+ limitation and the effect of NAD^+ on virulence.

In the first part of this thesis, I have identified two major pathways which regulate the TORC1 kinase and PKA kinase altering the ability to survive NAD^+ depletion. Both the Sea1/Npr2/Npr3 complex and Ira1 function as GTPase activating proteins (GAPs). The Sea1/Npr2/Npr3 complex is the GAP for the small G protein GTR1, which regulates TORC1 activation, and Ira1 is the GAP for RAS, the G protein responsible for PKA activation. Loss of *SEA1, NPR2, NPR3,* or *IRA1* results in marked defects in the cells ability to survive NAD^+ starvation, illustrating the importance of these particular genes. Based on these data, we suggest a model where the cell responds to NAD^+ depletion by inactivation both of the major pro-growth pathways by altering the activation state of TORC1 and PKA. Failure to appropriately sense this stress and respond with inactivation of the major growth pathways results in a loss in viability.

In the second part of the thesis, I followed up on a previous observation made in the lab which showed transcriptional up-regulation of *de novo* purine biosynthesis in response to NAD^+ limitation, independent of the previously known regulators of the cellular NAD^+ response. Naturally, this led to the question: why would NAD^+ limitation impact purine biosynthesis? Through a series of metabolomics experiments my work demonstrated that in response to NAD^+ limitation there is a massive accumulation of inosine monophosphate (IMP) and its breakdown products inosine and hypoxanthine. Importantly, metabolic flux labeling shows clearly that the *de novo* purine biosynthesis pathway is functional in starved cells, leading to new synthesis of IMP and downstream products. Through the generation of multiple mutants in the *de novo* pathway, I was able to demonstrate that *de novo* purine biosynthesis is absolutely required for virulence, whereas the salvage purine biosynthesis pathway was not required for virulence. Together these data minimally suggest that the upregulation of purine biosynthesis genes in response NAD^+ starvation has an effect on virulence. An additional piece of information received from the metabolomics experiments was that in response to NAD^+ limitation there is a definitive purine nucleotide imbalance between AMP and GMP. This raised the possibility that when cells are NAD^+ starved the signal they may actually be sensing is a purine nucleotide imbalance. Treatment of *C. glabrata* with the drugs MPA or 6AU, which function to specifically deplete cellular guanine pools, showed a transcriptional response which echoed that of NAD^+ depletion. Moreover, treatment of *C. glabrata* with MPA or 6AU prior to mouse infection phenocopied the hyper virulence phenotype we observe with NAD^+ depletion. This work suggests a model which connects

NAD^+ status and purine metabolism and potentially hints at a novel pathway relevant to virulence regulation by NAD^+ depletion.

Ph.D. DISSERTATION REFEREES FOR BASIL HUSSAIN

Thesis Advisor: Brendan Cormack, PhD

Thesis Reader: Jeffry Corden, PhD

ACKNOWLEDGMENTS

Graduate school was one of the most challenging experiences of my life. Without the help of numerous individuals this work, which culminated in a PhD, would have been impossible. I'm truly indebted to everyone that has helped and supported me through this process, there are so many words I can say, the most simple of which is thank you.

First, I'd like to thank my research advisor Brendan Cormack. Through the roller coaster ride that is graduate school Brendan was always patient with me and provided me with the freedom I needed to grow. His advice, support, and most importantly belief in me gave me confidence not only as a scientist but as a person. Brendan's passion for science was both inspiring and amazing. His persistence to never quit and never let any obstacle stop you from reaching your goal are lessons I will carry with me forever. What I will miss most about graduate school is coming in to the lab seeing the door to his office open and knowing I could walk in and talk with him about anything. If I had to start all over again I would choose his lab again without hesitation. Brendan, you were right, time in lab is valuable. Thank you for everything, I will miss you tremendously.

I would also like to thank the members of the Cormack lab who helped me daily, and made the lab an intellectually stimulating and fun experience. Particularly, I'd like to thank Shih-Jung Pan, Brian Green, Rebecca Zordan, and Jon Trow for their scientific advice, support, and most importantly friendship. During the weeks when science was not going well, coming into work was still enjoyable because of you all. I will always look back fondly on the many smiles and laughs we shared together.

I want to thank my friends for their unconditional support through my PhD. Thank you for everything you all have done for me. We have shared so many great moments together. First, I want to thank my friends Marcus Seldin, Michael Multhaup, Steven Wang, Christopher Bailey, and Allie Greene who were also students in the School of Medicine. They understood fully how difficult graduate school could be and provided timely advice, comedic relief, and unmatched support. Together we all made it through graduate school. I couldn't imagine my life without all of you. You all are among the best things that happened to me in my time at Hopkins. I also want to thank my friends who stuck by my side from the earlier years of my life. Particularly, Pranava Shah and his wife Nishma Shah, Aditya Koul, and Jen Rice. Your belief in me motivated me to accomplish this goal more then you will ever know. Your voices on the phones in times of need always cheered me up and kept me going. Thank you for always being there for me to lean on. I'm fortunate to have all of you in my life.

I want to give a heartfelt thank you to Elizabeth Kolar, who has been my partner through graduate school. We met very early in our careers at Hopkins and have never looked back. We have shared so many great moments together. My fondest memories of my time at Hopkins are with you. Thank you for your love, support, and patience. I relied on you so heavily through these last few years. Thank you for always being there, believing in me, and never letting me down. I love you more then you will ever know.

I want to thank my family who believed in me and sacrificed so much so I could chase this goal. Their unconditional support motivated me to never quit. To my brothers Esam and Shaji, we made it. When you put your mind to it you can do anything. I couldn't have done this without you. Your love and support through these past few years

have kept me going. I owe you both more then you will ever know. Words can't express my feelings for you both so I'll simply say I love you. Finally, I want to thank my mother, father, and uncle. They left their homes and everyone and everything they ever knew when they came to this country 40 years ago. They sacrificed so much so that I could have everything I needed and gave up many of their goals in favor of mine. In the quiet moments when I felt defeated I always thought of them, their sacrifice, how hard it was for them when they came to this country, how much they wanted me to succeed, and it kept me going. They taught me the value of hard work and commitment, that if you ever want something you have to work for it. You are my heroes, I love you.

TABLE OF CONTENTS

Abstract	ii
Acknowledgments	vi
Table of Contents	ix
List of Figures	x
List of Tables	xiii
Dedication	xiv
Introduction	1
References	9
Chapter1	13
Results	15
Discussion	76
Methods and Materials	82
References	91
Chapter 2	94
Results	97
Discussion	125
Methods and Materials	129
References	133
Curriculum Vitae	136

LIST OF FIGURES

Chapter 1

Figure 1A The NAD^+ biosynthetic pathway in *Saccharomyces cerevisiae*. 18

Figure 1B. Growth of wild type *C. glabrata* in media lacking NAD^+ and associated intracellular NAD^+ levels. 19

Figure 1C and 1D. *in vitro* assay for identifying mutants which fail to survive NAD^+ starvation. 21

Figure S1. Colony morphology on a recovery plate. 22

Figure 2A and 2B. Survival of *C. glabrata iml1*Δ *and iml1*Δ*tna1*Δ*tnr1*Δ*tnr2*Δ mutant strains in various nutrient-depleting media. 30

Figure 2C and 2D. Survival of *C. glabrata npr2*Δ strain in nutrient-depleting media. 32

Figure 3A. Survival of *S. cerevisiae* SEA complex deletions in –NA media. 34

Figure 3B. The robust survival defect for *bna6*Δ *pnc1*Δ *sea4*Δ *dnd1* strains. 37

Figure 3C. Transformation of pYES-nga into *S. cerevisiae.* 39

Figure 3D. Different transformation phenotypes between the *bna6*Δ *pnc1*Δ *sea4*Δ and *bna6*Δ *pnc1*Δ *sea4-1*Δ *dnd1* strains. 42

Figure 3E. The effect of restoring *PNC1* on viability in liquid NA starvation assay. 43

Figure 4A. Diploid Transformation with pYES-nga. 46

Figure 4B. Phenotypes of spores transformed with pYES-nga. 50

Figure 4C. *dnd1* spore phenotype in liquid NA starvation assay. 54

Figure 4D. Sequencing from *bna6*Δ *pnc1*Δ *sea4-1*Δ *dnd1* strain. 58

Figure 4E. Survival of *ira1*Δ mutants in liquid NA starvation assay. 59

Figure 4F. Transformation of *ira1*Δ strains with pYES-nga. 60

Figure 4G. Transformation of *pYES-nga* into *ira1*Δ diploid strain. 62

Figure S2. *ira2*Δ survival in response to NA limitation. 63

Figure S3. *C. glabrata ira1*Δ survival in response to NA limitation. 64

Figure 5A. Survival of *SEA* complex *IRA1* double mutants in liquid NA starvation assay. 67

Figure 5B. TOR signaling in response to NAD^+ starvation in *S. cerevisiae* mutants. 70

Figure 5C. TOR signaling in response to NAD^+ starvation in *C. glabrata* mutants. 73

Chapter 2

Figure 1B. Microarray analysis of *C. glabrata* cells grown in media lacking NAD^+. 98

Figure 1B. Microarray analysis of *C. glabrata* cells grown in media lacking NAD^+. 99

Figure 1C. Injection of mice with WT, *sir2*Δ*, hst1*Δ*, and sir2*Δ *hst1*Δ strains grown in media with and without NA. 100

Figure 1D. Additional factors must be involved in NA responsiveness. 101

Figure 2A. Purine metabolism genes upregulated in response to NA starvation mapped onto the purine metabolism pathway. 107

Figure 2B. Purine metabolism pathway in *S. cerevisiae*. 108

Figure 3. Infection of mice with *C. glabrata* purine metabolism mutants to determine virulence phenotypes. 112

Figure 4A. Growth of *C. glabrata* in minus NA media and associated NAD^+ levels. 117

Figure 4B. Cellular NAD^+ inosine and hypoxanthine levels in wild type *C. glabrata.* 119

Figure 4C. Cellular NMP levels in wild type *C. glabrata.* 120

Figure 5. The effect of virulence in *C. glabrata* due to treatment with MPA and 6AU. 123

LIST OF TABLES

Chapter 1

Table S1. Insertional mutants with decreased survival after NAD^+ starvation. 23

Table S2. Results from mating, sporulation and dissection of two *bna6*Δ *pnc1*Δ *sea4*Δ *dnd1* strains to wild-type. 47

Supplemental Table 3. Strains used in this study. 88

Chapter 2

Table 1. List of purine metabolism genes highly induced in response to NAD^+ limitation. 105

Table 2. Purine metabolism genes deleted in this study. 109

DEDICATION

This dissertation is dedicated to my family, for their unconditional support and belief in me. To my parents, I hope this achievement will help to complete the dreams you had when you came to this country forty years ago with nothing but hope. Thank you for your sacrifice. To my brothers, don't be afraid to dream big. If you put your mind to it you can accomplish anything.

INTRODUCTION

Biology of *Candida glabrata*

Candida glabrata is a fungal pathogen that belongs to the family Saccharomycetaceae in the phylum Ascomycota. Despite its name, *C. glabrata* is phylogenetically closer to the model yeast organism, *Saccharomyces cerevisiae*, than to other *Candida* species such as *Candida albicans* [1]. This is reflected in the whole-genome duplication event of the common ancestor of *S. cerevisiae* and *C. glabrata* that is lacking in the genomes of other *Candida* species [2]. *C. glabrata* is a nondimorphic haploid yeast and reproduces by budding, and is the only species within the genus that does not form pseudohyphae at temperatures above 37º C, and instead form blastoconidia (1 to 4 um) that are considerably smaller than that of *C. albicans.* This lack of pseudohyphae was the main reason *C. glabrata* was historically placed in the genus *Torulospsis* until 1978.

C. glabrata has lost various genes, such as those need for galactose, phosphate, nitrogen, sulfur metabolism, and pyridoxine biosynthesis [3, 4]. Generally, these natural auxotrophies of *C. glabrata*, which includes the inability to synthesize nicotinic acid and, are compensated for by the mammalian host environment [5].

Epidemiology

Traditionally, *C. albicans and C. glabrata* are very common nonpathogenic commensal fungi of humans, especially of the oral cavity and gastrointestinal tract. The majority of the human population are colonized by either or both species and are asymptomatic [6]. Due to the increase in antimicrobial resistance and the limited number

of antifungal drugs, infections caused by *Candida* species have been on the rise [7], and are now the most common cause of opportunistic mycoses worldwide [8]. Clinically, *Candida* infection is referred to as "candidiasis" and ranges from infections of oral and vaginal mucosa to systemic infection such as candidemia. In hospitalized patients Candida species are among the most frequently isolated fungi in blood stream infections (BSI) and represents a threat to hospitalized patients, particularly the immunocompromised [9, 10]. The number of individuals susceptible to *Candida* infections has increased dramatically over the past three decades for several reasons. The use of broad-spectrum antibiotics, catheters and parenteral nutrition, the presence of immunosuppression, the disruption of mucosal barriers, and the use of chemotherapy and radiotherapy are among the most significant predisposing factors for invasive fungal infections [4, 11-13].

C. albicans infection remains the major cause of candidiasis, and accounts for 50-70% of the invasive diseases [9, 10]. However, recent data has become available which reveals the emergence of non-*albicans* species in *Candida*-related BSI [9]. *C. glabrata, C. tropicalis* and *C. parapsilosis,* are the three leading non-*albicans* species responsible for invasive candidiasis [14]. Pfaller *et al.* showed a remarkable correlation between patient age and the proportion of *C. glabrata* BSI isolates. Indicating that as patients age, and presumably become more immunocompromised, they become more susceptible to *C glabrata* infection, supported by the fact that the highest percentage of *C. glabrata* BSIs are found in the 80-99 year age group [15]. Although *C. glabrata* is not the leading cause of systemic candidiasis, the mortality rate associated with *C. glabrata* BSI is estimated to be 35-50%, which is the highest in all studied non-*albicans Candida* species [9].

Virulence

Candida species use a variety of virulence factors which allow them to successfully infect their hosts. Common virulence factors found in *Candida* include adherence to host tissue, hyphae or pseudohyphae formation, biofilm production, and secretion of a variety of hydrolytic enzymes (*e.g.* protease, phospholipase and hemolysins) [4, 16]. Animal models of *C. glabrata* infection include immunocompetent mice or rats. However, in these animal models *C. glabrata* has a negligible mortality rate which is at odds with the remarkably high mortality rate in humans. This suggests that although these models may be of use in understanding the basic biology of *C. glabrata* infection, they do not fully recapitulate the events occurring in human infections.

Unlike *C. albicans*, very little is known about the pathogenicity of *C. glabrata*. The ability of *C. albicans* to form hyphae or pseudohyphae is essential for adherence and for invasion of host tissue. However, as it was mentioned earlier hyphae or pseudohyphae formation is not observed in *C. glabrata* [4]. This suggests that *C. glabrata* utilizes an alternative mechanism for adherence to epithelial cells than *C. albicans*. Additionally, it has previously been described that *C. albicans* possesses the ability to secrete aspartyl proteinases (SAP) and phospholipases [4]. The ability of *C.* glabrata to secrete similar enzymes has been poorly characterized to this point and only one study has shown that *C. glabrata* is able to produce secreted proteinase [16].

C. glabrata is an obligate NAD^+ auxotroph and can only grow in media supplemented with specific NAD^+ precursors: nicotinic acid (NA) nicotinamide (NAM) or nicotinamide riboside (NR) [17, 18]. This is because over time *C. glabrata* has lost the *BNA 1- 6* genes which are responsible for *de novo* NAD^+ biosynthesis from tryptophan

[19]. As a result, *C. glabrata* lacks the *de novo* NAD^+ synthesis pathway and requires an exogenous supply of the NAD^+ precursors in order to grow. Previous work has illustrated that an environmental limitation for NAD^+ precursors results in lower cellular NAD^+ levels in *C. glabrata,* which leads to cellular arrest [17, 18]. In this quiescent state *C. glabrata* is still viable but is not actively dividing. Following the supplementation of appropriate NAD^+ precursors to the starved cultures, the cells respond by commencing normal growth.

In previous work in our laboratory we have shown that starving *C. glabrata* for NAD^+ prior to infection has a marked impact on the virulence of the organism. *C.* glabrata was grown either in normal media (with normal levels of NA) or media completely lacking niacin (no NAD^+ precursors present). These cultures were then used to infect mice. What we found was remarkable was that cells that were starved for NAD^+ were hyper-virulent with 30 to 100 times more cells present in the kidney 7 days post infection when compared to cells grown in media with NA. This data clearly links the availably of NAD^+ to *C. glabrata* virulence and suggests that NAD^+ limitation of *C. glabrata* dramatically increases its virulence.

Adherence

From what is currently known, *C. glabrata* appears to have two key virulence factors that strongly contribute to its pathogenicity: adherence to host cells and subsequent biofilm formation. Typically, adhesins are proteins that are expressed on the cell surface that allow microbes to bind and adhere to both biological (e.g. surface of other fungal cells, host cells, or extracellular matrix) and non-biological surfaces (e.g. indwelling catheters, prosthetic devices). In *C. glabrata* we discovered a large family of

adhesins that are encoded by a set of genes called *EPAs* (Epithelial adhesins) [20-23]. The Epa proteins are similar to the ALS (agglutinin-like sequence) - proteins of *C. albicans* which help to mediate adherence in that organism. The Epa proteins are composed of an N-terminal signal sequence, followed by a ligand-binding domain, a serine- and threonine-rich central region, and a hydrophobic C-terminal sequence that is necessary for cross-linking of the protein to the cell wall through a GPI-anchor [24]. Analysis of the genome sequence of BG2, our lab *C. glabrata* strain, reveals that BG2 possesses 25 EPA genes 22 of which are located sub-telomerically.

Of the *EPA* genes three adhesins, *EPA1*, *6*, and *7,* are induced under NAD^+ limiting conditions and thus are of particular interest to us [19]. In previous work performed in the lab we have shown that these proteins mediate adherence to uroepithelial cells *in vitro* [21]. This suggests a model whereby when cells are starved for NAD^+ they respond by inducing expression of *EPA1, 6,* and *7.* The induction of these genes allow *C. glabrata* to bind and adhere to epithelial cells resulting in the kidney hyper-colonization phenotype that we observed. In fact, ectopic expression of *EPA1* in the normally no adherent yeast *S. cerevisiae* allow mediates adherence of *S. cerevisiae* to epithelial cells [21]. Thus, it is thought that these three proteins are likely to be involved in pathogen-host interactions *in vivo*. Interestingly, the *EPA* genes do not tell the full story of adherence. When experiments were performed with *C. glabrata* strains lacking all three *EPA* genes, we still saw a kidney colonization phenotype, albeit to a lesser extent. This result suggests that there are additional factors that play a role in the ability of *C. glabrata* to adhere to epithelial cells and puts forth the model that the functions of Epa1, 6, and 7 proteins account only partially for the hyper-colonization phenotype under

NAD^+ limiting conditions. One important inconsistency to note is that deletion of *EPA1* dramatically diminishes *in vitro* adherence to cultured epithelial cells however an *epa1*Δ strain of *C. glabrata* fails to show an altered hyper colonization phenotype in a mouse model of systemic infection suggesting key differences between the two assays [21]. Minimally, what we can say is adherence to the host is a key step in the pathogenicity of *C. glabrata* which at least in part is mediated through the action of the *EPA* gene family.

After attaching to either the host surface or a non-biological surface *Candida* can proliferate and in some cases form a biofilm. A biofilm is a group of microorganisms which physically stick to one another forming a complex microbial community on a given surface. Biofilm formation in microorganisms is of profound clinical importance due to the use of indwelling catheters, artificial valves of multiple types, and prosthetic devices in the medical community. Microbes can adhere to these surfaces and develop communities which are extremely hardy and exhibit multiple drug resistances. The long-lasting nature of these biofilms lead to persistent infections which are remarkably difficult to treat [16]. It has previously been documented that *C. glabrata* is capable of forming biofilms on wide range of plastic surfaces. Additionally, Iraqui et al. have previously demonstrated that the expression of EPA6 and EPA7 is induced in biofilm formation in vitro, and that deletion of EPA6 but not EPA1-5 greatly reduced the ability for *C. glabrata* to form biofilms [25]. This suggests that in addition to mediating binding to host epithelial cells Epas also mediate the binding of *C. glabrata* cells to one another leading to biofilm formation and highlighting the importance of these proteins in *C. glabrata* pathogenicity.

NAD^+ and *C. glabrata* Virulence

As it was mentioned earlier, of the 25 *EPA* genes encoded in our lab *C. glabrata* strain, BG2, 22 are located in the subtelomeric regions. The fact that the vast majority of these genes are located sub-telomerically is not by circumstance. Transcription of genes located next to telomeres is repressed in a process called telomere position effect (TPE), and has been the topic of much investigation [26]. TPE has been actively studied in *S. cerevisiae* where a group of proteins called sirtuins along with the Ku complex mediate subtelomeric silencing. Subtelomeric silencing also occurs in *C. glabrata*. In *C. glabrata* genes in telomeric and subtelomeric regions are subject to SIR2-dependent silencing and is mediated through SIR2 and other NAD^+-dependent histone deacetylases (HDAC) removal of acetyl groups from the lysine residues of histones [18, 27]. The removal of acetyl groups leads to repression of active gene transcription. In this reaction NAD^+ serves as a co-substrate and is consumed in the de-acetylation process. Thus, in order for subtelomeric silencing to constantly occur there is a continuous need for cellular NAD^+. The cell needs NAD^+ for additional functions and the result is a continuous need for NAD^+ synthesis to maintain the intracellular NAD^+ homeostasis and silencing. In *S. cerevisiae*, NAD^+ can be generated via two independent pathways. In the first NAD^+ can be made from tryptophan by the *BNA* genes, this is called the *de novo* pathway. Alternatively, cells can also generate NAD^+ from specific vitamin precursors such as nicotinic acid (NA), nicotinamide (NAM) and nicotinamide ribose (NR) via the Preiss-Handler pathway [28].

As it was mentioned earlier *C. glabrata* has lost the orthologues of the *S. cerevisiae BNA1-6* genes. As a result, *C. glabrata* is an obligate NAD^+ auxotroph that requires the appropriate NAD^+ precursors in the environment to grow. This sets up a

simple model, where NAD^+ starvation leads to a decrease in availability of exogenous supplies of NA precursors responsible for NAD^+ biosynthesis. As a result cellular NAD^+ levels drop dramatically. Because Sir2 is a NAD^+ -dependent enzyme the activity of the enzyme is severely compromised and since *C. glabrata* lacks the machinery necessary to make NAD^+ *de novo* the activity of the enzyme cannot be restored. Thus, repression of subtelomeric genes is relieved and the *EPA* genes are expressed leading to an enhanced ability to adhere to host cells.

REFERENCES

1. Fitzpatrick, D.A., et al., *A fungal phylogeny based on 42 complete genomes derived from supertree and combined gene analysis.* BMC Evol Biol, 2006. **6**: p. 99.
2. Dujon, B., et al., *Genome evolution in yeasts.* Nature, 2004. **430**(6995): p. 35-44.
3. Butler, G., et al., *Evolution of the MAT locus and its Ho endonuclease in yeast species.* Proc Natl Acad Sci U S A, 2004. **101**(6): p. 1632-7.
4. Kaur, R., et al., *A yeast by any other name: Candida glabrata and its interaction with the host.* Curr Opin Microbiol, 2005. **8**(4): p. 378-84.
5. Colombo, A.L., et al., *Prospective observational study of candidemia in Sao Paulo, Brazil: incidence rate, epidemiology, and predictors of mortality.* Infect Control Hosp Epidemiol, 2007. **28**(5): p. 570-6.
6. Li, L., S. Redding, and A. Dongari-Bagtzoglou, *Candida glabrata: an emerging oral opportunistic pathogen.* J Dent Res, 2007. **86**(3): p. 204-15.
7. Lass-Florl, C., *The changing face of epidemiology of invasive fungal disease in Europe.* Mycoses, 2009. **52**(3): p. 197-205.
8. Miceli, M.H., J.A. Diaz, and S.A. Lee, *Emerging opportunistic yeast infections.* Lancet Infect Dis, 2011. **11**(2): p. 142-51.
9. Pfaller, M.A., et al., *Candida bloodstream infections: comparison of species distribution and resistance to echinocandin and azole antifungal agents in Intensive Care Unit (ICU) and non-ICU settings in the SENTRY Antimicrobial Surveillance Program (2008-2009).* Int J Antimicrob Agents, 2011. **38**(1): p. 65-9.

10. Wisplinghoff, H., et al., *Nosocomial bloodstream infections in US hospitals: analysis of 24,179 cases from a prospective nationwide surveillance study.* Clin Infect Dis, 2004. **39**(3): p. 309-17.

11. Odds, F.C., *Activity of cilofungin (LY121019) against Candida species in vitro.* J Antimicrob Chemother, 1988. **22**(6): p. 891-7.

12. Odds, F.C. and C.E. Webster, *Effects of azole antifungals in vitro on host/parasite interactions relevant to Candida infections.* J Antimicrob Chemother, 1988. **22**(4): p. 473-81.

13. Pfaller, M.A., et al., *Variation in susceptibility of bloodstream isolates of Candida glabrata to fluconazole according to patient age and geographic location in the United States in 2001 to 2007.* J Clin Microbiol, 2009. **47**(10): p. 3185-90.

14. Mikulska, M., et al., *Invasive candidiasis in non-hematological patients.* Mediterr J Hematol Infect Dis, 2011. **3**(1): p. e2011007.

15. Pfaller, M.A., et al., *Variation in Candida spp. distribution and antifungal resistance rates among bloodstream infection isolates by patient age: report from the SENTRY Antimicrobial Surveillance Program (2008-2009).* Diagn Microbiol Infect Dis, 2010. **68**(3): p. 278-83.

16. Silva, S., et al., *Candida glabrata, Candida parapsilosis and Candida tropicalis: biology, epidemiology, pathogenicity and antifungal resistance.* FEMS Microbiol Rev, 2012. **36**(2): p. 288-305.

17. Ma, B., et al., *High-affinity transporters for NAD+ precursors in Candida glabrata are regulated by Hst1 and induced in response to niacin limitation.* Mol Cell Biol, 2009. **29**(15): p. 4067-79.

18. Ma, B., et al., *Assimilation of NAD(+) precursors in Candida glabrata.* Mol Microbiol, 2007. **66**(1): p. 14-25.

19. Domergue, R., et al., *Nicotinic acid limitation regulates silencing of Candida adhesins during UTI.* Science, 2005. **308**(5723): p. 866-70.

20. Cormack, B., *Can you adhere me now? Good.* Cell, 2004. **116**(3): p. 353-4.

21. Cormack, B.P., N. Ghori, and S. Falkow, *An adhesin of the yeast pathogen Candida glabrata mediating adherence to human epithelial cells.* Science, 1999. **285**(5427): p. 578-82.

22. De Las Penas, A., et al., *Virulence-related surface glycoproteins in the yeast pathogen Candida glabrata are encoded in subtelomeric clusters and subject to RAP1- and SIR-dependent transcriptional silencing.* Genes Dev, 2003. **17**(18): p. 2245-58.

23. Kaur, R., B. Ma, and B.P. Cormack, *A family of glycosylphosphatidylinositol-linked aspartyl proteases is required for virulence of Candida glabrata.* Proc Natl Acad Sci U S A, 2007. **104**(18): p. 7628-33.

24. Zupancic, M.L., et al., *Glycan microarray analysis of Candida glabrata adhesin ligand specificity.* Mol Microbiol, 2008. **68**(3): p. 547-59.

25. Iraqui, I., et al., *The Yak1p kinase controls expression of adhesins and biofilm formation in Candida glabrata in a Sir4p-dependent pathway.* Mol Microbiol, 2005. **55**(4): p. 1259-71.

26. Tham, W.H. and V.A. Zakian, *Transcriptional silencing at Saccharomyces telomeres: implications for other organisms.* Oncogene, 2002. **21**(4): p. 512-21.

27. Froyd, C.A. and L.N. Rusche, *The duplicated deacetylases Sir2 and Hst1 subfunctionalized by acquiring complementary inactivating mutations.* Mol Cell Biol, 2011. **31**(16): p. 3351-65.

28. Panozzo, C., et al., *Aerobic and anaerobic NAD+ metabolism in Saccharomyces cerevisiae.* FEBS Lett, 2002. **517**(1-3): p. 97-102.

CHAPTER 1

I would like to point out that although the majority of the work in this chapter is my own, portions of this chapter come from a prior member of the lab. The screen of the *Tn-7 C. glabrata* mutant library for mutants which failed to survive NAD^+ starvation as well as the follow up liquid starvation assays were performed by Shih-Jung Pan. Shih-Jung Pan also generated the *iml1*Δ and *npr2*Δ strains and tested them for survival in our liquid NA starvation assay as well as the plasmid constructs complementing these deletions (Figure 2).

RESULTS

Identification of genes essential for the survival of *C. glabrata* cells upon NAD^+ starvation

Saccharomyces cerevisiae has the ability to replenish intracellular NAD^+ via two mechanisms: *de novo* synthesis via the Kynurenine pathway or by salvage via the Priess-Handler pathway (Figure 1A) [1-3]. Interestingly, analysis of the genome sequence of the highly related yeast *Candida glabrata* reveals that *C. glabrata* has lost its *de novo* NAD^+ biosynthetic pathway [4]. As a result, *C. glabrata* can only synthesize NAD^+ via the salvage pathway from specific environmental NAD^+ precursors, such as nicotinic acid (NA), nicotinamide (NAM) and nicotinamide riboside (NR)[5, 6]. Growth of *C. glabrata* cells in media limited for NAD^+ precursors results in intracellular NAD^+ depletion, leading to a complete, reversible (by addition of NAD^+ precursors) cessation of cell division (Figure 1B)[5, 6]. Wild type *C. glabrata* strain BG2 doubles 4-5 times before ceasing growth. Over the course of the first 3 hours in media lacking NA, NAD^+ levels diminish from 31 amol/cell to 2 amol/cell. NAD^+ levels diminish via two mechanisms: dilution via doubling and the consumption of NAD^+ through NAD^+ dependent enzymes such as sirtuins. After the 3 hour time point NAD^+ levels continue remain consistently low and at 24 hours are approximately 60 fold lower than the 0 time point. Despite the fact that NAD^+ levels are remarkably low at these late time points *C. glabrata* remains viable and the addition of NA, even after days of starvation, results in a return to normal growth. We found it remarkable that even with dramatically low levels of intracellular NAD^+ these cells remain viable (approximately 61% viability after 4 days in –NA

media) and sought to understand the set of genes that were important for survival under these conditions.

In order to identify the genes essential for cellular survival in response to NAD^+ starvation, we developed a plate-based assay to screen a *C. glabrata* mutant library for mutants unable to survive NAD^+ starvation (Figure 1C). Briefly, NAD^+ starvation was achieved by replica plating mutant strains onto plates lacking niacin (SDC-NA plates) and incubating these at 30ºC for 7 days. We then assessed the abilities of mutants to survive NAD^+ starvation based on how well they recovered after replica plating the ghosts to recovery plates containing NA (SDC plates). The mutant strains were used were made in the BG2 background using *Tn7* –based insertional mutagenesis [7]. Figure S1 shows an example of the phenotypes exhibited by mutant strains on the recovery plates. The survival phenotype might not be specific to NA limitation, and could be associated with general growth defects or survival defects, for example, following carbon or nitrogen limitation. To differentiate these classes of mutants from mutants that were unable to survive NAD^+ starvation specifically, we checked all mutant strains with perturbed growth for growth defects in rich medium (YPD) and for recovery after nitrogen- or carbon- starvation. The latter experiment was done in a similar fashion as our NAD^+-starvation/recovery plate assay by using media lacking either a nitrogen source or glucose to achieve the nutrient starvation.

All of the mutants which failed to survive NAD^+ starvation but did not possess either general growth defects or defects related to nitrogen or carbon starvation were re-screened in a quantitative liquid-based assay. To quantify the survival rate after NAD^+ starvation for the mutants who failed to survive in our plate-based screen, we developed a

liquid media based assay (Figure 1D). Briefly, *C. glabrata* cells were grown in rich media possessing niacin overnight (SDC media). *C. glabrata* cells were then inoculated into media lacking niacin (SDC-NA media) and allowed to grow until growth arrest (2-3 doublings). After the cessation of doubling, cells were inoculated again into fresh media lacking niacin to ensure the cells were not starved for any other nutrients other than NAD^+. Samples were then plated and surviving CFUs assessed at different time points over 5 days to quantify survival. Mutants that failed so survive according to the parameters of both our plate based and liquid based assays were selected for further analysis. Out of the 24,000 mutants screened from the library, 91 mutants met our criteria and were selected for further analyses.

To identify the genes disrupted in these 91 mutant strains, genomic DNA flanking the *Tn7* insertion site was retrieved and sequenced. Sequence analysis revealed that these 91 mutants represented insertional disruptions in 47 genes. Multiple independent mutations were isolated for 20 genes. Only in one case, the same insertional mutation was isolated in 2 separate mutant strains. Table S1 lists those 47 genes for which disruption was associated with a NA depletion survival defect.

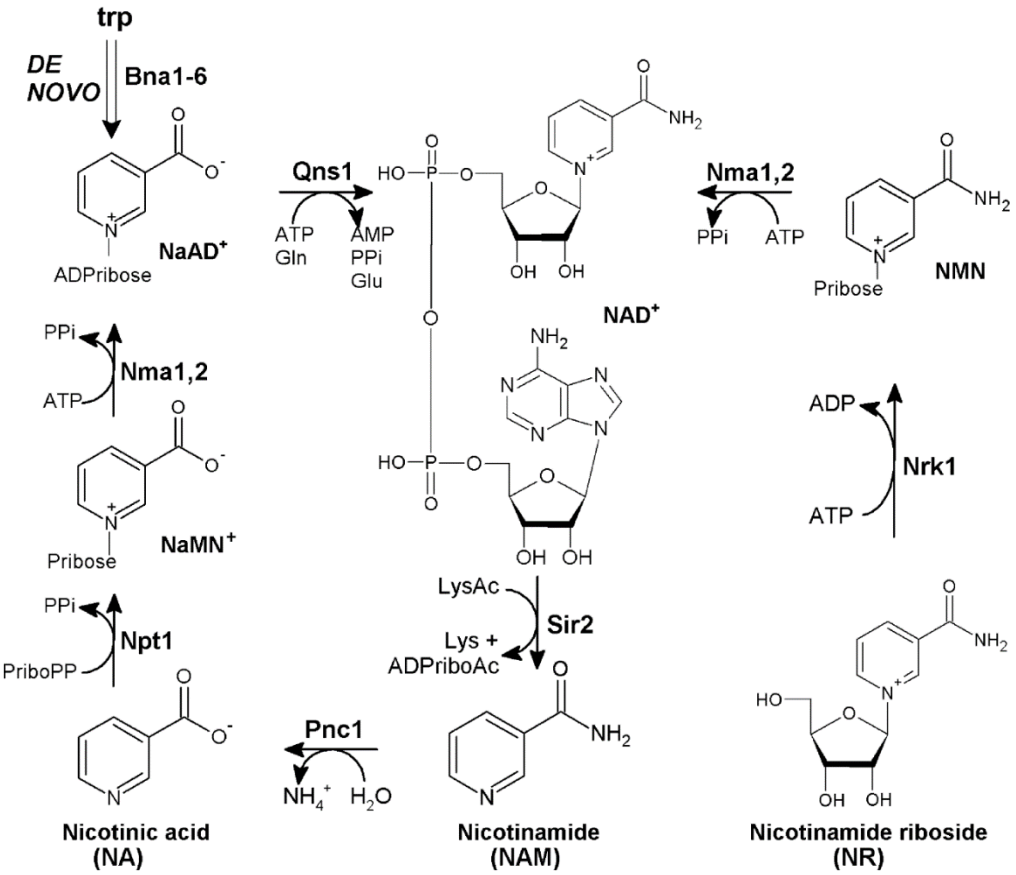

Figure 1A. The NAD^+ biosynthetic pathway in *Saccharomyces cerevisiae*.

NAD^+ can be synthesized *de novo* from tryptophan or by salvage pathway from the vitamin precursors nicotinic acid (NA), nicotinamide (NAM) or nicotinamide riboside (NR). PriboPP: phosphoribosyl pyrophosphate; Pribose: phosphoribose; LysAC: acetylated lysine; ADPriboAc: 2' and 3' O-acetylated ADPribose; $NAMN^+$: nicotinic acid mononucleotide; $NaAD^+$: nicotinic acid adenine dinucleotide; NMN: nicotinamide mononucleotide.

Figure 1B. Growth of wild type *C. glabrata* in media lacking NAD^+ and associated intracellular NAD^+ levels.

Top panel: In response to NAD^+ starvation WT *C. glabrata* doubles 4-5 times in media lacking NA before ceasing growth. Middle panel: In response to NAD^+ starvation intracellular NAD^+ levels diminish rapidly, and reach approximately $1/60^{th}$ of the original level after 24 hours of starvation. Error bars represent the standard deviation from a biological duplicate performed on two separate days. Bottom panel: Despite the fact that *C. glabrata* is growing with increasingly smaller amounts of intracellular NAD^+, the organism remains viable after days in –NA media.

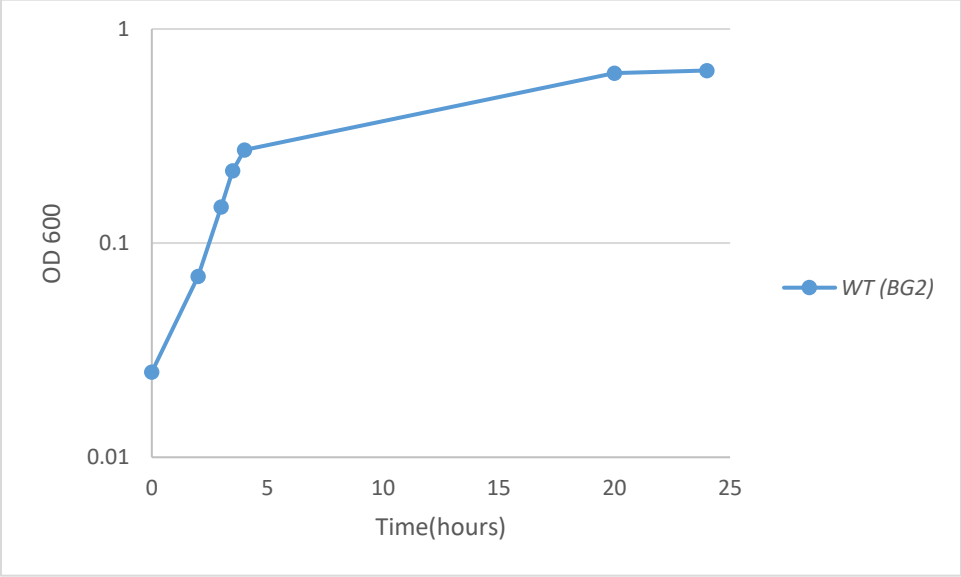

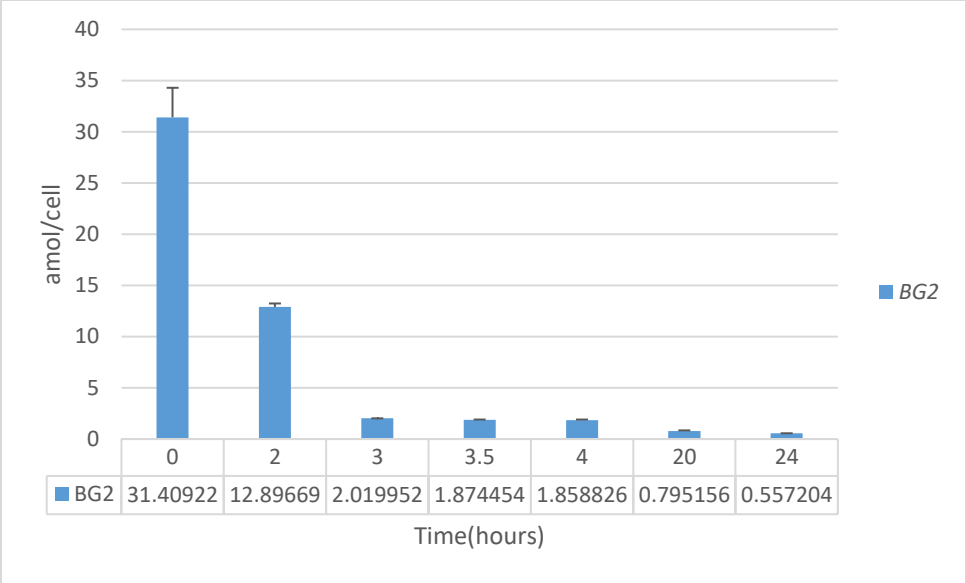
40
35
30
25
20
15
10
5
0
amol/cell
BG2
0
2
3
3.5
4
20
24
BG2
31.40922
12.89669
2.019952
1.874454
1.858826
0.795156
0.557204
Time(hours)

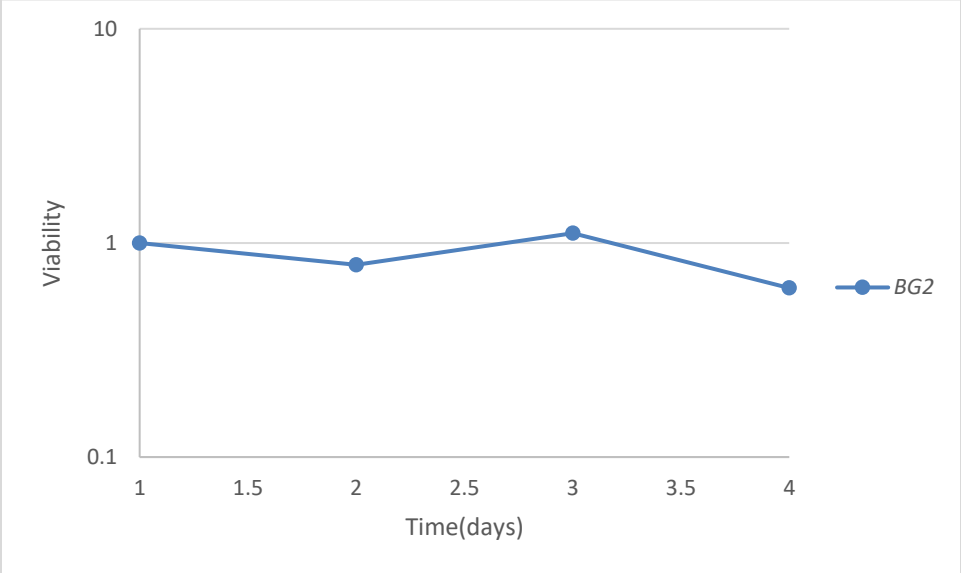
10
1
0.1
Viability
BG2
1
1.5
2
2.5
3
3.5
4
Time(days)

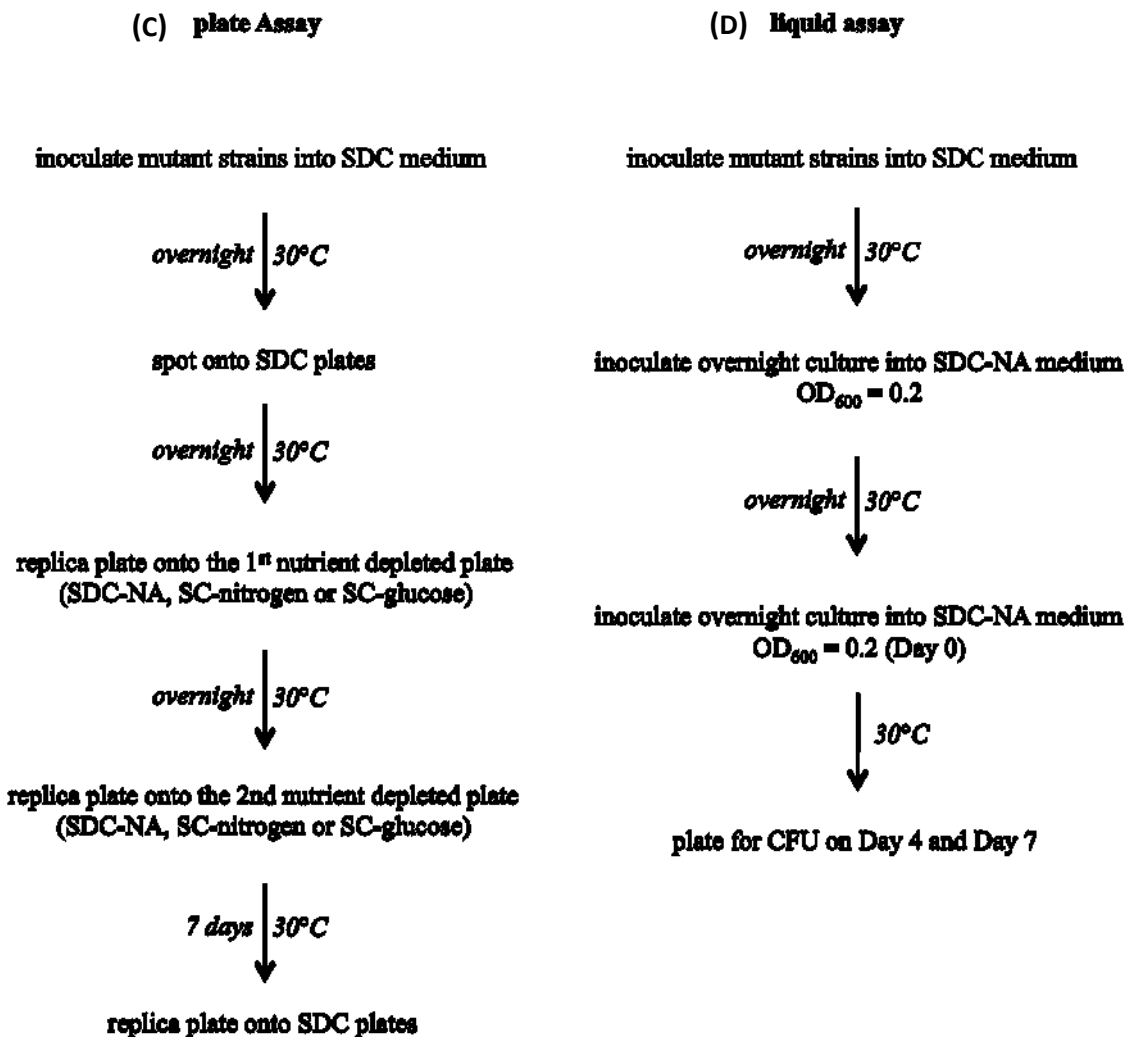

Figure 1C and 1D. *in vitro* assay for identifying mutants which fail to survive NAD^+ starvation.

(C) Procedure for plate based assay. (D) Procedure for liquid assay

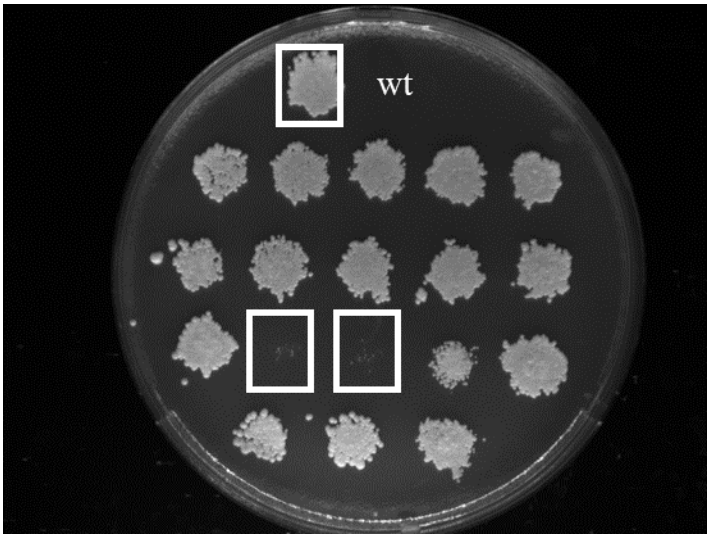

Figure S1. Colony morphology on a recovery plate.

The top white box marked the wild type. The boxes on the bottom marked two potential mutants that failed to recover after NAD^+ starvation.

Table S1. Insertional mutants with decreased survival after NAD^+ starvation.

The description associated with each gene was retrieved from

http://www.yeastgenome.org/ and may have been altered slightly.

Gene Name	# of times found	Description
ACT5	1	Actin-related protein of the dynactin complex
AIM23	1	Mitochondrial translation initiation factor 3 (IF3, mIF3)
ATG2	4	Peripheral membrane protein required for autophagic vesicle formation
BST1	1	GPI inositol deacylase of the endoplasmic reticulum
CCZ1	3	Subunit of a heterodimeric guanine nucleotide exchange factor
CHD1	1	Chromatin remodeler that regulates various aspects of transcription
CTF18	1	Subunit of a complex with Ctf8p; required for sister chromatid cohesion
DNA2	5	Tripartite DNA replication factor
DUG2	2	Component of glutamine amidotransferase (GATase II)
ENT2	1	Epsin-like protein required for endocytosis and actin patch assembly
ERG4	2	C-24(28) sterol reductase; catalyzes the final step in ergosterol biosynthesis
FPS1	2	Aquaglyceroporin, plasma membrane channel
GCN1	1	Positive regulator of the Gcn2p kinase activity

GCN2	7	Protein kinase; phosphorylates the alpha-subunit of translation initiation factor eIF2 (Sui2p) in response to starvation
GID8	1	Subunit of GID Complex, GID Complex is involved in proteasome-dependent catabolite inactivation of fructose-1,6-bisphosphatase
GPB1/GPB2	3	Multistep regulator of cAMP-PKA signaling; inhibits PKA downstream of Gpa2p and Cyr1p, thereby increasing cAMP dependency
HPR1	2	Subunit of THO/TREX complexes; this complex couple transcription elongation with mitotic recombination and with mRNA metabolism and export, subunit of an RNA Pol II complex
HSH155	1	U2-snRNP associated splicing factor
INO80	1	ATPase and nucleosome spacing factor
ISN1	2	Inosine 5'-monophosphate (IMP)-specific 5'-nucleotidase; catalyzes the breakdown of IMP to inosine; responsible for production of nicotinamide riboside and nicotinic acid riboside
LYS9	1	Saccharopine dehydrogenase (NADP+, L-glutamate-forming)
MED2	2	Subunit of the RNA polymerase II mediator complex
MTM1	1	Mitochondrial protein of the mitochondrial carrier family
NDC1	2	Subunit of the transmembrane ring of the nuclear pore complex (NPC)
NPR2	4	Subunit of the Iml1p/SEACIT complex; SEACIT (Iml1p-Npr2p-Npr3p) is a subcomplex of the SEA complex, a coatomer-related complex that associates dynamically with the vacuole;
PBP1	1	Component of glucose deprivation induced stress granules
PBS2	2	MAP kinase kinase of the HOG signaling pathway

PEP1/VTH1/2	1	Type I transmembrane sorting receptor for multiple vacuolar hydrolases
PRS3	1	5-phospho-ribosyl-1(alpha)-pyrophosphate synthetase; synthesizes PRPP, which is required for nucleotide, histidine, and tryptophan biosynthesis
RIS1	4	Swi2/Snf2-related translocase, SUMO-Targeted Ubiquitin Ligase (STUbL)
RSC3	1	Component of the RSC chromatin remodeling complex
RTG2	1	Sensor of mitochondrial dysfunction; regulates the subcellular location of Rtg1p and Rtg3p, transcriptional activators of the retrograde (RTG) and TOR pathways
SEA1	6	GTPase-activating protein (GAP) subunit of the Iml1p/SEACIT complex; SEACIT (Iml1p-Npr2p-Npr3p) is a subcomplex of the SEA complex
SIR2	1	Conserved NAD+ dependent histone deacetylase of the Sirtuin family
SKN7	4	Nuclear response regulator and transcription factor
SLA2	4	Adaptor protein that links actin to clathrin and endocytosis
SNA2	1	Protein of unknown function
SNX4	1	Sorting nexin; involved in retrieval of late-Golgi SNAREs from post-Golgi endosomes to the trans-Golgi network and in cytoplasm to vacuole transport
SRB8	1	Subunit of the RNA polymerase II mediator complex
SWI1	1	Subunit of the SWI/SNF chromatin remodeling complex
TOM7	1	Component of the TOM (translocase of outer membrane) complex
UBP3	1	Ubiquitin-specific protease involved in transport and osmotic response; negatively regulates Ras/PKA signaling

VPS45	1	Protein of the Sec1p/Munc-18 family; essential for vacuolar protein sorting
VPS70	2	Protein of unknown function involved in vacuolar protein sorting
YAF9	2	Subunit of NuA4 histone H4 acetyltransferase and SWR1 complexes
YPR084W	1	ORF , Uncharacterized
YRA1	1	Nuclear polyadenylated RNA-binding protein; required for export of poly(A)+ mRNA from the nucleus

Deletion of *SEA1* or *NPR2* leads to survival defect after prolonged NAD^+ depletion

Of the 47 genes identified that failed to survive NAD^+ depletion in vitro we chose to further analyze two: *NPR2 and SEA1* (formerly known as *IML1*). These two genes were of particular interest for two reasons. First, of all the mutants tested in the liquid NA starvation assay, these two mutants gave the strongest and most consistent phenotype. Second, it was previously described that *NPR2 and SEA1* function in a complex with one another in *S. cerevisiae* to regulate TORC1 activity [8-10]. This complex is known as the SEA complex (Seh1 associated Complex) and also contains Sea2-4, the nucleoporins Seh1 and Sec13, as well as Npr3 [8, 11]. Within the SEA complex Sea1, Npr2, and Npr3 function together in a sub-complex named SEACIT (SEA complex inhibiting TOR). SEACIT functions as a GTPase activating protein (GAP) which stimulates the upstream regulator of TORC1 GTR1 to convert bound GTP to GDP. GTP bound GTR1 is an activator of TORC1 activity, thus by promoting the exchange from GTP bound GTR1 to GDP bound GTR1 Sea1, Npr2, and Npr3 function as a negative regulator of TORC1 activity[9, 10]. Sea2, Sea3, and Sea4 correspondingly function together in a sub-complex named SEACAT (SEA complex activating TOR). SEACAT represses the activity of the Sea1, Npr2, Npr3 complex, thus acting as an activator of TORC1 [9, 10]. The results of our NA starvation screen in combination with the evidence that *NPR2* and *SEA1* function together in a complex led us to hypothesize that this complex may serve a role in response to NAD^+ depletion.

Six insertional mutations in *C. glabrata SEA1* and four in *NPR2* resulted in a survival defect upon NAD^+ starvation in our screen. To further investigate the effect of both these genes on NAD^+ starvation, we generated *sea1*Δ and *npr2*Δ strains in *C.*

glabrata in which the entire ORF was deleted. We then repeated the liquid NA starvation assay in the deletion mutant strains. The *sea1*Δ strain showed a 100-fold reduction in survival compared with the wild type after 4 days of NA starvation (Figure 2A. left panel). Moreover, the NAD^+ death phenotype was fully rescued after complementation with *SEA1* on a plasmid (Figure 2A). The *sea1*Δ strain resumed growth at later time points (day 5 and day 7) as evidenced by increased CFUs in many of our repeated experiments. We hypothesized that even though *C. glabrata* cells were starved for NAD^+ and entered growth arrest; there may still be a low level of NAD^+ or NAD^+ precursors stored within the cell. We reasoned that a proportion of NAD^+-starved *sea1*Δ cells might die and lyse, thus releasing their intracellular NAD^+ stores. The released NAD^+ could then be salvaged by the remaining cells allowing the cells to resume growth at late time points. We postulated that by blocking the uptake of NAD^+ precursors in the *sea1*Δ strain, this growth of cells after prolonged NAD^+ limitation could be prevented. In order to test this hypothesis, a *sea1*Δ *tna1*Δ *tnr1*Δ *tnr2*, quadruple mutant strain was generated.

In *C. glabrata*, Tna1, Tnr1 and Tnr2 are the high affinity transporters for NAD^+ precursors – niacin, nicotinamide and nicotinamide riboside [5]. Deletion of these genes render the cells unable to transport NAD^+ precursors when environmental concentrations of these precursors are low. The *sea1*Δ*tna1*Δ*tnr1*Δ*tnr2*Δ strain had no survival defects after carbon and thiamine limitation and showed slight survival defects after 15 days of nitrogen, phosphate or thiamine depletion as compared with the wild type. In contrast, the survival rate of the *sea1*Δ *tna1*Δ *tnr1*Δ *tnr2*Δ strain was five-log lower than that of the wild type after 15 days of NAD^+ starvation and there was no rebound of CFUs at any time points (Figure 2B). This data suggests that the survival defect seen in the *sea1*Δ is a

response specifically to NAD^+ starvation. Moreover, complementation with *SEA1* on a plasmid, rescued the survival defects of *sea1*Δ and *sea1*Δ *tna1*Δ *tnr1*Δ *tnr2*Δ strains upon NAD^+-starvation (Figure 2A). Together, these results indicate that *SEA1* is responsible for the death phenotype we observed and it has a role in the long-term survival of *C. glabrata* after NAD^+ starvation.

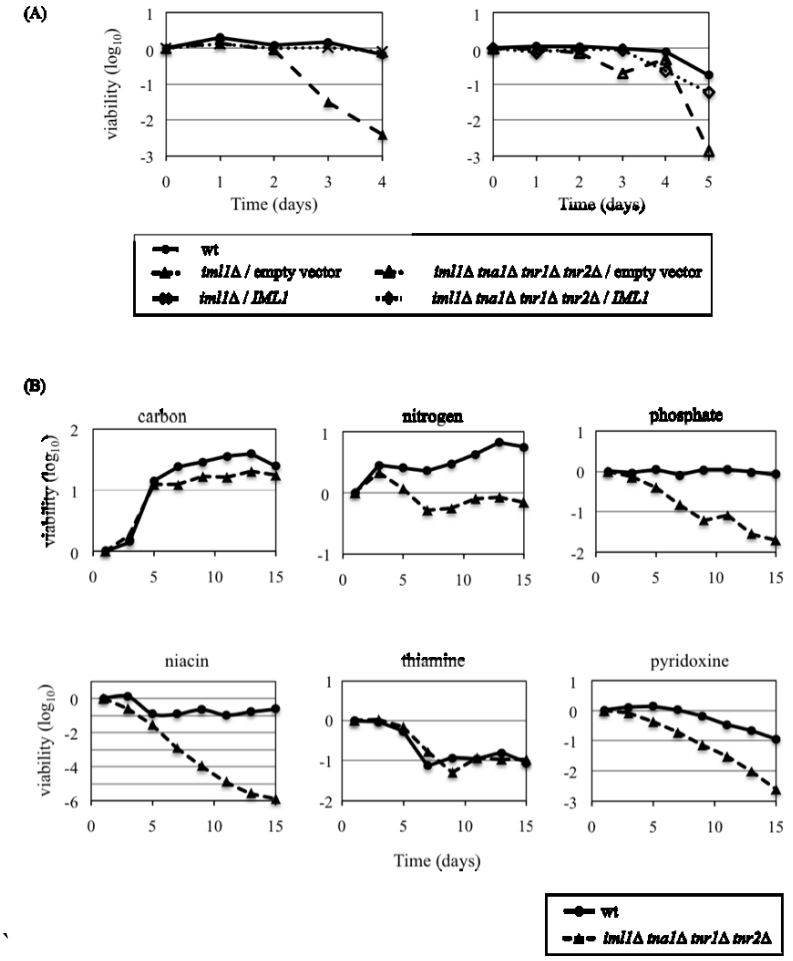

Figure 2A and 2B. Survival of *C. glabrata iml1*Δ *and iml1*Δ*tna1*Δ*tnr1*Δ*tnr2*Δ mutant strains in various nutrient-depleting media.

(A) *iml1*Δ and *iml1*Δ *tna1* Δ*tnr1* Δ*tnr2*Δ strains showed a 100-fold reduction in viability compared with wild type after 4 to 5 days of growth in NAD^+ depleting medium. This phenotype was reversed when *IML1* was provided ectopically on a plasmid. (B) *iml1*Δ *tna1*Δ *tnr1*Δ *tnr2*Δ strain showed minor or no survival defect after prolonged nitrogen, phosphate, pyridoxine, carbon or thiamine starvation but the viability was five orders of magnitude lower than that of the wild type after 15 days of NAD^+ starvation.

Next we wanted to determine if an *npr2*Δ strain also displayed a survival defect in response to NAD^+ starvation. To determine this, we conducted the liquid NA starvation assay with two unique *npr2*Δ strains. Interestingly, deletion of *NPR2* led to a 100-fold reduction in survival after 4 days of NAD^+ starvation in two *npr2*Δ isolates. In contrast, both carbon and nitrogen depletion had very mild effects on cell survival after 4 days of growth, again suggesting this survival defect is specific to NAD^+ starvation. (Figure 2C). Expression of *NPR2* from a plasmid restored survival to wildtype levels following NAD^+ depletion, whereas, an empty vector had no effect on survival to NAD^+ starvation (Figure 2D). Taken together these data strongly indicate that both *SEA1* and *NPR2* play a crucial role in survival in response to NAD^+ starvation, and suggest an important role for both genes in the long-term survival of *C. glabrata* after NAD^+ starvation. Furthermore, this data supports the idea that in addition to its roles in response to nitrogen starvation, amino acid biogenesis, and intracellular trafficking, the SEA complex may also be involved in response to NAD^+ depletion.

(C)

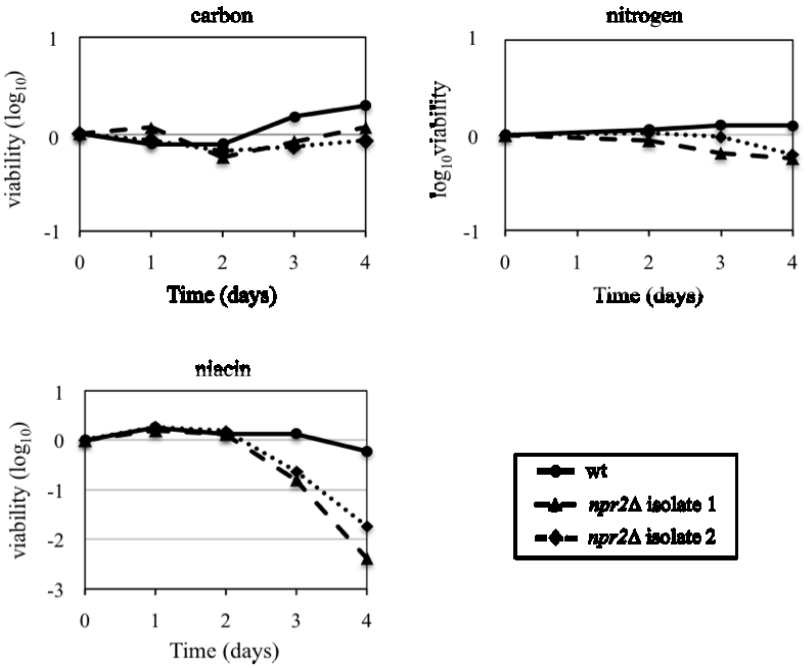

(D)

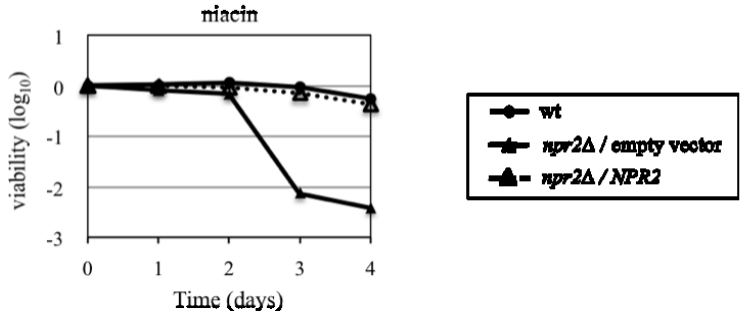

Figure 2C and 2D. Survival of *C. glabrata npr2*Δ strain in nutrient-depleting media.

(C) The *npr2*Δ strain showed no survival defect after 4 days of carbon or nitrogen starvation. However, the survival rate was 100-fold lower than that of the wild type after 4 days of NAD^+ starvation. (D) The survival defect of *npr2*Δ strain was restored by expressing NPR2 ectopically.

A background mutation implicated in death in response to NAD^+ starvation

We wanted to determine if the survival defect of the *C. glabrata sea1*Δ and *npr2*Δ strains was maintained in the closely related yeast *S. cerevisiae*. In contrast to *C. glabrata, S. cerevisiae* possesses a *de novo* pathway to synthesize cellular NAD^+ (Figure 1A)[1]. The *de novo* pathway utilizes tryptophan as a precursor and the activity of *BNA1-6* to synthesize NAD^+. In order to starve *S. cerevisiae* for NAD^+ synthesis via the *de novo* synthesis pathway needs to be blocked. To this end we generated a *bna6*Δ strain of *S. cerevisiae.* This strain is blocked in the first step of NAD^+ biosynthesis, and is an NAD^+ auxotroph which ceases to grow in media lacking NAD^+. In this strain background we then deleted members of the SEA complex: *sea1, sea2, sea3, sea4, npr2,* and *npr3.* We then performed the liquid NA starvation assay to determine if there was a survival defect for any of the strains (Fig. 3A). The survival defect seen for *sea1*Δ and *npr2*Δ strains that was present in *C. glabrata* was also seen in *S. cerevisiae,* though the effect was smaller: *bna6*Δ *sea1*Δ*, bna6*Δ *npr2*Δ*,* and *bna6*Δ *npr3*Δ (which comprise the SEACIT complex) showed a 5 fold reduction in survival relative to the *bna6*Δ strain. Interestingly, mutants in genes encoding the SEACAT complex showed no phenotype: *bna6*Δ *sea2*Δ*, bna6*Δ *sea3*Δ*,* and *bna6*Δ *sea4*Δ mutants survived as well as the *bna6*Δ control strain. The phenotype for *npr2* or *sea1* mutants in *C. glabrata* was stronger than for the corresponding mutants in *S. cerevisiae.* In the latter, the effect was highly reproducible and approximately 5-fold. We conclude that the absence of genes encoding the SEACIT complex impairs viability under conditions of NAD^+ starvation, and does so both *S. cerevisiae* and *C. glabrata*.

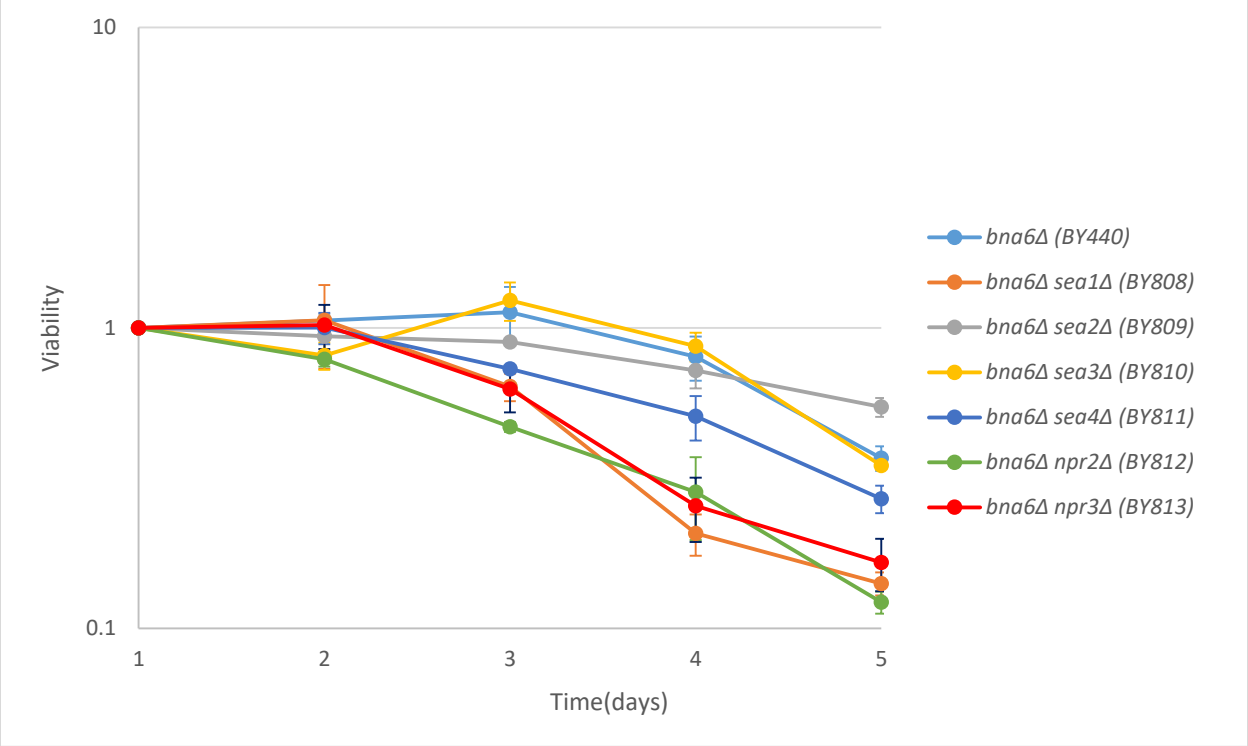

Figure 3A. Survival of *S. cerevisiae* SEA complex deletions in –NA media.

SEA complex components were deleted in a *bna6*Δ background and tested for survival in our liquid NA starvation assay. The *bna6*Δ *sea1*Δ, *bna6*Δ *npr2*Δ, and *bna6*Δ *npr3*Δ strains show an approximate 5-fold reduction in viability compared with the *bna6*Δ control strain after 5 days of growth in media lacking NAD^+. The error bars represent the standard error for 3 biological replicate experiments, carried out on three separate days.

We wanted to test if the survival defect for mutants in the SEACIT sub-complex could be exacerbated by disrupting the salvage pathway, which is known to reduce intracellular NAD^+ levels. After degradation of NAD^+ to nicotinamide (NAM), Pnc1 converts NAM to Nicotinic acid (NA) which can then be recycled back to NAD^+. To eliminate recycling we deleted *PNC1* in the *bna6*Δ background creating a *bna6*Δ *pnc1*Δ double mutant that is unable to synthesize or recycle NAD^+. In this *bna6*Δ *pnc1*Δ background we deleted the same members of the SEA complex described above and performed the liquid NA starvation assay. However the survival phenotype for *bna6*Δ *pnc1*Δ *sea1*Δ*, bna6*Δ *pnc1*Δ *npr2*Δ*,* and *bna6*Δ *pnc1*Δ *npr3*Δ strains was no worse than for the *bna6*Δ *sea1*Δ*, bna6*Δ *npr2*Δ*,* and *bna6*Δ *npr3*Δ strains.

Interestingly, however, we found that some of the *bna6*Δ *pnc1*Δ *sea4*Δ strains showed a robust death phenotype of approximately 10,000 fold for multiple independently derived *bna6*Δ *pnc1*Δ *sea4*Δ strains (Fig 3B). This very substantial phenotype was found in 4 out of 35 *bna6*Δ *pnc1*Δ *sea4*Δ we generated. Npt1 encodes another enzyme required for salvage of NAD^+ and we wondered if this same substantial survival defect would be found in a subset of *bna6*Δ *npt1*Δ *sea4*Δ mutants. We generated 6 *bna6*Δ *npt1*Δ *sea4*Δ mutants and found that 2 of these also showed the dramatic loss of viability upon limitation for NAD^+. This phenotype appeared in the *bna6 pnc1* or *bna6 npt1* backgrounds when we deleted *SEA4*. To ensure that the phenotype was not due to disruption of *SEA4*, we restored *SEA4* at the native locus in several strains showing the substantial survival phenotype (Fig 3B). Restoration of *SEA4* failed to rescue the death phenotype in the *bna6*Δ *pnc1*Δ *sea4*Δ. This suggested to us the presence of a background mutation that was responsible for or contributed to this substantial death phenotype in

response to NAD^+ starvation. For ease of discussion, we gave a provisional name to the corresponding gene: *DND1* (**d**eath from **N**AD^+ **d**epletion), and include *dnd1-6* as provisional genotypes for the 6 strains showing the dramatic death in response to NAD^+ depletion.

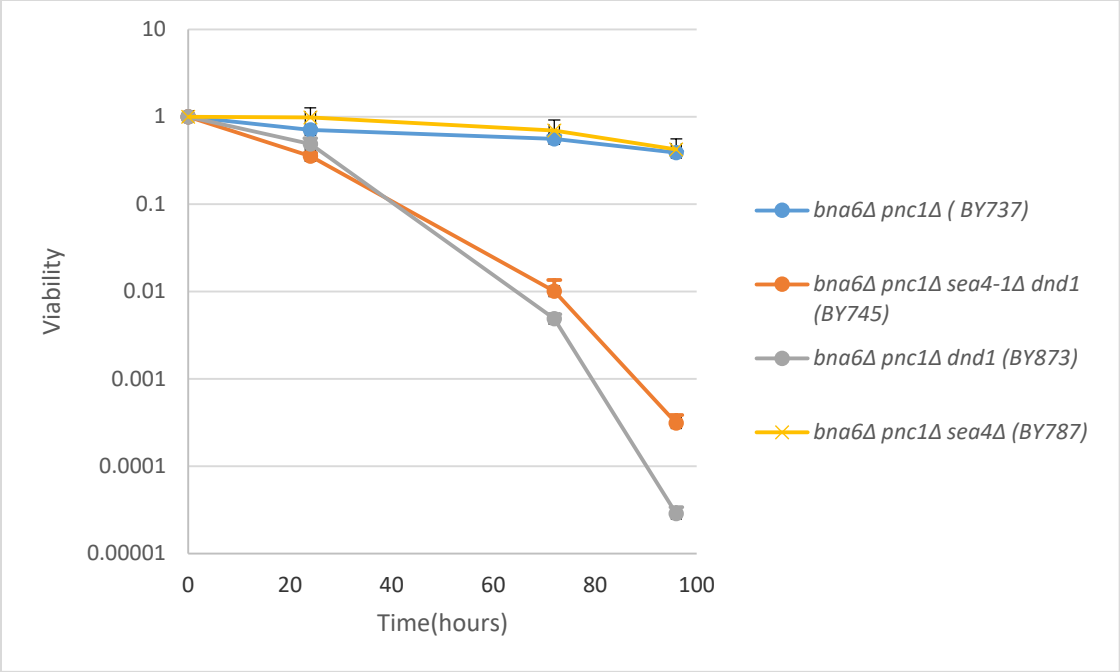

Figure 3B. The robust survival defect for *bna6*Δ *pnc1*Δ *sea4*Δ *dnd1* strains.

In a subset of *bna6*Δ *pnc1*Δ *sea4*Δ strains we acquired a background mutation which led to a failure to survive our liquid NA starvation assay. The *bna6*Δ *pnc1*Δ *sea4*Δ *-1 dnd1* strain tested above exhibits a 50,000 fold reduction in viability compared to the *bna6*Δ *pnc1*Δ control. This phenotype fails to revert to the *bna6*Δ *pnc1*Δ control phenotype even when *SEA4* is restored at the native locus strongly suggesting the presence of a background mutation. The error bars represent the standard error for 3 biological replicate experiments, carried out on three separate days.

To further analyze the survival defect seen in the *bna6*Δ *pnc1*Δ *sea4*Δ *dnd1* strain as it relates to NAD^+ depletion, we took advantage of a tool developed by Wessels et al. used to deplete intracellular NAD^+ levels. NAD-glycohydrolases are enzymes that catalyze the hydrolysis of the nicotinamide-ribose bond of NAD^+ to yield nicotinamide and adenosine diphosphoribose [12]. Wessels et al. demonstrated that expression of the NAD-glycohydrolase encoded by the *nga* gene from *Streptococcus pyogenes* (under the control of the *GAL1* promoter in vector pYES-nga depletes intracellular NAD^+ levels in *S. cerevisiae* [13].Consistent with this, we measured the levels of NAD^+ in strains carrying the pYES-nga plasmid (but not the control empty vector) after growth in galactose, and saw rapid depletion of NAD^+ within 30 minutes of addition of galactose. Consistent with growth inhibition seen by Wessels et al., we found that a wild-type *S. cerevisiae* strain grown on galactose (but not glucose) transformed with pYES-nga showed a dramatic inhibition of growth. Cells transformed with the empty vector grew fine on both galactose and glucose containing plates (Figure 3C).

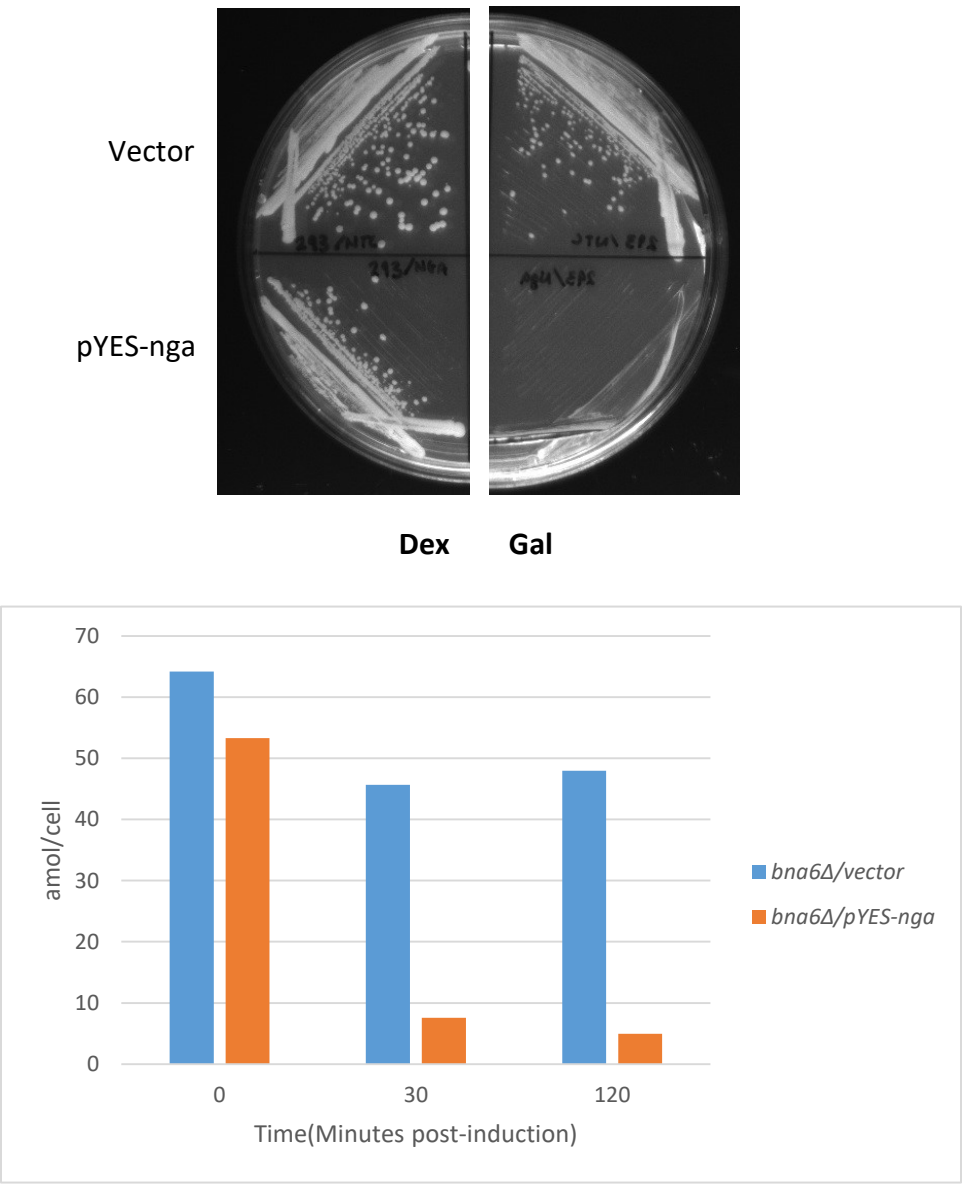

Figure 3C. Transformation of pYES-nga into *S. cerevisiae.*

S. cerevisiae transformed with pYES-nga is responsive to induction through plating on galactose. When the strains are plated on media with dextrose as the carbon source both strains grow very similar to the wild-type control strain. When the same strains are plated on galactose the *nga* gene is induced and growth defects are seen for both strains relative

to the control. Induction of *nga* results in rapid depletion of cellular NAD^+ levels within 30 minutes.

We transformed the *bna6*Δ *pnc1*Δ *sea1*Δ, *bna6*Δ *pnc1*Δ *sea2*Δ, *bna6*Δ *pnc1*Δ *sea3*Δ, *bna6*Δ *pnc1*Δ *sea4*Δ strains as well as *bna6*Δ *pnc1*Δ *sea4*Δ *dnd1* with pYES-nga and assessed growth on SDC-URA plates (Fig 3D). We found a striking difference in transformation by pYES-nga between the *bna6*Δ *pnc1*Δ *sea4*Δ dnd1 *s*train and the other strains (including *bna6*Δ *pnc1*Δ *sea4*Δ. The *bna6*Δ *pnc1*Δ *sea4*Δ (Figure 3D) as well as all the other strains (*bna6*Δ *pnc1*Δ *sea1*Δ, *bna6*Δ *pnc1*Δ *sea2*Δ , *bna6*Δ *pnc1*Δ *sea3*Δ) all transformed well with the plasmid and produced a lawn of transformants as well as isolated single colonies. In contrast the *bna6*Δ *pnc1*Δ *sea4*Δ *dnd1* cannot be transformed with the pYES-nga at all, and if the lawn was re-streaked no single isolated colonies grew. The few isolated colonies seen on *bna6*Δ *pnc1*Δ *sea4*Δ *dnd1* transformation plate (Figure 3D) are mutants in which the pYES-nga is no longer active and causes no growth inhibition when grown in the presence of galactose. By contrast, all transformants from *bna6*Δ *pnc1*Δ *sea1*Δ, *bna6*Δ *pnc1*Δ *sea2*Δ, *bna6*Δ *pnc1*Δ *sea3*Δ, and *bna6*Δ *pnc1*Δ *sea4*Δ failed to grow, as expected, when plated on galactose. We conclude therefore that the *bna6*Δ *pnc1*Δ *sea4*Δ *dnd1* strain cannot be transformed with the pYES-nga likely due to leaky expression of the pYES-nga even on the glucose-repressing SDC transformation plates. Notably, the *bna6*Δ *pnc1*Δ *sea4*Δ *dnd1* strains can be readily transformed with other plasmids, including pYES2/NT/C the empty parent vector of pYES-nga. The failure of the *bna6*Δ *pnc1*Δ *sea4*Δ *dnd1* strain to survive transformation with a plasmid that depletes cellular NAD^+ levels is consistent with this strains rapid death when grown

without NA (Figure 3B). From a practical perspective, we used transformability by pYES-nga as a test for the presence of the putative *dnd1* mutation.

To further show that the death phenotype of the *bna6*Δ *pnc1*Δ *sea4*Δ *dnd1* strains is related to NAD^+ metabolism, we examined whether survival could be modulated by restoring *PNC1*. *PNC1* is required for recycling NAM back to NAD^+ and a *pnc1*Δ mutation eliminates NAD^+ recycling and further disrupts NAD^+ biosynthesis. Restoration of *PNC1* at the native locus in the *bna6*Δ *pnc1*Δ *sea4-1*Δ *dnd1* strain substantially increases the survival following NA starvation (Fig 3E) by about 50 fold in two independently generated isolates. Notably, the *bna6*Δ *sea4*Δ *dnd1* strain still dies much faster than *bna6*Δ *sea4*Δ or *bna6*Δ strains, showing that the effect of the *dnd1* mutation does not depend absolutely on *pnc1* being deleted.

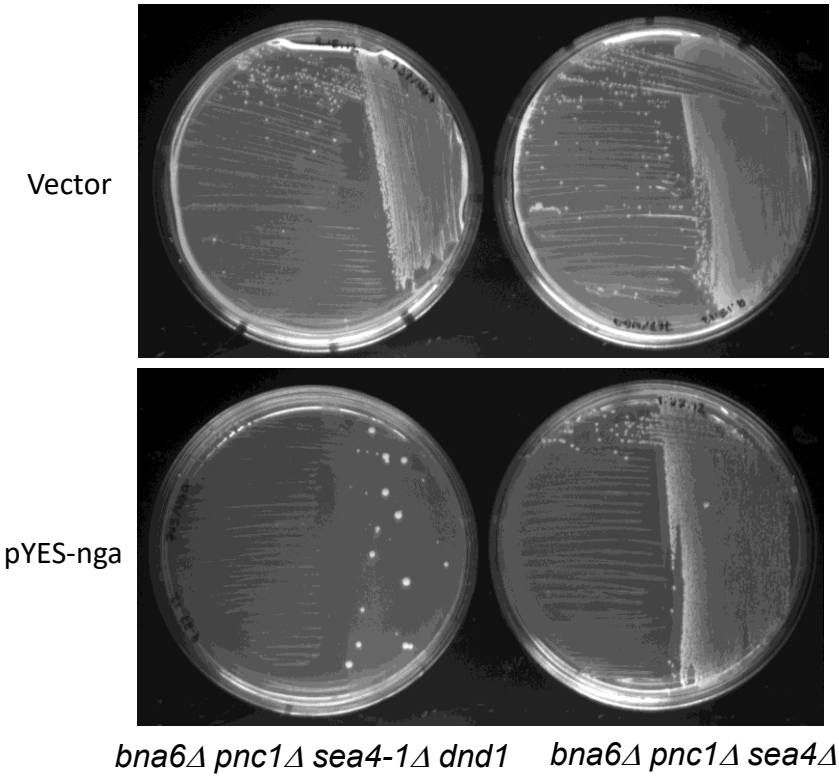

Figure 3D. Different transformation phenotypes between the *bna6*Δ *pnc1*Δ *sea4*Δ *and bna6*Δ *pnc1*Δ *sea4-1*Δ *dnd1* strains.

The *bna6*Δ *pnc1*Δ *sea4*Δ and *bna6*Δ *pnc1*Δ *sea4-1*Δ *dnd1* strains were transformed with pYES-nga. Although the strains are expected to be genotypically identical, the *bna6*Δ *pnc1*Δ *sea4-1*Δ *dnd1* strain has a clear transformation defect when compared to the *bna6*Δ *pnc1*Δ *sea4*Δ strain suggesting the presence of a second-site mutation.

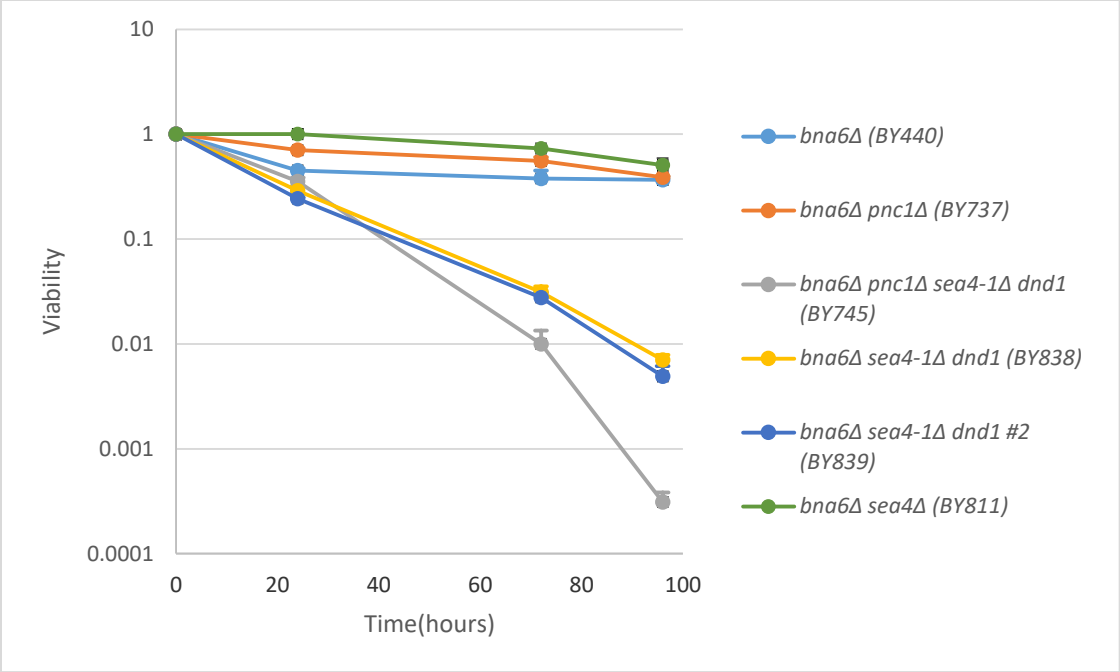

Figure 3E. The effect of restoring *PNC1* on viability in liquid NA starvation assay. *PNC1* was restored at the native locus in the *bna6Δ pnc1Δ sea4-1Δ dnd1* strain background. Restoration of PNC1 in two isolates decreased the survival defect from approximately 50,000 fold to 100 fold, linking the death phenotype seen specifically to NAD^+ metabolism. The error bars represent the standard error for 3 biological replicate experiments, carried out on three separate days.

Identification of the background mutation which causes death in response to NAD^+ starvation

To identify the *DND1* gene, we mated strain BY745 (*bna6*Δ *pnc1*Δ *sea4*Δ *dnd1*) with *S. cerevisiae* strain BY4742. We transformed the resulting diploid strain (BY293-745) with either pYES-nga or empty vector (Fig 4A). The diploid transformed equally well with pYES-nga and empty vector, suggesting that the *dnd1* phenotype is recessive, at least as far as the impact on transformability by the pYES-nga plasmid.

We sporulated strain BY293-745 and analyzed progeny spores of 11 tetrads with 4 surviving spores. We genotyped the deleted genes based on antibiotic resistance (*bna6*Δ*::NAT, pnc1*Δ*::HYG, sea4*Δ*::G418*) (Table S2). Next, to determine if any of the spores exhibited the *dnd1* phenotype, we first transformed all 44 spores with pYES-nga and assessed their transformation phenotypes. Strikingly, two spores from each tetrad could be transformed with pYES-nga and two spores could not be transformed. Thus the *dnd1* transformation phenotype segregated 2:2. Figure 4B shows representative samples of a subset of spores transformed with pYES-nga. Among the spores that could not be transformed with pYES-nga, all genotypes for the three antibiotic marked genes were represented suggesting that the *dnd1* phenotype is, remarkably, independent of any of these genes. From the above data, we concluded that the NAD^+ depletion mediated death seen in strain BY745 is independent of the *bna6*Δ *pnc1*Δ *sea4*Δ mutations and that the causative mutation (*dnd1*) is likely caused by a single mutation that segregates 2:2. We had independently isolated 6 strains that had the strong DND phenotype. We wished to formally demonstrate that *dnd2-dnd6* are allelic with *dnd1*. We performed a complementation assay: we mated spore T11-2 (matα *bna6*Δ *sea4*Δ *dnd1*) to BY807

(*bna6*Δ *pnc1*Δ *sea4*Δ*)*. The resulting diploid could be transformed with pYES-nga. By contrast diploids obtained by mating spore T11-2 with BY746, BY834, BY835, BY773 and BY851 (containing the *dnd2-6* mutations) could not be transformed with pYES-nga (Data not shown). This strongly suggested that *dnd1 -6* are all alleles of the same gene

Vector pYES-nga

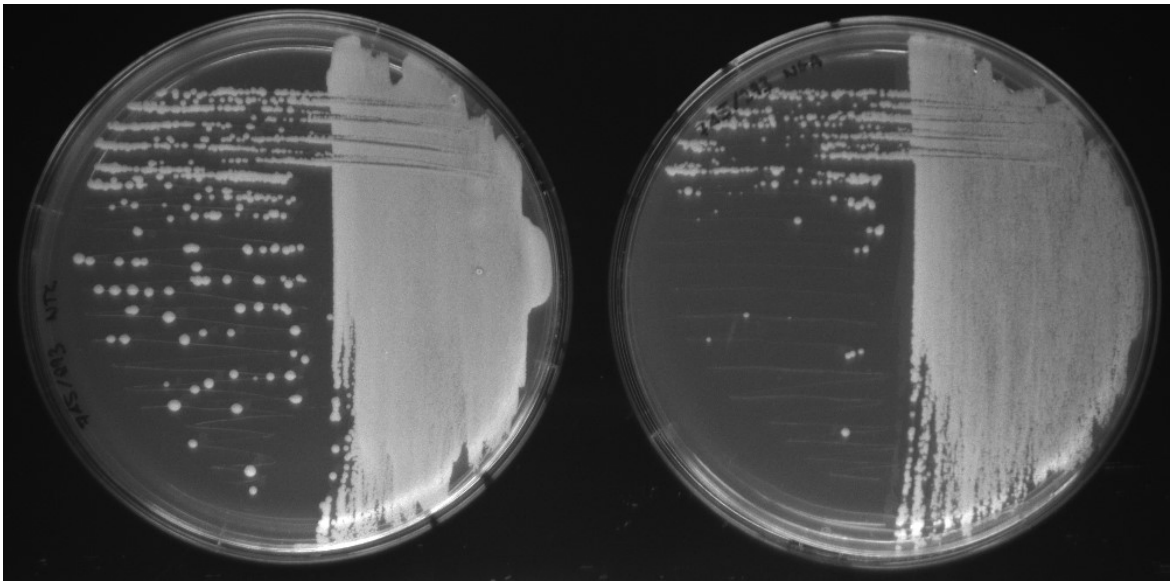

WT/*bna6Δ pnc1Δ sea4-1Δ dnd1*

Figure 4A. Diploid Transformation with pYES-nga.

A WT/ *bna6*Δ *pnc1*Δ *sea4-1*Δ *dnd1* diploid strain was generated and transformed with pYES-nga. The diploid strain has no transformation defect when transformed with pYES-nga indicating complementation of the *dnd1* mutant by the WT strain.

Table S2. Results from mating, sporulation and dissection of two *bna6*Δ *pnc1*Δ *sea4*Δ *dnd1* strains to wild-type.

For the pYES-nga column (+) means that the strain was successfully transformed with the plasmid whereas (-) means that the strain had a marked growth defect upon transformation with the plasmid. For *lys2*Δ*0* and *met15*Δ*0* (+) indicates the growth of that strain on media lacking that particular amino acid, (-) means the strain failed to grow on media lacking that particular amino acid. For the *bna6*Δ*::NAT, pnc1*Δ*::HYG,* and *sea4*Δ*::G418* (+) indicates the growth of that strain on media supplemented with the corresponding antibiotic, (-) indicates failure of that strain to go on media containing the antibiotic.

Tetrad #	Spore #	Mating type	pYES-nga	*lys2*Δ*0*	*bna6*Δ*::NAT*	*pnc1*Δ*::HYG*	*sea4*Δ*::G418*	*met15*Δ*0*
1	1	α	+	-	+	+	-	+
1	2	a	-	+	-	-	+	+
1	3	α	-	+	-	+	-	-
1	4	a	+	-	+	-	+	-
2	1	a	+	-	-	+	+	+
2	2	α	+	-	+	-	-	+
2	3	a	-	+	-	-	+	-
2	4	α	-	+	+	+	-	-
3	1	a	+	-	+	-	+	-

3	2	α	-	+	-	+	-	-
3	3	α	+	-	-	-	+	+
3	4	a	-	+	+	+	-	+
4	1	α	-	+	+	-	-	+
4	2	a	+	-	-	-	-	-
4	3	a	+	-	+	+	+	-
4	4	α	-	+	-	+	+	+
5	1	a	-	-	+	-	-	-
5	2	α	+	-	-	+	+	-
5	3	a	+	+	+	-	-	+
5	4	α	-	+	-	+	+	+
6	1	a	-	+	+	-	+	-
6	2	α	+	-	-	+	-	+
6	3	a	-	-	-	-	+	+
6	4	α	+	+	+	+	-	-
7	1	a	+	-	+	+	-	+
7	2	a	-	+	+	-	-	-
7	3	α	+	-	-	+	+	+
7	4	α	-	+	-	-	+	-
8	1	a	-	+	-	-	+	-

8	2	α	+	-	+	-	-	+
8	3	a	-	-	-	+	+	-
8	4	α	+	+	+	+	-	+
9	1	α	-	+	-	-	+	+
9	2	a	-	+	+	-	+	+
9	3	α	+	-	-	+	-	-
9	4	a	+	-	+	+	-	-
10	1	α	+	-	-	+	-	-
10	2	a	-	+	+	-	-	-
10	3	α	+	-	+	+	+	+
10	4	a	-	+	-	-	+	+
11	1	a	-	+	-	+	+	-
11	2	α	-	-	+	-	+	+
11	3	a	+	-	+	+	-	-
11	4	α	+	+	-	-	-	+

Figure 4B. Phenotypes of spores transformed with pYES-nga.

All spores generated through the mating of two *bna6*Δ *pnc1*Δ *sea4*Δ *dnd1* strains with wild-type were transformed with pYES-nga. A subsection of spores of these spores with seemingly identical genotypes but different transformation phenotypes are illustrated below. The genotypes of the spores used in this experiment are: *bna6*Δ*::NAT, bna6*Δ *::NAT pnc1*Δ*::HYG,* and the *bna6*Δ*::NAT pnc1*Δ*::HYG sea4*Δ*::G418.*

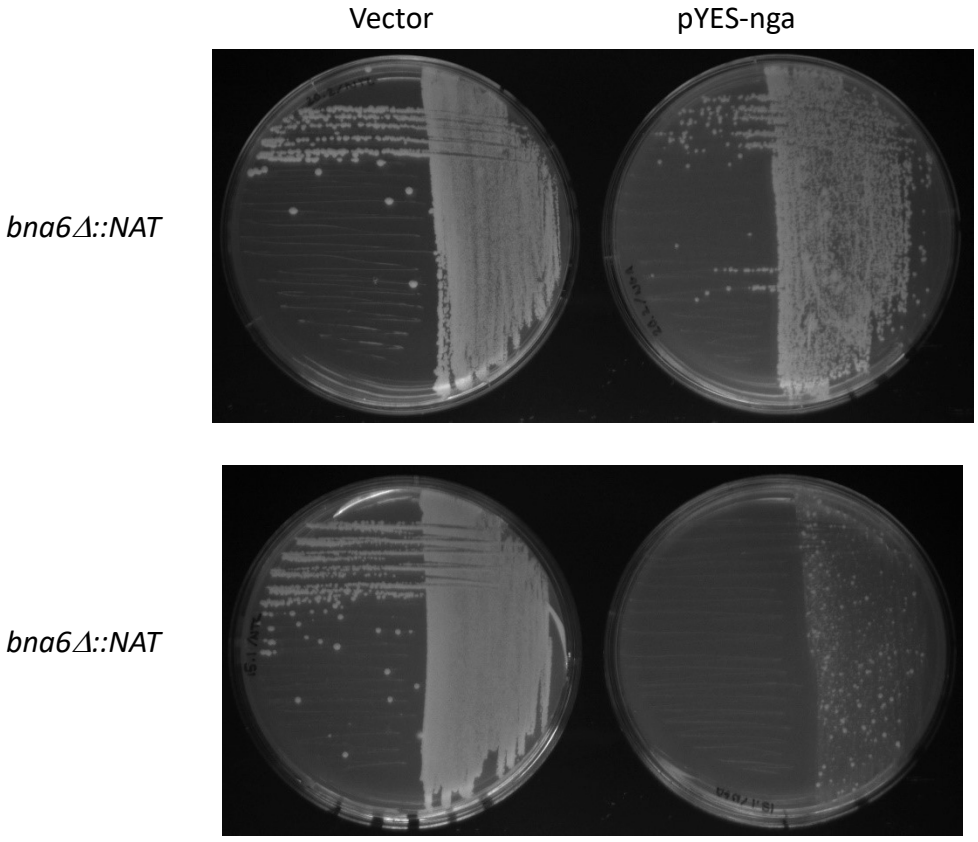

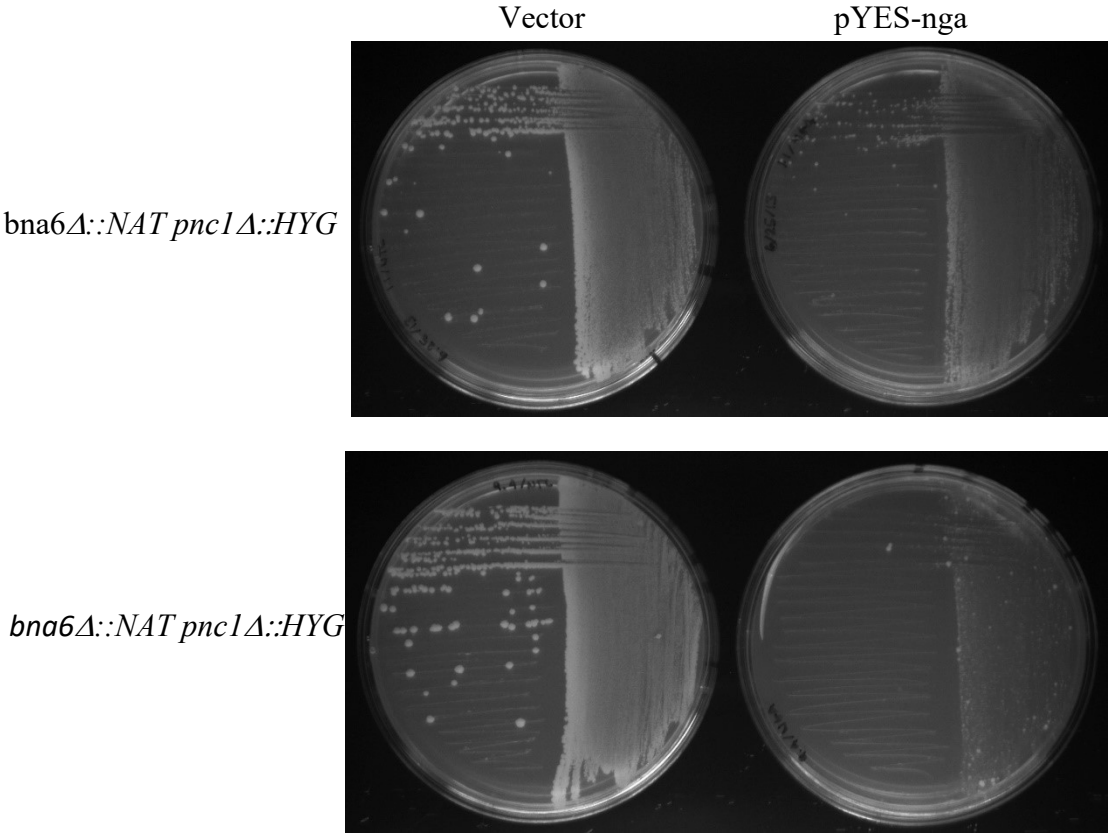
Vector
pYES-nga
bna6Δ::NAT pnc1Δ::HYG
bna6Δ::NAT pnc1Δ::HYG

Vector pYES-nga

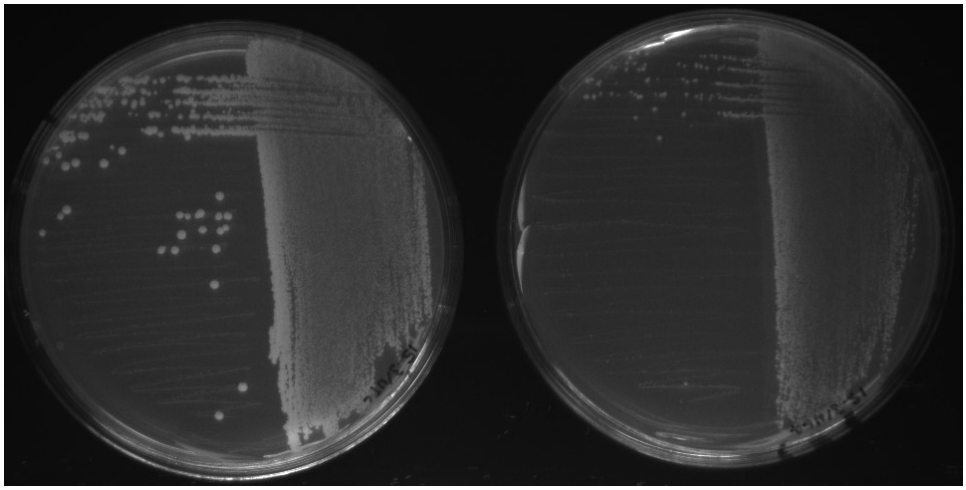

bna6Δ::NAT pnc1Δ::HYG sea4Δ::G418

Next, we performed the liquid NA starvation assay on all spores that were *bna6*Δ. Cells possessing *BNA6* can continually synthesize NAD^+ through the *de novo* pathway and thus are unable to be starved. Figure 4C monitors the survival of a subset of representative spores tested. All spores that failed to transform with pYES-nga, but not those that could be transformed with pYES-nga had marked survival defects when starved for NAD^+ relative to the control strains (*bna6*Δ *or bna6*Δ *pnc1*Δ*)*. Moreover, the tested spores quantitatively had similar survival to the original parental *bna6*Δ *pnc1*Δ *sea4*Δ *dnd1* and *bna6*Δ *sea4*Δ *dnd1* strains. Thus, we conclude that *dnd1* confers two phenotypes – a rapid and dramatic death when cells are grown in media lacking NA, and an inability to be transformed with pYES-nga even under glucose repressing conditions.

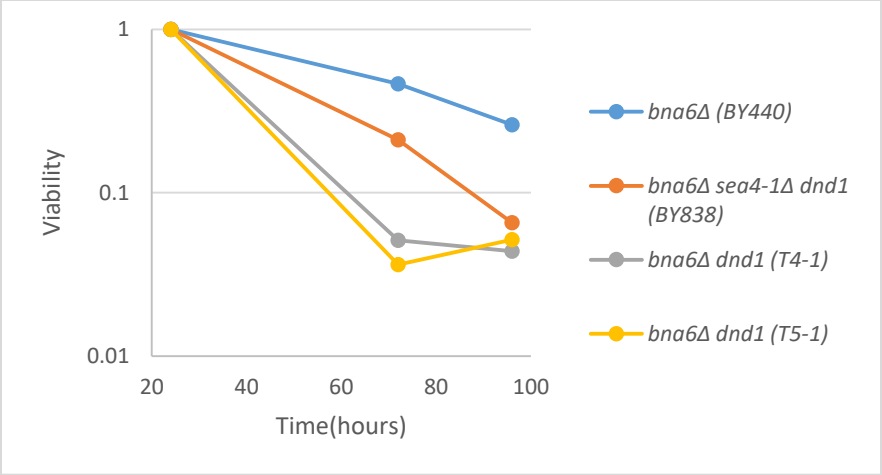

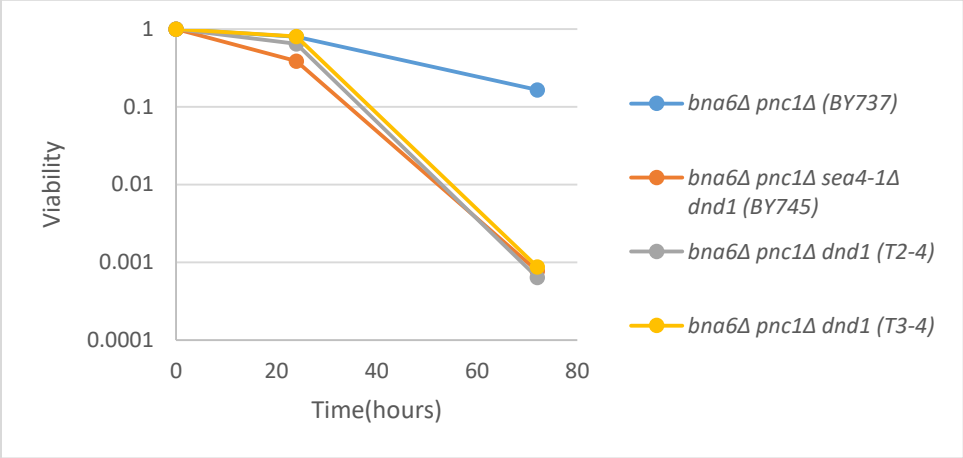

Figure 4C. *dnd1* spore phenotype in liquid NA starvation assay.

Four representative spores 2 with *bna6*Δ *dnd1* genotypes and 2 with *bna6*Δ *pnc1*Δ *dnd1* genotypes were tested for survival in response to NAD^+ starvation. All spores tested have a definitive survival defect relative to the appropriate control strain. The *bna6*Δ *dnd1* spores have similar viability as the original *sea4-1*Δ mutant where *PNC1* was restored at the native locus. The survival of the *bna6*Δ *pnc1*Δ *dnd1* spores is remarkably similar to the original *bna6*Δ *pnc1*Δ *sea4-1*Δ *dnd1* strain. Repeat experiments with the same spores yielded quantitatively similar results.

To identify the causative mutation underlying the *dnd1* phenotype, we used whole-genome sequencing. We isolated genomic DNA from three independently derived *bna6*Δ *pnc1*Δ *sea4*Δ *dnd1* strains that showed survival defects in both the liquid NAD^+ starvation assay and our pYES-nga transformation assay as well as genomic DNA from the *bna6*Δ *pnc1*Δ parental strain from which the strains were created. We identified high confidence SNPs differing between the *sea4* parents. Strikingly, all three *bna6*Δ *pnc1*Δ *sea4*Δ *dnd1* strains possessed a single T insertion after nucleotide 72 in *IRA1,* which was absent in the sequence of the *sea4*Δ parental strain (Figure 4D). *IRA1* is a GTPase activating protein, which negatively regulates RAS by converting it from the GTP to the GDP bound inactive form [14-16]. We used PCR to amplify and sequence this region of IRA1 from 12 spores – 6 that showed the *dnd1* phenotype, and 6 that did not. All 6 *dnd1* spores had the T72 indel mutation, while all of the spores we identified as lacking the *dnd1* mutation had fully wild-type *IRA1* sequences.

Whole genome sequencing of strains BY745 (*dnd1*) BY746 (*dnd2*), BY834 (*dnd4*) all showed the same T72 insertion in *IRA1*.We confirmed by PCR amplification and sequencing this same mutation was present in BY835 (*dnd5*), BY773 (*dnd3*) and BY851 (*dnd6*) and not in the immediate parental strains (BY729 and BY709), for which the *IRA1* ORF sequence was wild type. To demonstrate that *IRA1* loss of function was indeed the cause of the DND phenotype, we created *ira1*Δ strains in *S. cerevisiae* and examined their survival of NAD^+ starvation, as well as transformability by pYES-nga. We compared survival of *bna6*Δ and *bna6*Δ *pnc1*Δ strains to *bna6*Δ *ira1*Δ and *bna6*Δ *pnc1*Δ *ira1*Δ strains, and found a dramatic decrease in survival of NA starvation conferred by loss of *IRA1* (Figure 4E). Likewise, disruption of *IRA1* resulted in an

inability to tolerate transformation by pYES-nga. For the transformation assay, the magnitude of the phenotype was correlated with the degree to which the NAD^+ biosynthetic pathway was altered. In an *ira1*Δ strain transformation with pYES-nga produces an area with a lawn of colonies but single colonies cannot grow. Transformation of a *bna6*Δ *ira1*Δ strain gave a lawn with few colonies and no colonies in the section of the plate where isolated colonies should exist. Finally, in a *bna6*Δ *pnc1*Δ *ira1*Δ strain transformation with pYES-nga results in a complete failure of transformation (Figure 4F). Consistent with *ira1*Δ being allelic with *dnd1*, a diploid made by mating *bna6*Δ *ira1*Δ *with* strain BY745 (*dnd1*) could not be transformed with pYES-nga (Figure 4G).

These data convinced us that the strong DND phenotype which emerged 6 times independently in *bna6*Δ *pnc1*Δ *sea4*Δ or *bna6*Δ *npt1*Δ *sea4*Δ backgrounds was due in each case to a loss of function mutation in *IRA1* by insertion of a T residue at nucleotide position 72.

Loss of *IRA2* also confers a loss of viability under NA depletion conditions.

Ira1 and Ira2 function together in a complex, and loss of either results in a loss of RAS GAP activity [17, 18]. We constructed mutants of *IRA2* both alone and in combination with *bna6*Δ and *bna6*Δ *pnc1*Δ mutants to determine if these had the same phenotypes as the corresponding *ira1*Δ mutants. As shown in figure S2 both *bna6*Δ *ira2*Δ mutants and *bna6*Δ *pnc1*Δ *ira2*Δ showed a dramatic loss of viability when starved for NAD^+ In addition, as with *ira1*Δ mutants, *ira2*Δ mutants could not be efficiently transformed with pYES-nga.

Loss of *IRA1* also confers a loss of viability under NA depletion conditions in *C. glabrata*.

We showed (Figure 2A-D) that mutants in the SEA complex in *C. glabrata* show a loss of viability under NA starvation conditions. We did not isolate an *ira1* or *ira2* mutants in the initial *Tn7* plate screen for failure to survive NA depletion. To determine if *ira1* mutants had a NA starvation viability loss in *C. glabrata*, we deleted *IRA1* and assessed ability of the mutant to survive NAD^+ depletion (Figure S3). As in *S. cerevisiae*, loss of *IRA1* resulted in a dramatic loss of viability, showing that this role of IRA1 is conserved between the two species.

As a precaution, we were concerned, that the *C. glabrata sea1*Δ and *npr2*Δ strains analyzed in Figure 2 might have acquired a mutation in *IRA1*, as occurred in certain strains of S. cerevisiae, We therefore PCR amplified and sequenced the ORF sequence of both *IRA1* and *IRA2* of strain CG2398 (*sea1*Δ). Both ORFs had no mutations, consistent with the NA depletion viability loss in C. glabrata strains being due to loss of Sea1 or Npr2.

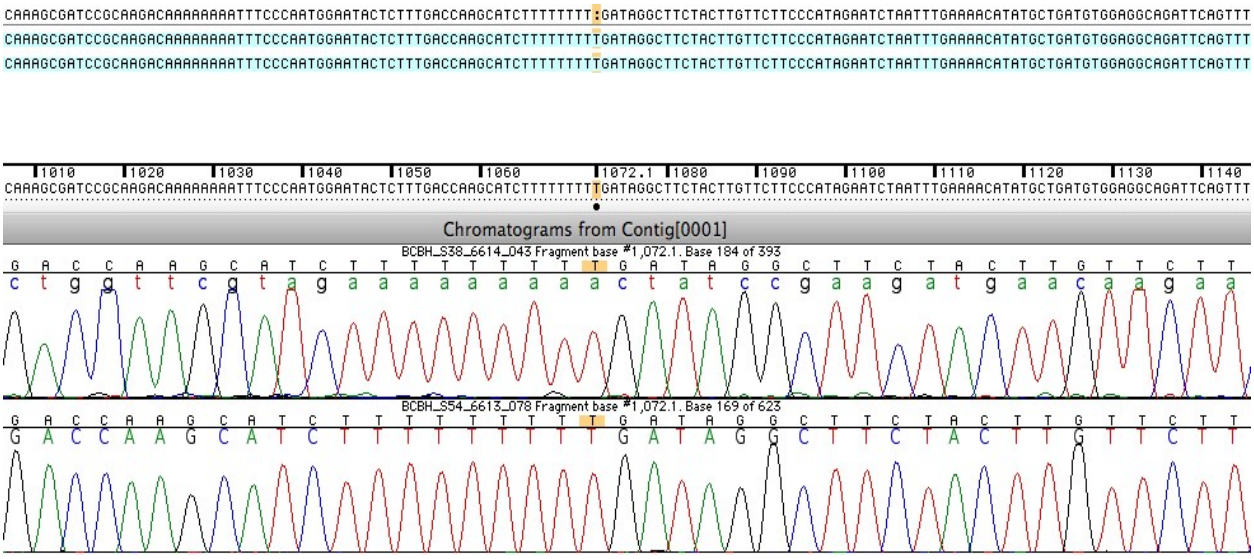

Figure 4D. Sequencing from *bna6*Δ *pnc1*Δ *sea4-1*Δ *dnd1* strain.

Whole-genome sequencing data revealed a single "T" insertion after nucleotide 72 in *IRA1* in all three of the *bna6*Δ *pnc1*Δ *sea4*Δ *dnd1* strains sequenced. The *sea4*Δ parental strain lacks this "T" insertion.

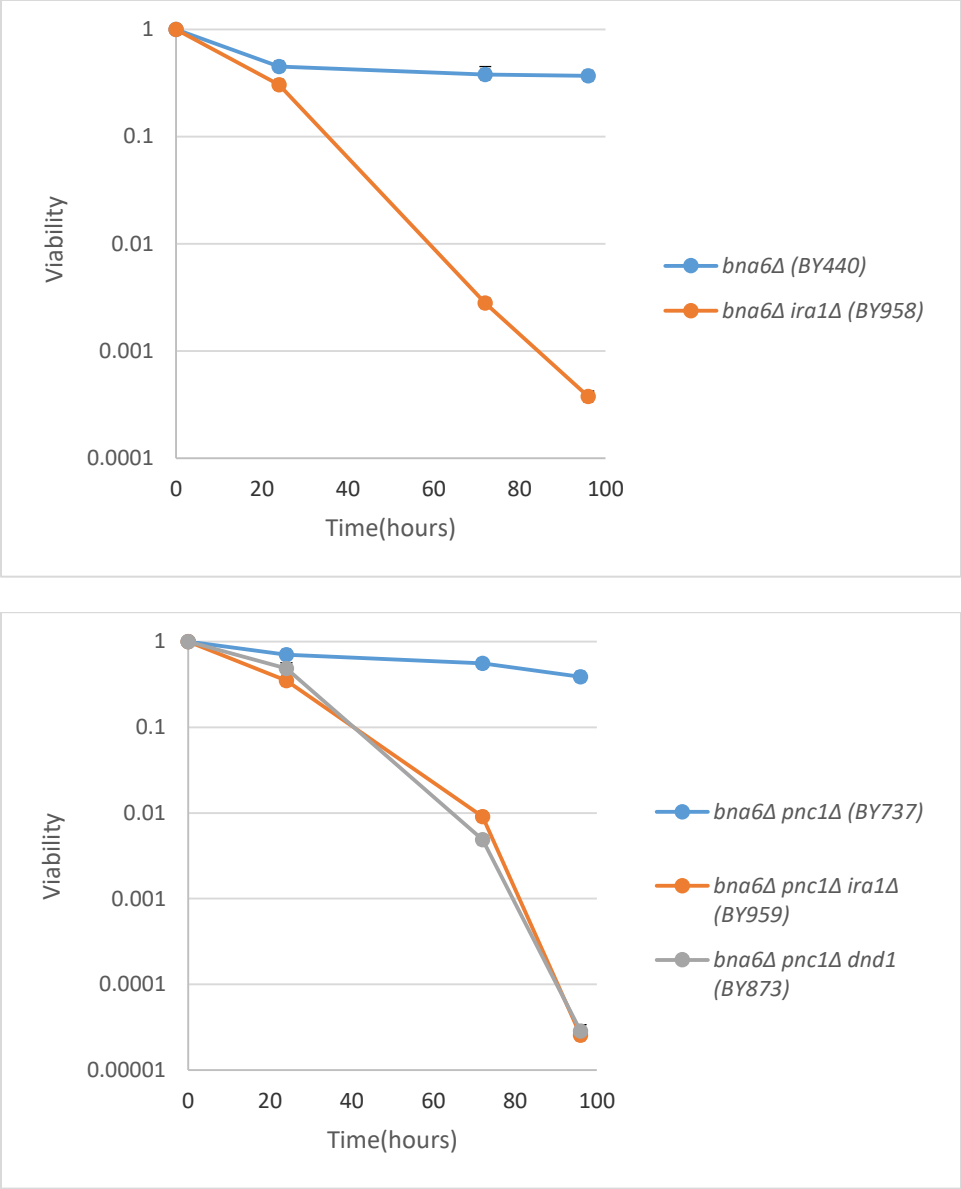

Figure 4E. Survival of *ira1*Δ mutants in liquid NA starvation assay.

*ira1*Δ strains were generated and were tested for survival in response to NAD^+ starvation. In both the *bna6*Δ *ira1*Δ, and *bna6*Δ *pnc1*Δ *ira1*Δ strains there is a robust survival defect relative to the control strains. The error bars represent the standard error for 3 biological replicate experiments, carried out on three separate days.

Figure 4F. Transformation of *ira1*Δ strains with pYES-nga.

Transformation of the *bna6*Δ, *ira1*Δ *bna6*Δ *ira1*Δ, and *bna6*Δ *pnc1*Δ *ira1*Δ strains causes a notable growth defect in both the *bna6*Δ *ira1*Δ**,** and *bna6*Δ *pnc1*Δ *ira1*Δ strains. The *bna6*Δ *ira1*Δ strain produces single isolated colonies where a lawn is expected and the *bna6*Δ *pnc1*Δ *ira1*Δ strain fails to produce any isolated colonies on the plate.

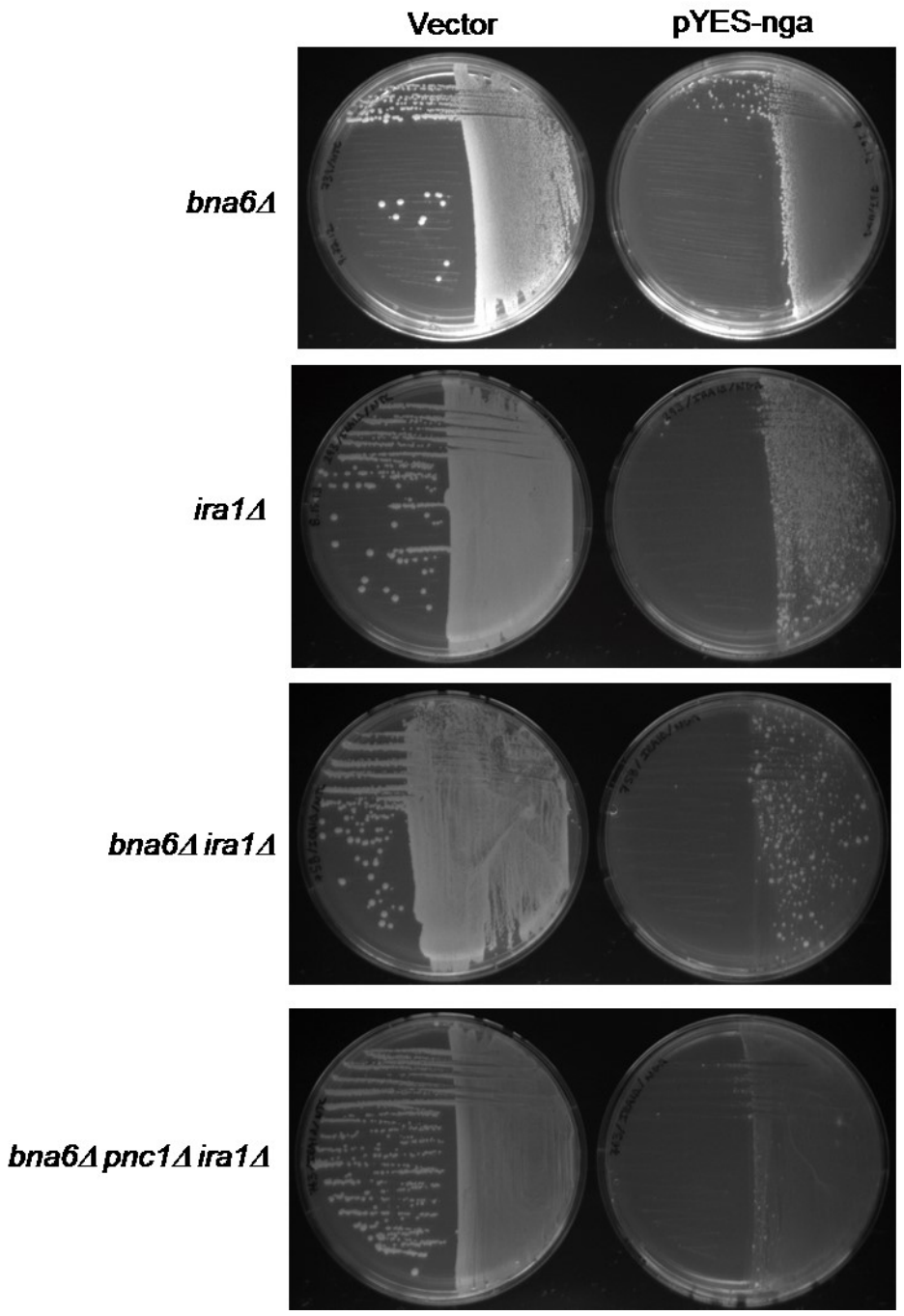
Vector
pYES-nga
bna6Δ
ira1Δ
bna6Δ ira1Δ
bna6Δ pnc1Δ ira1Δ

Figure 4G. Transformation of *pYES-nga* into *ira1*Δ diploid strain.

The *bna6*Δ *pnc1*Δ *ira1*Δ *bna6*Δ *pnc1*Δ *sea4*Δ *dnd1* diploid has a marked transformation defect relative to the WT/ *bna6*Δ *pnc1*Δ *sea4-1*Δ *dnd1* diploid which transforms successfully. This indicates the failure of bna6Δ *pnc1*Δ *sea4-1*Δ *dnd1* to complement the *ira1*Δ.

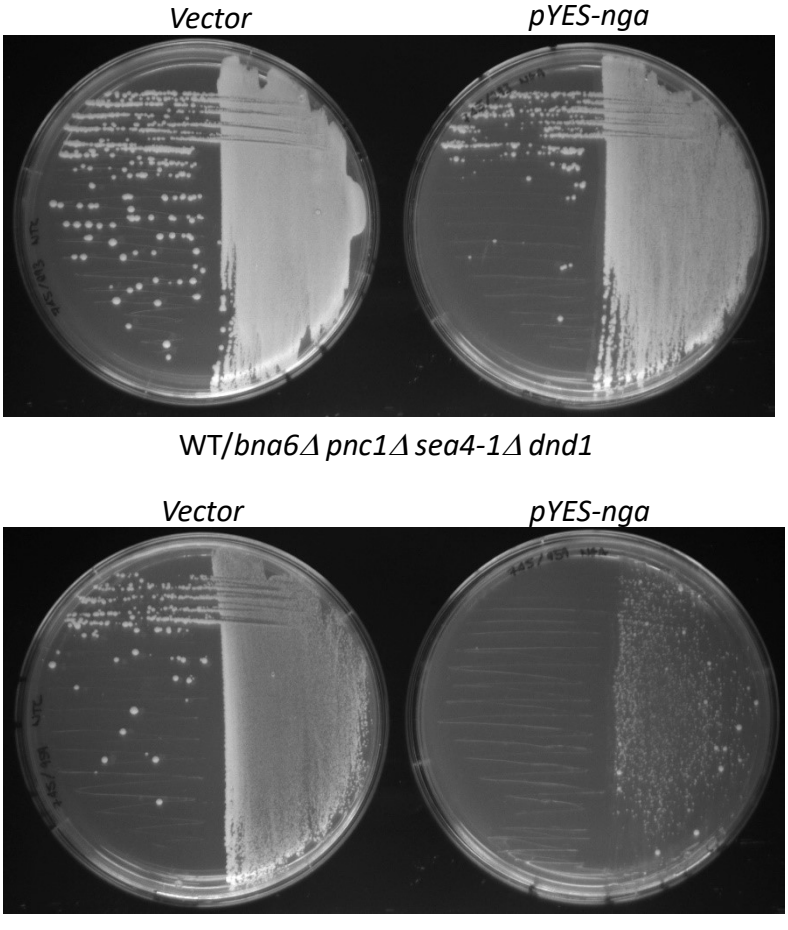

Figure S2. *ira2*Δ survival in response to NA limitation.

*ira2*Δ strains were generated and were tested for survival in response to NAD^+ starvation. In both the *bna6*Δ *ira2*Δ**,** and *bna6*Δ *pnc1*Δ *ira2*Δ strains there is a robust survival defect relative to the control strain. The error bars represent the standard error for 3 biological replicate experiments, carried out on three separate days.

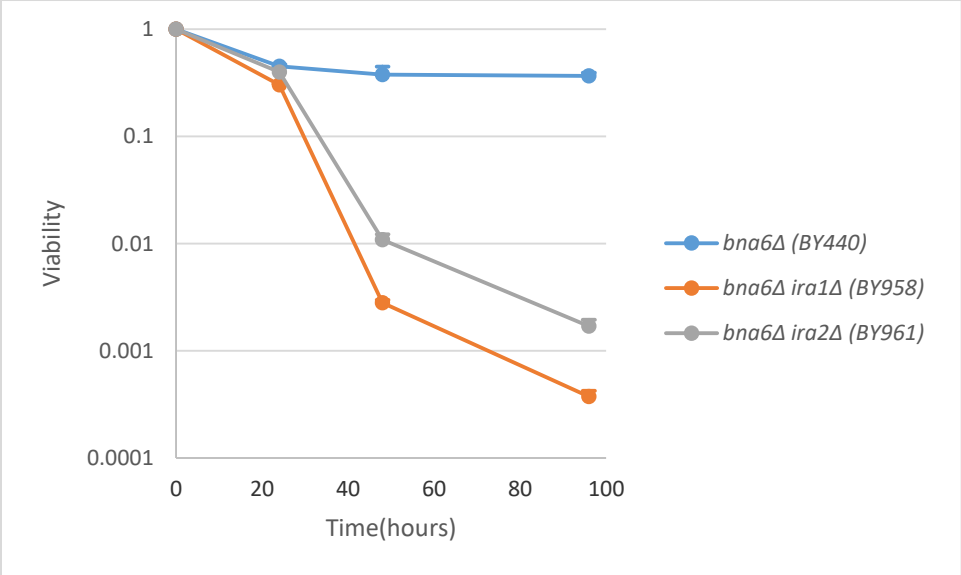

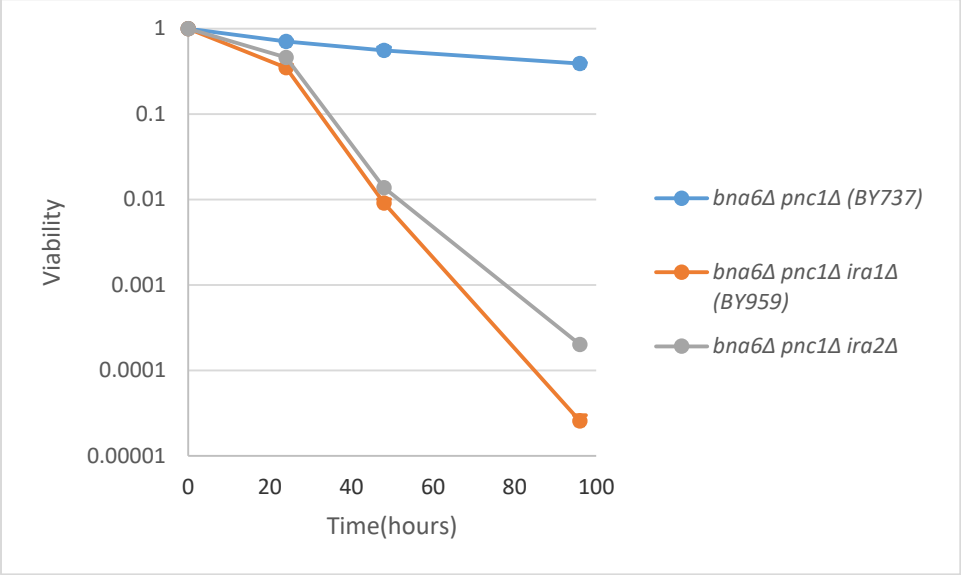

Figure S3. *C. glabrata ira1*Δ survival in response to NA limitation.

An *ira1*Δ strain was generated in *C. glabrata* and was tested for survival in response to NA limitation. As in *S. cerevisiae* the *C. glabrata ira1*Δ strain has a tremendous growth defect relative to the WT control strain.

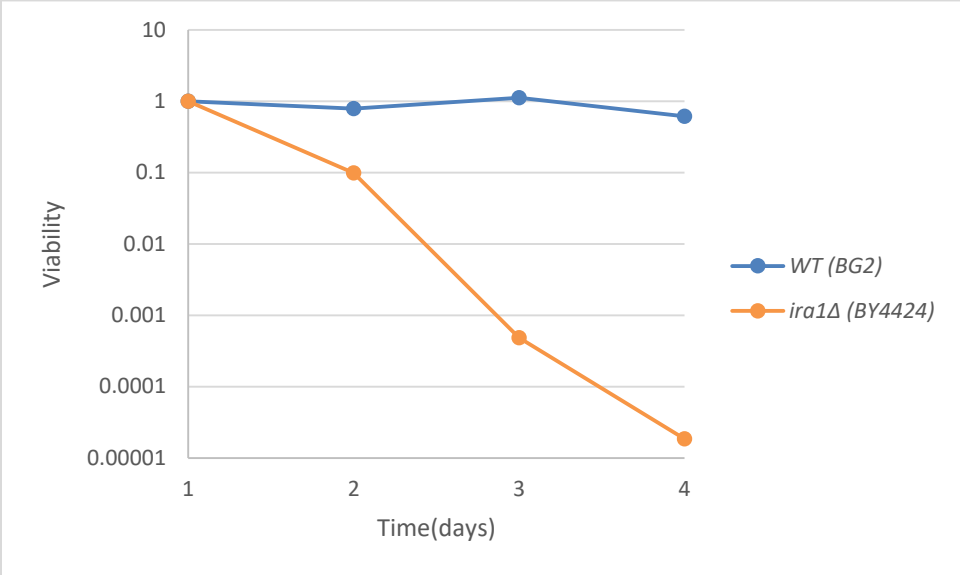

Interaction between SEA complex and *IRA1*

We have shown that in *S. cerevisiae* the loss of either SEACAT complex members or *IRA1* results in a failure to survive NAD^+ depletion. The SEACAT complex is a GAP regulating TOR activity and IRA1 is a GAP regulating PKA activity. Herman et al. have previously demonstrated broad cross-talk between the TOR and RAS pathways in *S.* cerevisiae which is essential for the coordination of cell growth in response to nutrient availability [19]. Furthermore, Herman et al. concluded that mutations in one of the two pathways results in compensatory elevation or dampening of levels of the other pathway in an effort to compensate to maintain proper cell growth. We wished to see how these pathways interact in controlling survival following NAD^+ depletion [19]. To do this we generated a set of SEA complex and *IRA1* double mutants in the *bna6*Δ *pnc1*Δ background in *S. cerevisiae* and tested these in NAD^+ starvation assays (Figure 5A). *ira1* mutants, which eliminate RAS GAP activity are hyperactive for RAS. The SEACAT sub complex (*SEA1, NPR2,* and *NPR3*) functions as the GAP for Gtr1 which positively regulates TOR activity. *sea1*Δ*, npr2*Δ or *npr3*Δ mutants are therefore hyperactive for TOR. SEACIT mutants act upstream of and repress SEACAT and thus *sea2*Δ*, sea3*Δ*,* and *sea4* mutants are predicted to be hypo active for TORC1. Interestingly, mutation of any member of the SEACAT sub complex (*SEA1, NPR2,* or *NPR3*) combined with an *ira1*Δ exacerbated the loss of viability phenotype seen in *ira1*Δ mutants. By contrast, a *sea4*Δ (SEACIT complex) in concert with *ira1*Δ partially rescued the loss of viability of the *ira1*Δ mutant. Together, these data suggest that survival of NAD^+ depletion requires both TOR and PKA pathways to be down regulated, and GAP mutants that regulate either GTR1 or RAS compromise the ability of the cell to survive NAD^+ depletion.

Figure 5A. Survival of *SEA* complex *IRA1* double mutants in liquid NA starvation assay.

The survival of *SEA* complex *IRA1* double mutants generated in the *bna6*Δ pnc1Δ background was assessed in our liquid NA starvation assay. In the *bna6*Δ pnc1Δ background the *ira1*Δ *sea1*Δ, *ira1*Δ *npr2*Δ, and *ira1*Δ *npr3*Δ exacerbate the failure to survive. In contrast, the *ira1*Δ *sea4*Δ strain blunts the survival defect seen in the *ira1*Δ strain illustrating differing phenotypes between the SEACIT and SEACAT sub complexes.

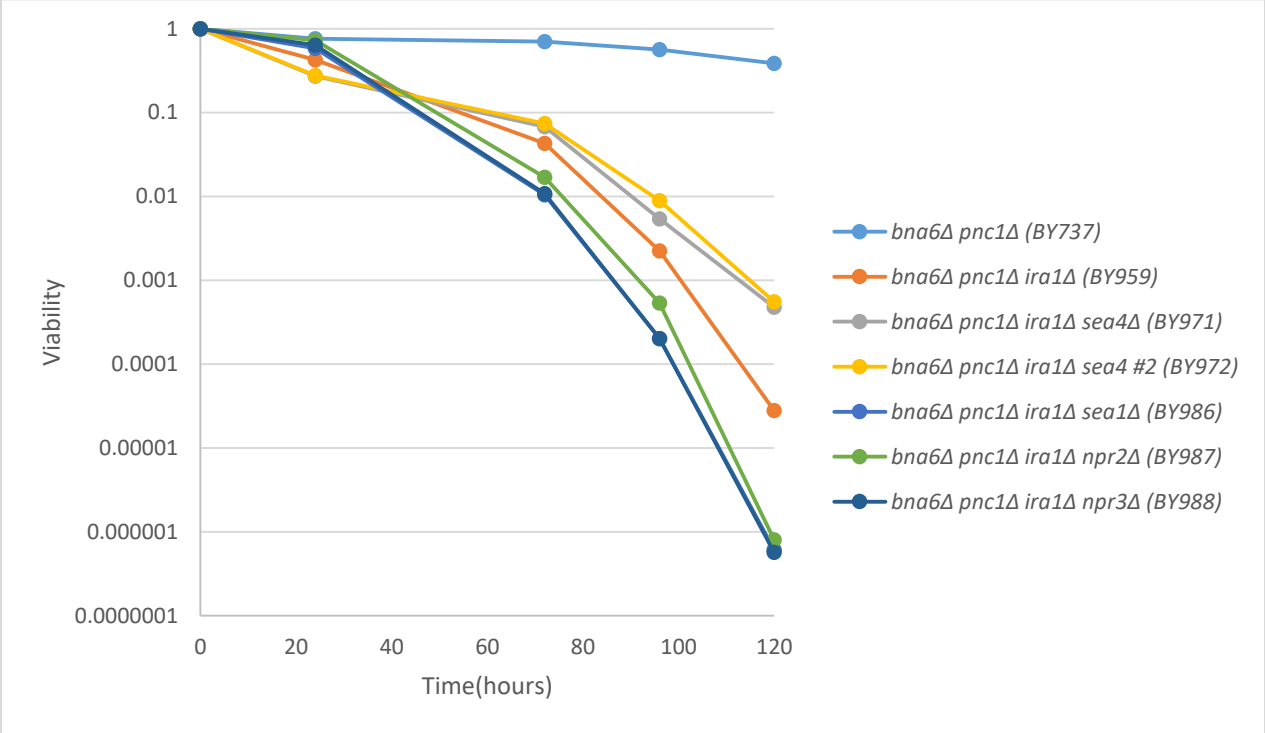

*sea1*Δ and *ira1*Δ strains inappropriately activate TOR signaling

We have shown that SEACAT mutants are compromised for survival of NAD^+ depletion. Next, we wished to demonstrate an effect on TOR signaling. To this end, we utilized ribosomal protein S6 (P-S6) as a proxy to monitor TOR activity. It has previously been described that S6 is phosphorylated specifically in response to TOR activation [20-22]. The availability of phospho-specific antibodies to P-S6 combined with its phosphorylation as a specific downstream event of TOR activation allow for a readout of TOR activity through western blot analysis. To monitor the activation of TOR we grew *S. cerevisiae bna6*Δ*, bna6*Δ *sea1*Δ*, bna6*Δ *npr2*Δ*,* and *bna6*Δ *ira1*Δ strains overnight to mid-log phase (OD_{600} of approximately 0.5) and collected the same number of all cells for the strains listed above. We then washed the cells with media that lacking NA to remove all NA in the media and inoculated fresh SDC-NA media to a low OD and allowed the cells to grow collecting cells at various time points. These cellular samples were then processed and run on poly-acrylamide gels and probed with anti-P-S6 antibody (Figure 5B). Remarkably, the *bna6*Δ *sea1*Δ*,* and *bna6*Δ *ira1*Δ strains which we tested showed consistent differences when compared to the *bna6*Δ control strain. The *bna6*Δ *npr2*Δ strain also behaved in the same manner as the *bna6*Δ *sea1*Δ strain as expected since both are components of the SEACIT sub complex (data not shown). The *bna6*Δ *sea1*Δ*,* and *bna6*Δ *npr2*Δ strains both have robust P-S6 signals for two hours after the *bna6*Δ control strain. This data suggests that the *bna6*Δ *sea1*Δ*,* and *bna6*Δ *npr2*Δ strains both have aberrant TOR signaling relative to wild-type. More specifically, it is clear that these two mutant strains fail to promptly shut of TOR signaling when starved for cellular

NAD^+. Even more dramatically, the *bna6*Δ *ira1*Δ strain completely fails to shut off TOR signaling as indicated by the persistent P-S6 signal even after 24 hours of growth

Figure 5B. TOR signaling in response to NAD^+ starvation in *S. cerevisiae* mutants.

Phosphorylation of ribosomal protein S6 is used as a measure of activation of TOR in the *sea1*Δ and *ira1*Δ mutants. Both mutants tested fail to stop signaling growth through TOR relative to the *bna6*Δ control strain. The *bna6*Δ *sea1*Δ strain maintains pS6 signal for an additional 2 hours compared to the *bna6*Δ control and the *bna6*Δ *ira1*Δ strain maintains a persistent signal through the entire experiment.

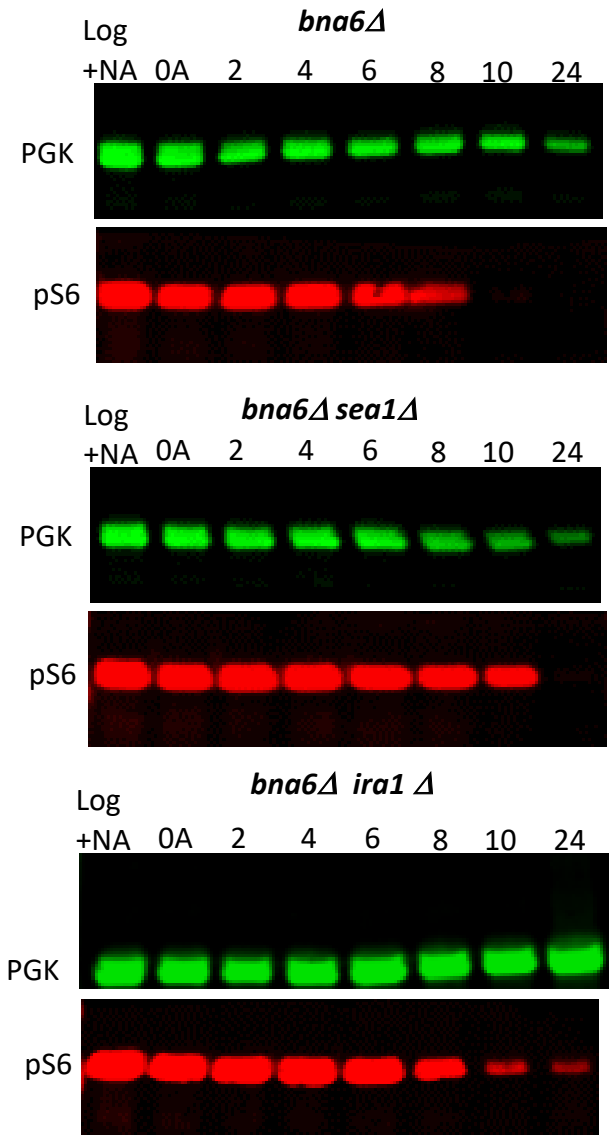

To demonstrate that this phenomena was widespread and not confined solely to *S. cerevisiae* we performed the same experiment on *C. glabrata* wild-type, *sea1*Δ and *ira1*Δ strains (Figure 5C). As we expected, the results in *C. glabrata* paralleled the *S. cerevisiae* results, albeit on a slightly faster scale. The *sea1*Δ strain maintained a P-S6 signal longer than the wild-type control strain, and the *ira1*Δ strain maintained a persistent signal through the entirety of the experiment save the 24 hour time point. In both organisms the aberrant signaling appears to be independent of cellular NAD^+ levels and OD_{600}, as cellular NAD^+ levels are very similar between the control strain and mutants (Figure 5C).

Figure 5C. TOR signaling in response to NAD^+ starvation in *C. glabrata* mutants.

Phosphorylation of ribosomal protein S6 can also be used as a measure of activation of TOR in the *sea1*Δ and *ira1*Δ *C. glabrata* mutants. As in *S. cerevisiae* both the *sea1*Δ and *ira1*Δ mutants failed to stop signaling through TOR relative to the *bna6*Δ control strain. Additionally, the aberrant signaling through TOR is independent of both OD600 and intracellular NAD^+ levels as both those values remain extremely similar from strain to strain.

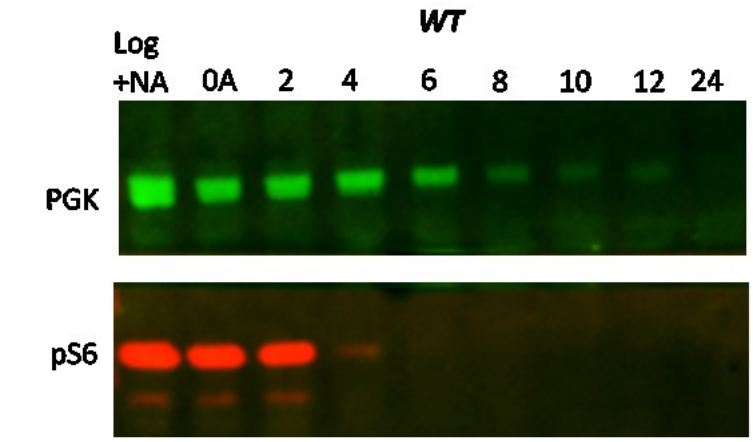
WT
Log
+NA 0A 2 4 6 8 10 12 24
PGK
pS6

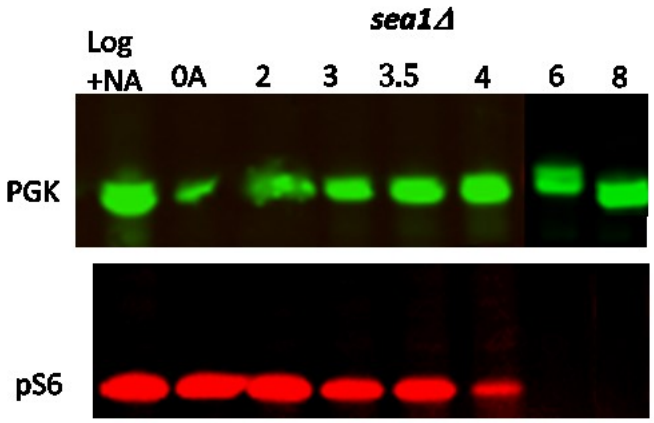
sea1Δ
Log
+NA 0A 2 3 3.5 4 6 8
PGK
pS6

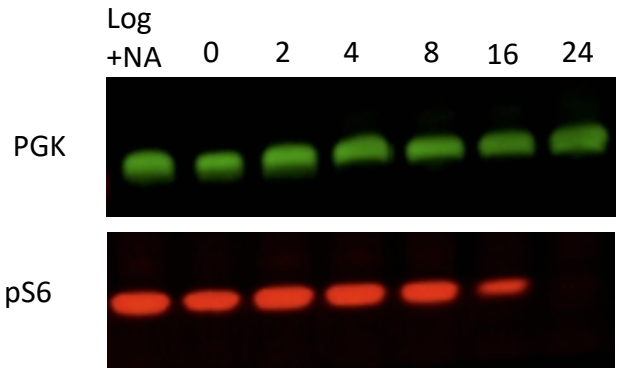
Log
+NA 0 2 4 8 16 24
PGK
pS6

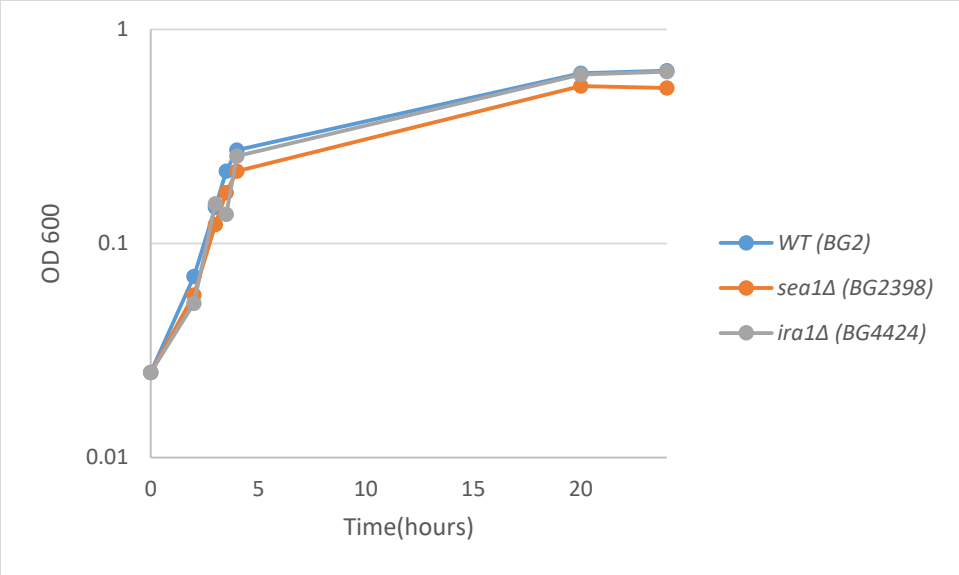

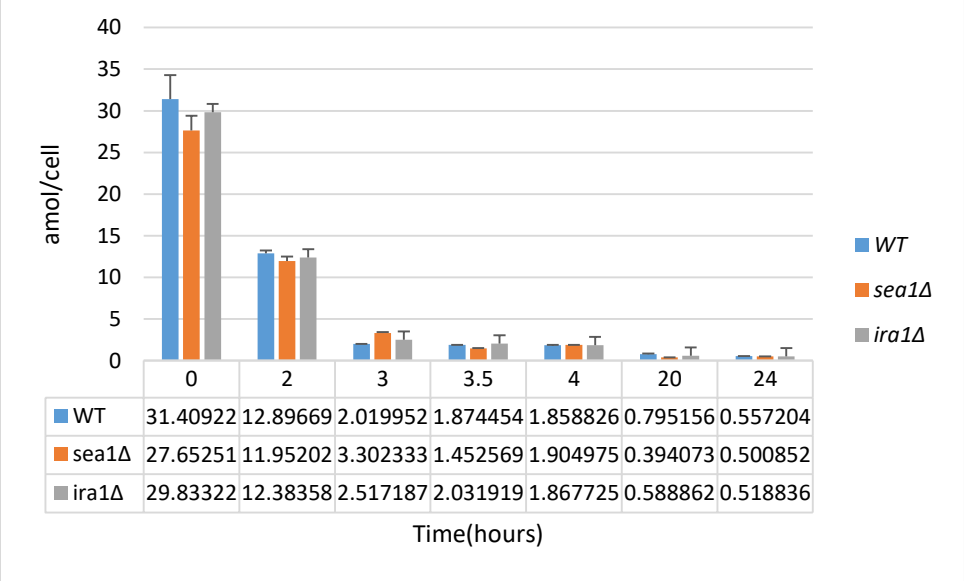

	0	2	3	3.5	4	20	24
WT	31.40922	12.89669	2.019952	1.874454	1.858826	0.795156	0.557204
sea1Δ	27.65251	11.95202	3.302333	1.452569	1.904975	0.394073	0.500852
ira1Δ	29.83322	12.38358	2.517187	2.031919	1.867725	0.588862	0.518836

Discussion

The pathogenic yeast *Candida glabrata* lacks the machinery needed to synthesize NAD^+ *de novo*. As such *C. glabrata* is a NAD^+ auxotroph, and can only grow when NAD^+ precursors can be salvaged from its environment [4-6]. When growth occurs in media lacking these NAD^+ precursors, *C. glabrata* senses this nutrient limitation and responds by entering a quiescent state. In this state *C. glabrata* is still viable for several days, but is simply inactive. Addition of NAD^+ precursors to the environment is followed by a short lag phase and then normal growth resumes. Notably, cellular levels of total NAD^+ fall during starvation to a fraction of homeostatic levels - as low as 10 □M. Yet, both *C. glabrata* and for *bna6*Δ mutants of *S. cerevisiae* are able to return to growth within minutes of NAD^+ precursors being added back to the media. We wished to know what genes play an important role in the cellular response to NAD^+ starvation.

We screened approximately 24,000 mutants from a *Tn-7* insertional mutant library and identified 91 mutant strains, corresponding to 47 genes that failed to survive NAD^+ starvation. We have not verified the phenotypes of all of these, but the fact that many were recovered multiple times in the screen increases confidence that the disrupted gene is responsible for the phenotype. We concentrated on analysis of two genes from the initial screen: *SEA1* and *NPR2.* These two genes were of particular interest to us because Dokudovskaya et al. showed that Sea1 and Npr2 function together as components of a newly identified protein complex known as the SEA complex [8, 11]. Furthermore, Panchaud et al. illustrated that Sea1, Npr2, and Npr3 function together in a sub complex of the SEA complex known as SEACIT [9, 10]. The SEACIT sub complex functions as a GTPase-activating protein (GAP) for the GTPase GTR1. GTP bound

GTR1 activates TORC1 signaling providing a pro-growth signal [9, 10]. Under conditions where nutrients in the environment are limited the SEACIT sub complex stimulates the GTPase activity of GTR1. This shifts GTR1 from the active GTP bound form to the GDP bound, form which does not activate TORC1 signaling leading, to cellular growth arrest.

Our data suggest that in addition to its described role in response to amino acid deprivation and nitrogen starvation, the SEA complex could play a role in response to NAD^+ depletion. Indeed *sea1*Δ and *npr2*Δ *C. glabrata* mutants showed a 100-fold reduction in viability after prolonged starvation for NAD^+ relative to wild type control. To determine if the roles of *SEA1* and *NPR2* in response to NAD^+ starvation were conserved beyond *C. glabrata* the *sea1*Δ and *npr2*Δ mutants were also generated in the closely related yeast *Saccharomyces cerevisiae.* Here mutants in combination with *bna6*Δ*,* which disrupts *de novo* NAD^+ biosynthesis were tested for viability, and *sea1*Δ and *npr2*Δ yield a milder but reproducible death phenotype in response to NAD^+ starvation, indicating the importance of these genes in response to NAD^+ starvation across species.

While testing the other components of the SEA complex for viability in response to NAD^+ starvation in *S. cerevisiae,* 6 strains independently acquired the same background mutation which resulted in an astonishing 10,000 fold death phenotype relative to control strain. Because the magnitude of this phenotype was so impressive we sought to identify the mutation causing the phenotype. Whole-genome sequencing combined with tetrad analysis confirmed that the background mutation was an insertion in the coding region of *IRA1*. Interestingly, *IRA1* functions to downregulate PKA in the

cell functioning as a GAP which negatively regulates RAS by converting it from the GTP to the GDP bound inactive form [15, 16].

Our data suggests that under conditions where cells are starved for NAD^+ in a wild type cell the SEA complex and *IRA/IRA2* sense the starvation, and convert GTR1-GTP and RAS-GTP to the corresponding GDP states and downregulating TOR and PKA pathways. In *sea1*Δ*, npr2*Δ*,* and *npr3*Δ mutants the SEACIT inhibitory complex is compromised. As a result the GTP binding protein GTR1 is locked in its active GTP bound state, generating a persistent pro-growth signal through the TOR pathway. Likewise, in the *ira1*Δ mutant RAS is locked in its active GTP bound state providing a pro-growth signal to the PKA pathway. In ways we do not yet understand, growth signaling through these pathways under conditions in which cellular NAD^+ levels are low, results in a crisis leading to inviability.

Herman et al. have previously carefully documented crosstalk between the TOR and PKA pathways, demonstrating a coordination of these two major growth pathways to appropriately integrate cellular nutrient availability and properly regulate growth. They conclude that the PKA and TORC1 pathways function in parallel to promote proper cellular growth [19]. Our data is consistent with this view as it pertains to changes in NAD^+ cellular levels. Under conditions of NAD^+ depletion, both pathways need to be downregulated for the cell to respond optimally to NAD^+ depletion.

We identified the same mutation in *ira1* in 6 different isolates. These were all obtained in the process of deleting the *SEA4* gene in different *bna6*Δ backgrounds. The deletions were made with no difficulty at all, but of 35 independent *sea4* deletions, 6

acquired the *ira1* mutation. We interpret this to mean a strong selection for suppression of some phenotype during the transformation. Notably, we obtained this *ira1* mutant only while disrupting *SEA4*, and not in more than 200 disruptions of *SEA1*or *NPR2* (data not shown). *sea4* mutants are hypoactive for TOR activity, and we suggest that this places a strong pressure for compensatory activation of the PKA pathway by mutation of *IRA1*. This explanation fits well within the current understanding of TOR-PKA pathway antagonism. Herman et al. have shown conclusively that the two pathways can act antagonistically to each other in the sense that TORC1 activity increased in response to lower levels of PKA signaling and decreased TORC1 activity was associated with increased levels of PKA activity suggesting a model in which activity of the two pathways in parallel promotes growth and that decreased signaling in one can be compensated by increased activity in the other [19].

Interestingly, Dokudovskaya et al. who discovered the SEA complex found a survival defect for nitrogen starvation in specific mutant combinations. Specifically, they showed that *sea2*Δ *sea4*Δ, *sea3*Δ *sea4*Δ, and *sea2*Δ *sea3*Δ mutants, but not the single mutants exhibited significantly reduced survival after 7 days of nitrogen starvation [8]. By contrast, Tu and Wu who demonstrated a role of the SEA complex in signaling autophagy under conditions of non-nitrogen starvation (NNS) found no nitrogen starvation defect for any of the Sea complex mutants [23]. We checked our mutants for nitrogen starvation defects and found none for any of *sea1, sea2 sea3, sea4, npr2* or *npr3*. So what explains the discrepancy in our results and those of Tu and Wu with those of Dokudovskaya? *ira1* mutants are well known to have a nitrogen starvation defect. We found that our *ira1* mutants, either with the point mutation or the whole deletion were

highly sensitive to Nitrogen starvation using the plate starvation assay also used by Dokudovshaya et al. We suggest that in the process of creating the combinatorial mutants deleted for multiple genes of the SEA complex, the authors picked up an *ira1* mutant in the background and that this is what is responsible for the nitrogen starvation phenotype documented in the Dokudovskaya study.

In recent systematic studies of yeast evolution over thousands of generations, *IRA1* mutants are among the most common mutations that give a fitness advantage [24, 25]. Botstein et al. investigated sequence evolution in 40 replicate *S. cerevisiae* populations growing in rich medium for 1,000 generations. Of the 24 genes that acquire mutations more often than expected by chance, and are inferred to give a fitness advantage, the top gene mutated through their analysis was *IRA1* [24]. In a recent study from Sherlock and Petrov, they also identified *ira1* mutations as giving a fitness benefit in long term culture under glucose limitation [25].

It is remarkable that we identified the same "T" insertion mutation in each of our strains rather than independent mutants in *ira1*. In both systematic studies, many inactivating mutations of *IRA1* were found. By contrast, all of our *ira1* mutants had the same insertion of a "T" nucleotide at the end of a string of 7 T's suggesting that in the *sea4*Δ background, this error occurred with elevated frequency.

In addition to identifying *SEA1* and *NPR2* through our *in vitro* screen we identified 45 additional mutants which failed to survive in response to NAD^+ starvation. Several of the additional mutants correspond to pathways that touch on TORC1 and PKA signaling. *GCN2* is the key protein kinase in the TORC1 pathway responsible for

phosphorylating translation initiation factor eIF2 in response to amino acid starvation. *GPB1/GPB2* encode additional regulators of the cAMP-PKA signaling pathway, *RTG2* which is a transcriptional activator downstream in TORC1 pathway. Additionally, many of the mutants are global regulators of transcription and chromatin, and analysis of these may shed light on the transcriptional response of cells to NAD^+ depletion.

Materials and methods

Strains

The strains used in this study can be found in supplemental table 3

Intracellular NAD^+ concentrations. The acid extraction for NAD^+ was modified from the method described by Lin et al. [26]. Briefly, 1 ml of ice-cold 0.05 N NaOH-1 mM EDTA was added to 1×10^8 to 2×10^8 frozen *C. glabrata* cells. For acid extraction, 300 µl of 0.125 N HCl was added to 300 µl of the above alkali extract. The remaining alkali extract and the acid extract were frozen, and cells were broken up with a bead beater. Following incubation at 60°C for 30 min, 100 µl of 0.4 M Tris base was added to 400 µl of acid extract and 100 µl of 100 mM Tris-HCl (pH 8.1)-0.1 N HCl was added to 200 µl of alkali extract for neutralization. The mixtures were centrifuged, and the supernatants were stored at −80°C prior to use.

The enzyme cycling method for measuring intracellular NAD^+/NADH was adapted from Shah et al.[27]. The reaction mixture containing 0.17 M bicine (pH 7.8), 0.85 M ethanol, 7.1 mM EDTA, 1.4 mg/ml bovine serum albumin, 0.71 mM 3-(4,5-dimethyl-2-thiazolyl)-2,5-diphenyl-2H-tetrazolium bromide, and 2.8 mM phenazine ethosulfate was made fresh each time. A 100-µl volume of this reaction mixture was added to 50-µl samples or 0 to 80 pmol standard NAD^+ or NADH in a 96-well plate. The reaction was started by the addition of 20 µl of 1 U of alcohol dehydrogenase (0.168 mg/ml in 0.1 M bicine, pH 7.8). The color was developed in the dark at 30°C, and the absorbance was measured at 570 nm every 5 minutes for a total of 30 min after the addition of the enzyme.

Plate based assay for *Tn7*-insertional mutant library screen

The mutant library was made by Castano et al.[7]. For the plate-based assay, *C. glabrata* mutant strains were grown overnight in SDC medium in 96-well plates and spotted onto SCD plates the next day. After 24 hours of incubation, cells on SDC plates were replica plated onto SDC-NA plates and incubated overnight followed by another replica plating onto the second SDC-NA plates. The second SDC-NA plates were incubated at 30°C for seven days then replica plated onto SDC plates with 5 μM niacin (recovery plates). The recovery plates were incubated at 30°C and colony morphology was recorded after 24 and 48 hours of incubation.

We used several parameters to score the phenotypes: first, whether the density of growth of a mutant strain on the recovery plate was greater or less than 50% of that of the wild type; second, whether the size of the colonies of a mutant strain was similar to or smaller than that of the wild type. The mutant strains were then classified into 4 categories: (1) >50% in growth density, normal size colony, (2) >50% in growth density, small size colony, (3) <50% in growth density, normal size colony, (4) <50% in growth density, small size colony. For mutants which fell into categories 2, 3, or 4 the plate assay was repeated to ensure the phenotype could be replicated. Finally, we eliminated mutants that had defects after nitrogen-or carbon-starvation, and that had growth phenotypes on YPD plates.

Liquid assay for *Tn7*-insertional mutant library screen

For NAD^+ starvation in liquid media, cells were grown in 5ml SDC overnight. The next day, the cells were inoculated into 5 ml SDC-NA to an initial OD_{600} of 0.1. After an

overnight growth at 30°C, the cells were diluted 1:5 into 5 ml SDC-NA (Day 0). The cells were then incubated at 30°C and appropriate dilutions were plated on YPD on Days 0, 2, 4 and 7. Colonies were counted after 40 hours of growth at 30°C. The ratio of viable cell count on Day 7 to that on Day 0 corresponded to the survival rate of an individual mutant after 7 days of NAD+ starvation. We then calculated the "killing index" by taking the ratio of the survival rates between the wild type and a mutant. A mutant with a reduced survival rate would have a "killing index" of greater than 1. Only mutants that had a killing index of 5 or greater in the liquid assay were selected for further analyses.

Nutrient limitation of the selected mutants in liquid media

C. glabrata strains were grown in 5 ml SDC medium overnight. The next day, cells were washed once with PBS then inoculated into media lacking different nutrients (thiamine, pyridoxine, nitrogen, carbon or phosphate) to an initial OD_{600} of 0.1 and incubated at 30°C. Appropriate dilutions were plated on YPD plates at various time points as indicated in the main text. The YPD plates were incubated at 30°C and colonies were counted after 40 h of growth at 30°C.

Mating, sporulation, and dissection of *S. cerevisiae* yeast strains

S. cerevisiae diploid construction, sporulation, and dissection was performed as described in Current protocols in molecular biology Volume 2 sections 13.2.3-13.2.8.

Nitrogen Starvation plate assay to screen *ira* and *sea* double mutants

The nitrogen starvation plates were made by combining 1.7 grams of Difco Yeast Nitrogen Base minus amino acids and ammonium sulfate with 20 grams of BD Bacto-

agar and 950 mL of water. After autoclaving dextrose is added to a final concentration of 2% and the plates are poured and allowed so solidify overnight.

To perform the assay the strains of interest were spotted onto YPD plates and incubated overnight at 30 degrees Celsius. After overnight growth a sterile velvet is used to transfer the yeast from YPD to a nitrogen starvation plates described above. This initial plate is allowed to grow overnight at 30 degrees Celsius. After overnight growth a sterile velvet is used once again to transfer yeast from the nitrogen starvation plate to a fresh nitrogen starvation plate. This plate is incubated at 30 degrees Celsius and allowed to grow for 9 days. After 9 days a sterile velvet is used to transfer the yeast from the nitrogen starvation plate back to YPD, and the YPD plate is incubated at 30 degrees Celsius overnight. Phenotypes of the spots are then analyzed and photographed. If additional time points are desired the process above can be altered to include more plates so that for each time point a fresh nitrogen starvation plate can be used.

Gene deletion in *Candida glabrata*

Gene deletion in *C. glabrata* was done via a split-marker transformation. The ORF of the gene was replaced with a nourseothricin (NAT) cassette. The sequence information for generating gene deletion constructs came from the Candida Genome Database website (http://www.candidagenome.org) combined with the Cormack laboratory *C. glabrata* genome sequence. For deletion with NAT cassette, we utilized a split marker replacement method. Briefly, approximately 500 bp of both the 5' and 3' untranslated regions (UTR) of each gene to be deleted were amplified. The anti-sense primer for the 5’ UTR amplification and the sense primer for the 3’ UTR amplification contained 20 additional

nucleotides found specifically in our NAT deletion cassette. The NAT cassette was then amplified as two distinct portions. The 5' portion of the NAT cassette is amplified with a 20 nt primer that is the reverse complement of the tailed anti-sense primer used to amplify the 5' UTR. The 3' portion of the Nat cassette is amplified with a 20 nt primer that is the reverse complement of the tailed sense primer used to amplify the 3' UTR. For a total of 4 PCR amplified fragments. All 4 of those reactions were cleaned up with the QIAquick PCR Purification Kit.

The 5' UTR fragment and the 5' portion of the NAT cassette are fused together in a Splicing by Overlap Extension (SOEing) PCR reaction. The 3' UTR fragment and 3' portion of the NAT cassette are fused together in the same manner. The two fused fragments were purified with the Qiaquick PCR Purification Kit, and then transformed into *C. glabrata* via the lithium acetate method and selected on YPD plates supplemented with 200 µg/ml NAT. Homologous recombination and allele replacement of each locus was verified by PCR analysis using a primer that anneals in the sequences external to the cloned fragments and a primer annealing within the NAT cassette. We also verified the absence of a gene by inability to PCR amplify an internal fragment from each deleted gene.

Gene deletion in *S. cerevisiae*

S. cerevisiae gene deletion was achieved via PCR-mediated one-step gene disruption as described in Current protocols in molecular biology Volume 2 sections 13.10.5-13.10.7. The ORF of the gene was either replaced with a nourseothricin (NAT) cassette, a hygromycin (HYG) resistance cassette. The NAT cassette was amplified with using the

template plasmid PCR2.1 NAT. They HYG cassette was amplified using the template plasmid pAP599. The protocol was adapted only slightly by using 50 nucleotides of homology to the target gene for all primers used instead of 30-40 nucleotides described in the reference. Transformation was performed via the lithium acetate method and plated first onto YPD. After overnight growth on YPD at 30 degrees Celsius, the lawn of yeast was replica-plated using a sterile velvet to a YPD plate supplemented with either 200 µg/ml NAT or 500 µg/ml hygromycin.

Sample preparation and Western Blotting for P-S6

2 OD units of cells were collected on nitrocellulose filters at each time point of interest, and the filters were flash frozen in liquid nitrogen and stored at -80 degrees Celsius until processing. Cells were recovered from the filters through washing with ice-cold PBS and pelleting the re-suspended solution by a 30 second spin at 13,200 RPM in a centrifuge pre-chilled to 4 degrees Celsius. For processing 200 µL of SDS loading buffer was added to 2 OD units of cells in a microfuge tube. Approximately 100 µL of acid washed class beads were then added and the mixture was placed in a bead beater homogenizer which was set on high for 45 seconds. Each mixture went through a total of 4 cycles on the bead beater. The mixture was then centrifuged at 4 degrees Celsius for 5 minutes at 13,200 RPM and the supernatant was transferred to a new microfuge tube which was then boiled for 5 minutes. 10 µL of the final mixture was then loaded on a NuPAGE Novex 4-12% Bis-Tris Gel. Western blots were performed as described on the ThermoFisher website for One-Dimensional SDS Gel Electrophoreiss of Proteins with NuPAGE Novex Pre-Cast Gels https://www.thermofisher.com/us/en/home/references/protocols/proteins-

expression-isolation-and-analysis/sds-page-protocol/one-dimensional-sds-gel-electrophoresis-of-proteins-pre-cast-gels-.html#intro.

Analysis of the Western Blots was performed according to the Odyssey Classic Application Protocols which can be found at http://biosupport.licor.com. P-S6 was detected by using Cell Signaling Technology Phospho-S6 Ribosomal Protein (Ser235/236) (91B2) Rabbit mAb (product number 4857) at a 1:5000 dilution. The secondary antibody used was ThermoFisher Donkey anti-Rabbit IgG (H+L), Alexa Flour 680 conjugate (product number A10043) at a 1:15,000 dilution. Phosphoglycerate Kinase was used as a control and was detected using ThermoFisher Phosphoglycerate Kinase Antibody (catalog number 22C5D8) at a 1:10,000 dilution. The secondary antibody used was Rockland-Inc. Mouse IgG (H&L) Antibody DyLight 800 Conjugated Pre-Adsorbed (catalog number 610-132-121) at a 1:15,000 dilution. The western blots were detected on the Li-cor Odyssey imaging system.

Supplemental Table 3. Strains used in this study.

C. glabrata

strain number	relevant genotype
BG2781	*Wild type BG2*
BG2398	*ura3Δ::G418, iml1Δ*
BG2410	*ura3Δ::G418, iml1Δ/pGRB2.2 (URA3)*
BG2412	*ura3Δ::G418, iml1Δ/pSP181 (IML1 URA3)*
BG2409	*ura3Δ::G418, iml1Δ, tna1Δ, tnr1Δ, tnr2Δ/pGRB2.2 (URA3)*
BG2411	*ura3Δ::G418, iml1Δ, tna1Δ, tnr1Δ, tnr2Δ/pSP181 (IML1 URA3)*
BG2399	*ura3Δ::G418, npr2Δ*
BG2400	*ura3Δ::G418, npr2Δ isolate 2*
BG2461	*ura3Δ::G418, npr2Δ /pGRB2.2 (URA3)*
BG2462	*ura3Δ::G418, npr2Δ /pSP183 (NPR2 URA3)*

S. cerevisiae

strain number	relevant genotype
BY292	*BY4741 (MATa his3Δ1 leu2Δ0 met15Δ0 ura3Δ0)*
BY293	*BY4742 (MATα his3Δ 1 leu2Δ 0 lys2Δ 0 ura3Δ 0)*
BY758	*BY4742 bna6Δ*
BY808	*BY4742 bna6Δ sea1Δ::NAT*
BY809	*BY4742 bna6Δ sea2Δ::NAT*
BY810	*BY4742 bna6Δ sea3Δ::NAT*
BY811	*BY4742 bna6Δ sea4Δ::NAT*
BY812	*BY4742 bna6Δ npr2Δ::NAT*
BY813	*BY4742 bna6Δ npr3Δ::NAT*
BY440	*BY4741 bna6Δ::G418*
BY737	*BY 4741bna6Δ::NAT pnc1Δ::G418*
BY745	*BY4741 bna6Δ::NAT pnc1Δ::HYG sea4-1Δ::G418 dnd1*
BY958	*BY4742 bna6Δ ira1Δ::NAT*
BY959	*BY4742bna6Δ pnc1Δ ira1Δ::NAT*
BY838	*BY4741 bna6Δ::NAT sea4-1Δ::G418 dnd1*
BY839	*BY4741 bna6Δ::NAT sea4-1Δ::G418 dnd1 isolate 2*
BY873	*BY4741 bna6Δ::NAT pnc1Δ::HYG dnd1*
BY991	*BY4741 bna6Δ::G418/pYes2NTC isolate #1*
BY998	*BY4741 bna6Δ::G418/pYes-nga isolate #1*
BY787	*BY4742 bna6Δ pnc1Δ sea4Δ::HYG*
BY969	*BY4742 bna6Δ ira1Δ::NAT sea4Δ::HYG*
BY980	*BY4742 bna6Δ ira1Δ::NAT sea1Δ::HYG*

BY981	*BY4742 bna6Δ ira1Δ::NAT npr2Δ::HYG*
BY982	*BY4742 bna6Δ ira1Δ::NAT npr3Δ::HYG*
BY971	*BY4742 bna6Δ pnc1Δ ira1Δ::NAT sea4Δ::HYG*
BY972	*BY4742 bna6Δ pnc1Δ ira1Δ::NAT sea4::HYG isolate 2*
BY986	*BY4742 bna6Δ pnc1Δ ira1Δ::NAT sea1Δ::HYG*
BY987	*BY4742bna6Δ pnc1Δ ira1Δ::NAT npr2Δ::HYG*
BY988	*BY4742bna6Δ pnc1Δ ira1Δ::NAT npr3Δ::HYG*

References

1. Panozzo, C., et al., *Aerobic and anaerobic NAD+ metabolism in Saccharomyces cerevisiae.* FEBS Lett, 2002. **517**(1-3): p. 97-102.
2. Preiss, J. and P. Handler, *Biosynthesis of diphosphopyridine nucleotide. II. Enzymatic aspects.* J Biol Chem, 1958. **233**(2): p. 493-500.
3. Preiss, J. and P. Handler, *Biosynthesis of diphosphopyridine nucleotide. I. Identification of intermediates.* J Biol Chem, 1958. **233**(2): p. 488-92.
4. Domergue, R., et al., *Nicotinic acid limitation regulates silencing of Candida adhesins during UTI.* Science, 2005. **308**(5723): p. 866-70.
5. Ma, B., et al., *High-affinity transporters for NAD+ precursors in Candida glabrata are regulated by Hst1 and induced in response to niacin limitation.* Mol Cell Biol, 2009. **29**(15): p. 4067-79.
6. Ma, B., et al., *Assimilation of NAD(+) precursors in Candida glabrata.* Mol Microbiol, 2007. **66**(1): p. 14-25.
7. Castano, I., et al., *Tn7-based genome-wide random insertional mutagenesis of Candida glabrata.* Genome Res, 2003. **13**(5): p. 905-15.
8. Dokudovskaya, S., et al., *A conserved coatomer-related complex containing Sec13 and Seh1 dynamically associates with the vacuole in Saccharomyces cerevisiae.* Mol Cell Proteomics, 2011. **10**(6): p. M110 006478.
9. Panchaud, N., M.P. Peli-Gulli, and C. De Virgilio, *SEACing the GAP that nEGOCiates TORC1 activation: evolutionary conservation of Rag GTPase regulation.* Cell Cycle, 2013. **12**(18): p. 2948-52.

10. Panchaud, N., M.P. Peli-Gulli, and C. De Virgilio, *Amino acid deprivation inhibits TORC1 through a GTPase-activating protein complex for the Rag family GTPase Gtr1.* Sci Signal, 2013. **6**(277): p. ra42.

11. Dokudovskaya, S. and M.P. Rout, *A novel coatomer-related SEA complex dynamically associates with the vacuole in yeast and is implicated in the response to nitrogen starvation.* Autophagy, 2011. **7**(11): p. 1392-3.

12. Everse, K.E., J. Everse, and L.S. Simeral, *Bacillus subtilis NADase and its specific protein inhibitor.* Methods Enzymol, 1980. **66**: p. 137-44.

13. Michos, A., et al., *Enhancement of streptolysin O activity and intrinsic cytotoxic effects of the group A streptococcal toxin, NAD-glycohydrolase.* J Biol Chem, 2006. **281**(12): p. 8216-23.

14. Colombo, S., et al., *Involvement of distinct G-proteins, Gpa2 and Ras, in glucose- and intracellular acidification-induced cAMP signalling in the yeast Saccharomyces cerevisiae.* EMBO J, 1998. **17**(12): p. 3326-41.

15. Tanaka, K., K. Matsumoto, and E.A. Toh, *IRA1, an inhibitory regulator of the RAS-cyclic AMP pathway in Saccharomyces cerevisiae.* Mol Cell Biol, 1989. **9**(2): p. 757-68.

16. Tanaka, K., et al., *S. cerevisiae genes IRA1 and IRA2 encode proteins that may be functionally equivalent to mammalian ras GTPase activating protein.* Cell, 1990. **60**(5): p. 803-7.

17. Tanaka, K., et al., *IRA2, an upstream negative regulator of RAS in yeast, is a RAS GTPase-activating protein.* Proc Natl Acad Sci U S A, 1991. **88**(2): p. 468-72.

18. Tanaka, K., et al., *IRA2, a second gene of Saccharomyces cerevisiae that encodes a protein with a domain homologous to mammalian ras GTPase-activating protein.* Mol Cell Biol, 1990. **10**(8): p. 4303-13.

19. Ramachandran, V. and P.K. Herman, *Antagonistic interactions between the cAMP-dependent protein kinase and Tor signaling pathways modulate cell growth in Saccharomyces cerevisiae.* Genetics, 2011. **187**(2): p. 441-54.

20. Ruvinsky, I. and O. Meyuhas, *Ribosomal protein S6 phosphorylation: from protein synthesis to cell size.* Trends Biochem Sci, 2006. **31**(6): p. 342-8.

21. Ruvinsky, I., et al., *Ribosomal protein S6 phosphorylation is a determinant of cell size and glucose homeostasis.* Genes Dev, 2005. **19**(18): p. 2199-211.

22. Urban, J., et al., *Sch9 is a major target of TORC1 in Saccharomyces cerevisiae.* Mol Cell, 2007. **26**(5): p. 663-74.

23. Wu, X. and B.P. Tu, *Selective regulation of autophagy by the Iml1-Npr2-Npr3 complex in the absence of nitrogen starvation.* Mol Biol Cell, 2011. **22**(21): p. 4124-33.

24. Lang, G.I., et al., *Pervasive genetic hitchhiking and clonal interference in forty evolving yeast populations.* Nature, 2013. **500**(7464): p. 571-4.

25. Venkataram, S., et al., *Development of a Comprehensive Genotype-to-Fitness Map of Adaptation-Driving Mutations in Yeast.* Cell, 2016. **166**(6): p. 1585-1596 e22.

26. Lin, S.S., J.K. Manchester, and J.I. Gordon, *Enhanced gluconeogenesis and increased energy storage as hallmarks of aging in Saccharomyces cerevisiae.* J Biol Chem, 2001. **276**(38): p. 36000-7.

27. Shah, G.M., et al., *Methods for biochemical study of poly(ADP-ribose) metabolism in vitro and in vivo.* Anal Biochem, 1995. **227**(1): p. 1-13.

CHAPTER 2

I would like to point out that although the majority of the work in this chapter is my own, portions of this chapter come from previous members of the lab. Biao Ma performed the microarray analysis which identified the purine metabolism genes as being up-regulated in response to NAD^+ starvation. Biao Ma and Brian Green performed the experiments demonstrating that starving *C. glabrata* for NAD^+ prior to infection results in a kidney hyper colonization phenotype. Biao Ma and Brian green also performed the systemic mouse infection experiments with the *sir2*Δ, *hst1*Δ, and *sir2*Δ *hst1*Δ strains. Carlos Gomez performed one set of systemic mouse infection experiments with 5 mice injected with MPA treated *C. glabrata.*

RESULTS

Purine metabolism genes are up-regulated in response to NAD^+ starvation

In previous work conducted in the laboratory, in a mouse model of systemic infection starving *C. glabrata* for NA prior to infection led to a 30-100 fold increase in colonization in the mouse kidney (Figure 1A). In order to better understand this phenotype and the associated transcriptional response to NAD^+ starvation, Ma et al. performed a microarray analysis of *C. glabrata* cells grown in media lacking NA (Figure 1B). In total we found 249 genes which were induced in response to NA limitation. Of those 249 genes the vast majority were regulated by the sirtuin *SIR2* (30 genes) and a homolog of *SIR2* called *HST1* (227 genes)[1]. Both *SIR2* and *HST1* are NAD^+ dependent enzymes and the dependence of these enzymes on NAD^+ links their activity directly to cellular NAD^+ levels [2]. Due to their clear involvement in response to cellular NAD^+ starvation *SIR2* and *HST1* were two obvious candidates for regulatory factors responsible for the response to NA starvation. Through the microarray analysis and subsequent follow-up experiments we learned that *SIR2* is the primary regulator of sub-telomeric genes, including the *EPA* adhesins which are responsible for allowing *C. glabrata* to adhere to epithelial cells, *HST1* is the primary regulator of many genes distributed throughout the genome, including the high-affinity NAD^+ transporters *TNA1, TNR1,* and *TNR2* which are responsible for salvaging NAD^+ precursors from the environment [1, 3]. We reasoned that if the mouse kidney hyper colonization phenotype was a result of reduced activities of *SIR2* and *HST1* then deleting *SIR2* and *HST1* should phenocopy the kidney hyper colonization phenotype we saw after NAD^+ starvation. This hypothesis provides additional predictions: 1.) The high kidney colonization should be seen even in

media replete with NA , and 2.) NAD^+ starvation will not lead to any further increase in kidney colonization. We generated *C. glabrata sir2*Δ*, hst1*Δ*, and sir2*Δ *hst1*Δ strains and injected mice with all three strains and wild type *C. glabrata* control (Figure 1C). For the wild type control strain we saw an approximate 100 fold increase in kidney CFUs in response to NA starvation which was expected. However, what was startling was that for the *sir2*Δ*, hst1*Δ*, and sir2*Δ *hst1*Δ strains both of our predictions were incorrect. The kidney colonization in NA replete media for the mutant strains was very similar to wild type levels in media with NA. Furthermore, all 3 mutant strains were still responsive to NA starvation indicated by increased CFUs in all 3 mutant strains grown in media lacking NA. This data suggests there are factors other than *SIR2* and *HST1* that are involved the cellular response to NA starvation (Figure 1D).

Figure 1A. NAD^+ starvation of *C. glabrata* cells prior to infection into mice.

C. glabrata cells starved for NAD^+ prior to injection into mice hyper colonize the kidney by approximate 30-100 fold 7 days after infection. Each dot represents a single mouse. The horizontal bar represents the average CFUs for each cohort of mice.

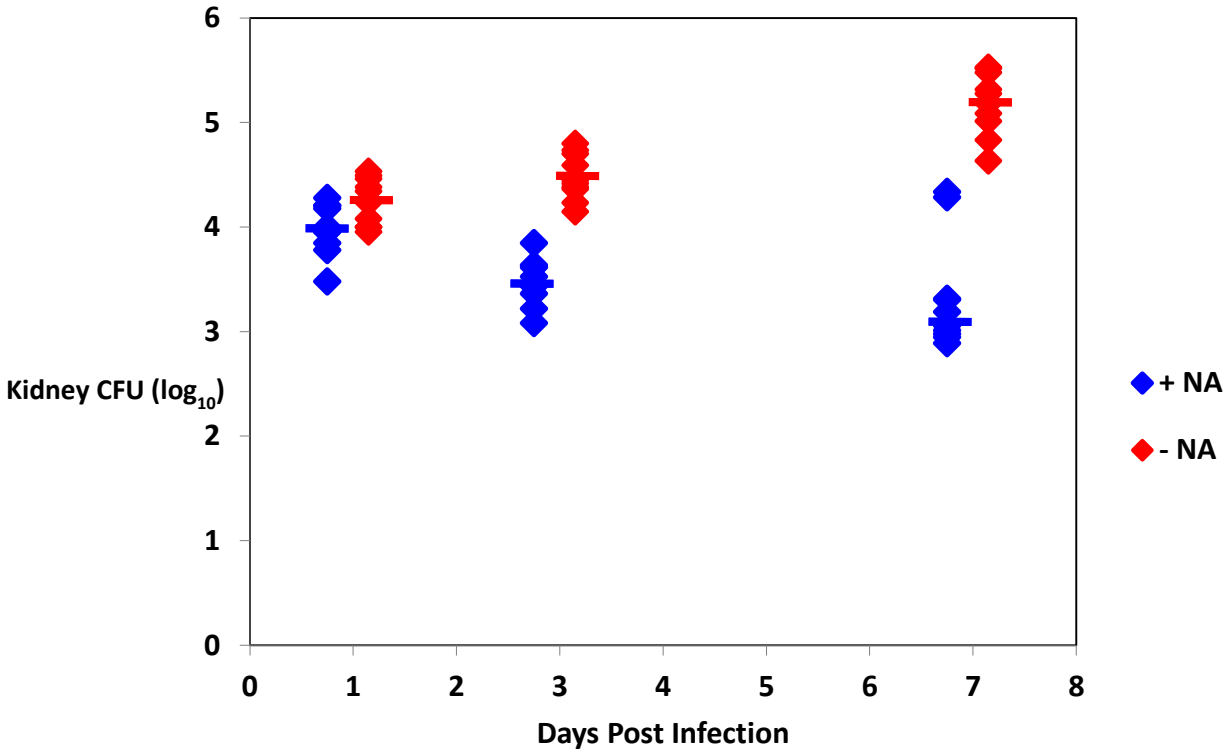

Figure 1B. Microarray analysis of *C. glabrata* cells grown in media lacking NAD$^+$.

To understand transcriptional changes that occur in C. glabrata cells in response to NAD+ starvation cells were grown in media lacking NAD$^+$ microarray analysis was performed. The results from the experiment reveals that the response to NA limitation is mediated primarily by Hst1 and Sir2.

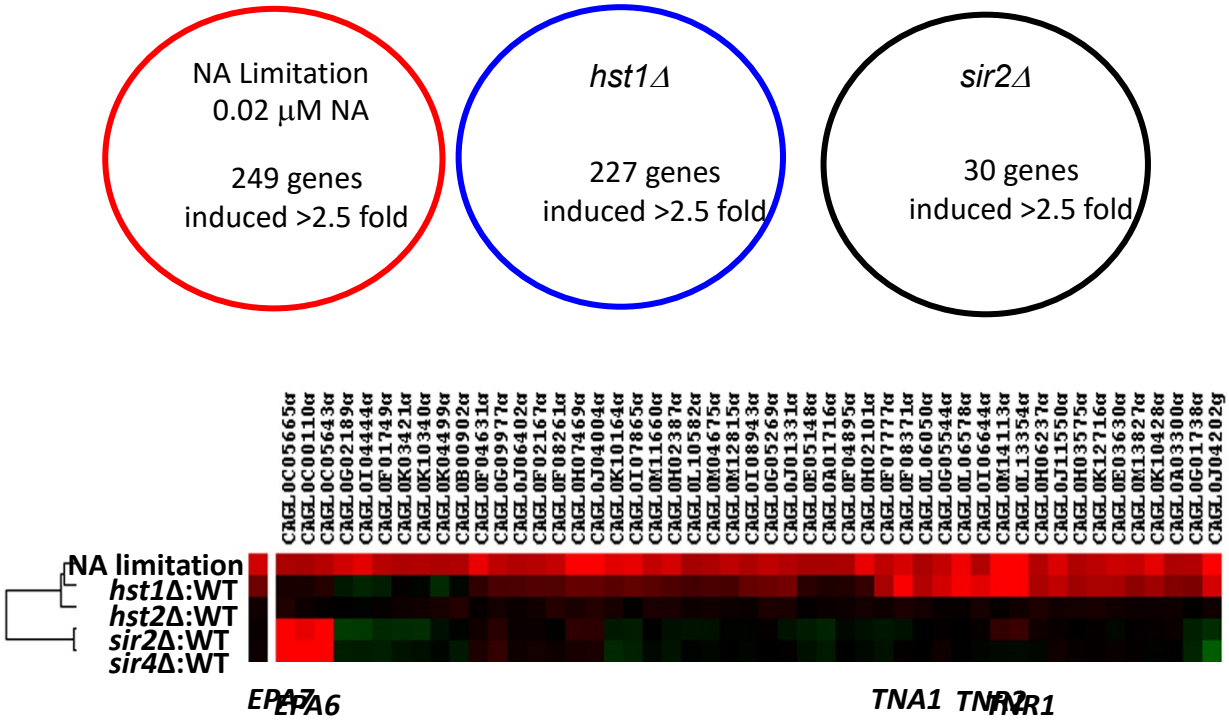

Figure 1C. Injection of mice with WT, *sir2*Δ, *hst1*Δ, *and sir2*Δ *hst1*Δ strains grown in media with and without NA.

Mice were injected with wild type (WT) *C. glabrata* along with *sir2*Δ, *hst1*Δ, *and sir2*Δ *hst1*Δ mutant strains. After 7 days the kidneys were harvested from all mice and CFUs were counted after plating. All strains tested were still responsive to NA starvation showing hyper colonization of the kidneys in response to NA starvation. The *sir2*Δ, *hst1*Δ, *and sir2*Δ *hst1*Δ strains did not demonstrate the hyper colonization phenotype when grown in media with NA, indicating that NAD^+ status affects virulence independently of Sir2 or Hst1. Each dot represents a single mouse. The horizontal bar represents the average CFUs for each cohort of mice.

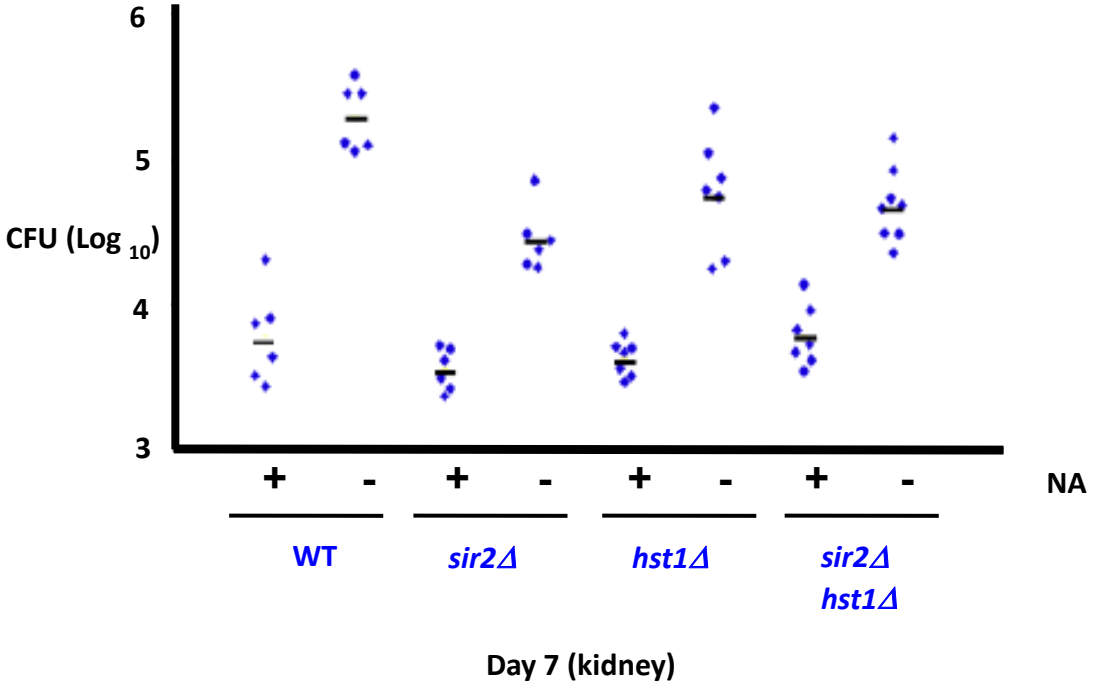

Figure 1D. Additional factors must be involved in NA responsiveness.

The failure of the sir2Δ*, hst1*Δ*, and sir2*Δ *hst1*Δ strains to recapitulate the kidney hyper colonization phenotype suggests the possibility that additional factors may be involved in response to NAD^+ limitation.

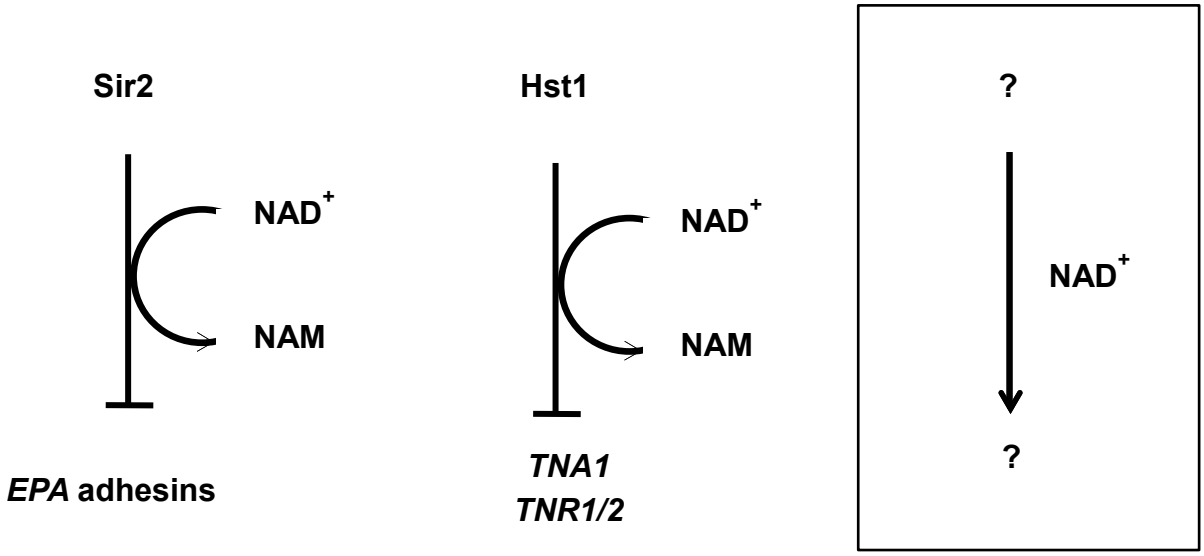

Interestingly, through our analysis we were able to identify an additional set of genes that were upregulated in response to NAD^+ limitation, that were regulated independent of either *SIR2* or *HST1* (Table 1) [1]. What we found was particularly remarkable about this set of genes was that they seemed to be all involved in the process of purine nucleotide biosynthesis (Figure 2A and 2B). Naturally, this led to our next question: Why would NA limitation lead to induction of a set of genes involved in purine nucleotide biosynthesis? Furthermore, how would purine nucleotide metabolism have an effect on *C. glabrata* virulence?

To address these questions we generated a set of strains with deletions in key genes involved in purine metabolism in *C. glabrata*. The complete list of genes deleted and the functions of the genes can be found in Table 2. It should also be noted that in *C. glabrata,* all the genes deleted represent uncharacterized ORFs that were identified through homology with the *S. cerevisiae* versions of the genes.

The deleted genes broadly fall into three categories. First, genes involved in *de novo* production of inosine monophosphate (IMP). IMP is a common precursor to the purine nucleotides (AMP and GMP) which are involved in almost all aspects of cellular life, and thus is an extremely important molecule [4, 5]. IMP is generated *de novo* through two independent pathways, the ADE pathway and the HIS pathway. These pathways produce the IMP intermediate 5-Aminoimidazole-4-carboxamide ribonucleotide (AICAR) which subsequently produces IMP. To determine the importance of the *de novo* production of IMP in response to NA starvation we constructed single *ade4*Δ and *his1*Δ strains as well as, the *ade4*Δ his1Δ double mutant. *ADE4* catalyzes the first step of the *de novo* purine nucleotide biosynthetic pathway [6, 7]. Construction of

the *ade4*Δ was verified by the failure of the strain to grow on media lacking adenine as well as junctional and ORF PCR reactions. *HIS1* catalyzes the first step in *de novo* histidine biosynthesis [8]. Likewise, *his1*Δ mutant was verified via failure to grow on media lacking histidine, and the *ade4*Δ *his1*Δ double mutant needed both adenine and histidine in the media in order to survive, and furthermore should fully eliminate *de novo* IMP production. This set of mutants would tell us about the relative importance of each branch of the IMP *de novo* synthesis pathway as well as the combinatorial effect of the double mutant which presumably would completely inhibit *de novo* IMP biosynthesis.

The second set of genes we deleted were involved in interconverting IMP to adenosine monophosphate (AMP) or guanosine monophosphate (GMP). Once IMP is synthesized it is subject to multiple fates. IMP could be converted to either GMP or AMP. To interrogate the set of genes involved in conversion of IMP to either GMP or AMP, and to determine the relative importance of AMP and GMP, we sought to create an *imd1*Δ *strain* and an *ade12*Δ strain. In *S. cerevisiae*, a family of 4 genes *IMD1-4* convert IMP to xanthosine monophosphate (XMP) through the activity IMP dehydrogenase (IMD), which then ultimately gets converted to GMP [9, 10]. In *C. glabrata,* the *IMD* gene family remains an uncharacterized, but blasting the sequence of any member of the *S. cerevisiae IMD1-4* gene family against the *C. glabrata* genome maps to a single gene CAGL0K10780g. We deleted this ORF, and subsequently showed that *C. glabrata* deletions in this gene lead to guanine auxotrophy. Thus, we named this gene *IMD1* in *C. glabrata* and concluded that unlike in *S. cerevisiae, C. glabrata* has only one gene responsible for converting IMP to XMP. We also attempted to delete *ADE12,* however, were unable to do so in numerous attempts. In *S. cerevisiae ADE12* is a non-essential

gene that catalyzes the first step in synthesis of AMP from IMP [11, 12]. The only circumstances under which we were able to delete *ADE12* was if a wild type copy of the gene was provided on the plasmid. Consistent with ADE12 being essential, this plasmid could not be subsequently lost from the strain (with a chromosomal deletion of ADE12).

The final set of genes deleted were involved in degradation, recycling, and salvaging metabolites of IMP. In addition to *de novo* synthesis, IMP can be generated through recycling from preformed bases or nucleosides. As it was mentioned earlier IMP can be converted to GMP or AMP, however IMP can have additional fates. IMP can also can be broken down first to inosine via Isn1 [13, 14]. The inosine generated through the action of Isn1 can be further metabolized to hypoxanthine through the action of Pnp1 [15]. Also, exogenous adenine can be brought into the cell via the permease Fcy2 converted to hypoxanthine through Aah1 which can then be recycled back to IMP through the activity of Hpt1 [7, 16-19]. AMP can also be converted directly back to IMP through Amd1 [5, 20]. We created single deletions in the genes corresponding to all these enzymes. We also generated an *aah1*Δ *amd1*Δ double mutant which should lead to a complete block of conversion of exogenous adenine to IMP.

Table 1. List of purine metabolism genes highly induced in response to NAD^+ limitation.

Fold induction of subset of genes strongly upregulated under conditions of NAD^+ depletion. Microarrays were completed in biological triplicate with duplicate spots on each array.

Gene Name	Fold Induction	Pathway
ADE1	15.9X	Ade(de novo IMP) biosynthesis
ADE6	7.9X	Ade(de novo IMP) biosynthesis
ADE4	7.1X	Ade(de novo IMP) biosynthesis
ADE5/7	7.0X	Ade(de novo IMP) biosynthesis
ADE13	6.4X	Ade(de novo IMP) biosynthesis
ADE17	4.2X	Ade(de novo IMP) biosynthesis
ADE8	3.1X	Ade(de novo IMP) biosynthesis
HIS4	8.3X	Ade(de novo IMP) biosynthesis
HIS2	6.5X	Ade(de novo IMP) biosynthesis
HIS7	4.7X	Ade(de novo IMP) biosynthesis
HIS1	3.1X	Ade(de novo IMP) biosynthesis
MTD1	12.6X	Once carbon Metabolism
SHM2	9.3X	Once carbon Metabolism
GCV1	4.3X	Once carbon Metabolism
GCV3	3.5X	Once carbon Metabolism
SHM1	2.6X	Once carbon Metabolism

Figure 2A. Purine metabolism genes upregulated in response to NA starvation mapped onto the purine metabolism pathway.

The genes identified as induced in response to NA starvation through microarray analysis all mapped to the purine metabolism pathway, indicating the importance of these genes in response to NA limitation. The red numbers indicate fold induction level of the gene.

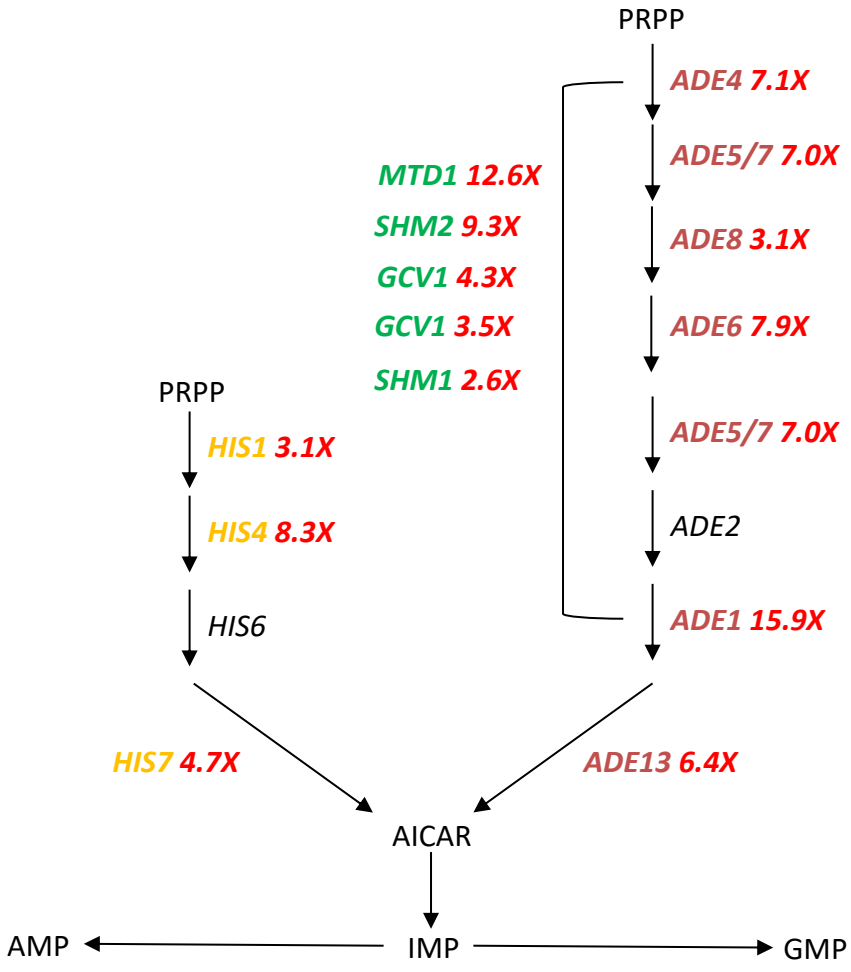

Figure 2B. Purine metabolism pathway in *S. cerevisiae*.

Schematic diagram of purine metabolism in *S. cerevisiae.* Gene names are italicized.

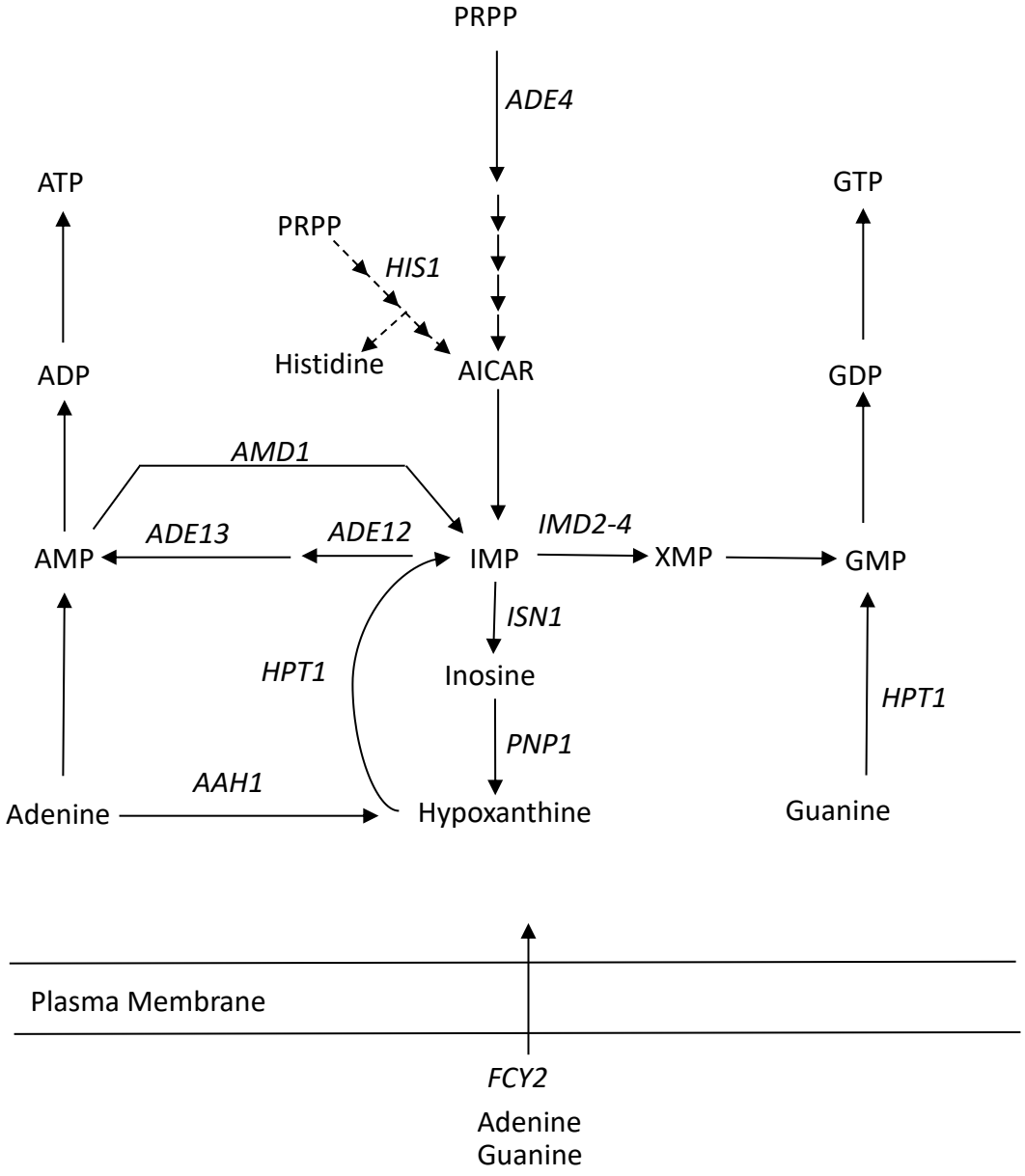

Table 2. Purine metabolism genes deleted in this study.

The function associated with each gene was retrieved from http://www.yeastgenome.org/ and may have been altered slightly.

Gene	Function
AAH1	Adenine deaminase responsible for converting adenine to hypoxanthine
ADE4	Phosphoribosylpyrophosphate amidotransferase (PRPPAT); catalyzes first step of the *de novo* purine nucleotide biosynthetic pathway
AMD1	AMP deaminase; catalyzes the deamination of AMP to form IMP and ammonia; thought to be involved in regulation of intracellular purine (adenine, guanine, and inosine) nucleotide pools
FCY2	Purine-cytosine permease; mediates purine (adenine, guanine, and hypoxanthine) and cytosine accumulation
HIS1	ATP phosphoribosyltransferase; catalyzes the first step in histidine biosynthesis
HPT1	Hypoxanthine-guanine phosphoribosyltransferase; catalyzes the transfer of the phosphoribosyl portion of 5-phosphoribosyl-alpha-1-pyrophosphate to a purine base (either guanine or hypoxanthine) to form pyrophosphate and a purine nucleotide (either guanosine monophosphate or inosine monophosphate)
IMD4	Inosine monophosphate dehydrogenase; catalyzes the rate-limiting step in the de novo synthesis of GTP
ISN1	Inosine 5'-monophosphate (IMP)-specific 5'-nucleotidase; catalyzes the breakdown of IMP to inosine; responsible for production of nicotinamide riboside and nicotinic acid riboside; expression positively regulated by nicotinic acid and glucose availability
PNP1	Purine nucleoside phosphorylase; specifically metabolizes inosine and guanosine nucleosides; involved in the nicotinamide riboside salvage pathway

Systemic infection of mice with *C. glabrata* purine metabolism mutants.

The entire set of *C. glabrata* purine metabolism mutants described above along with wild type controls were starved for NAD^+ and injected into mice to determine what effect, if any, they would have on the kidney hyper colonization phenotype (Figure 3). Strikingly, the *ade4*Δ*, ade4*Δ *his1*Δ*, isn1*Δ*, and imd1*Δ strains showed a dramatic decrease in colonization of the kidney by approximately 1,000-10,000 fold relative to the wild type control. Minimally, what this means is that certain aspects of purine metabolism play a vital role in *C. glabrata* virulence. The failure of the *ade4*Δ and the *ade4*Δ *his1*Δ strains but not the *his1*Δ to hyper colonize the kidney definitively illustrates the importance of the adenine *de novo* biosynthetic pathway to the virulence phenotype. Practically, what this means is that in the host *C. glabrata* must not have access to extra-cellular adenine, and thus must rely on *de novo* synthesis of adenine in order to hyper colonize the kidney. If adenine was exogenously available Fcy2 would transport it into the cell where it could be converted to IMP either via the action of Aah1 and Hpt1 or Amd1. Furthermore, this illustrates the importance of IMP biosynthesis. In the absence of both the *de* novo adenine biosynthetic pathway and lack of exogenous adenine there is no source for synthesis of IMP. The importance of IMP biosynthesis in virulence is further supported by the hyper colonization phenotype in the *aah1*Δ amd1Δ double mutant which would fail to make IMP from exogenous adenine but presumably is still virulent because IMP can be synthesized via the *de novo* pathway. The avirulence of the *isn1*Δ strain suggests that the breakdown of IMP to inosine is of utmost importance. This result is slightly strange because IMP can still be converted to both AMP and GMP in the *isn1*Δ mutant. This results suggests several possibilities, the first suggests the avirulence may

not be directly related to a buildup of IMP but may instead have something to do with the failure to metabolize IMP to inosine. The second possibility suggests that the failure of Isn1 to breakdown to IMP may result in an accumulation of IMP that is unable to be resolved even if IMP can be converted to both AMP and GMP. Finally, the failure of the *imd1*Δ strain to hyper colonize the kidney indicates the importance of converting IMP to GMP. Presumably, this suggests that in the host *C. glabrata* may not have access to guanine or that guanine in the host is limited and thus an *imd1*Δ strain would have blunted levels of guanine nucleotides as there are no other sources for GMP biosynthesis. Still, these results beg the question why would defects in purine metabolism affect virulence?

Figure 3. Infection of mice with *C. glabrata* purine metabolism mutants to determine virulence phenotypes.

Mice were injected with wild type (WT) *C. glabrata* along with the complete set of purine metabolism mutants described above. After 7 days the kidneys were harvested from all mice and CFUs were counted after plating. The *ade4*Δ, *ade4*Δ *his1*Δ, *isn1*Δ, and *imd1*Δ strains showed a dramatic decrease in kidney colonization relative to the wild type control. Each dot represents a single mouse. The horizontal bar represents the average CFUs for each cohort of mice.

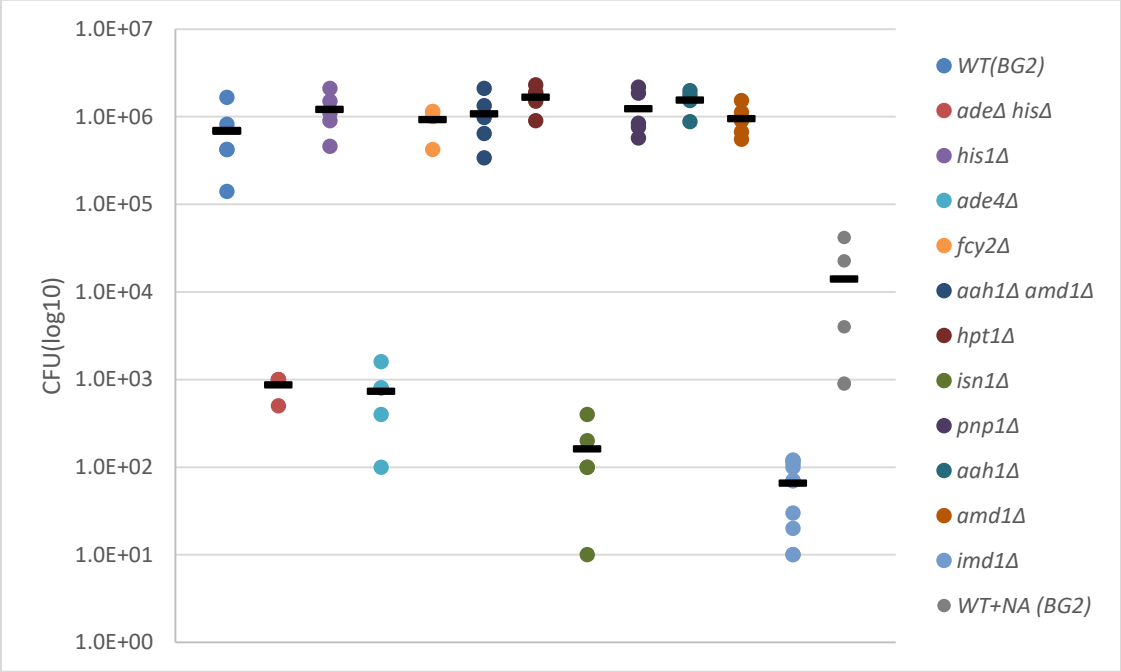

Metabolomic analysis of *C. glabrata* in response to NAD^+ starvation

The microarray data generated by Ma et al. described earlier suggests that the in response to NAD^+ limitation, there is transcriptional activation of the genes involved in purine nucleotide biosynthesis. To better understand if the transcriptional induction we saw in response to NAD^+ limitation actually correlated to the function of the pathway and how flux through purine metabolism was impacted by NAD^+ limitation we performed metabolomic analysis of wild type *C. glabrata* under conditions of NA starvation. Briefly, wild type *C. glabrata* was grown overnight in media with NA to log phase. Cells were collected at this point as a reference to see how metabolites changed in response to NA starvation. Cells were then washed in media that lacked NA and re-suspended to OD and allowed go grow in minus NA media for 10 hours. Cells were collected over two hour increments during the starvation. After the 10 hour collection NA was spiked into the culture and cells were collected at 20, 40, and 60 minutes after the addition of NA. The cells were then processed and analyzed for metabolites through mass spectrometry. Figure 4A (top panel) shows the growth of wild type *C. glabrata* through the course of the experiment.

As a first step to ensure that we were performing the experiment properly without compromising metabolites and to give us confidence in analyzing the various metabolites, we looked at cellular NAD^+ levels over the course of the experiment (Figure 4A). We predicted based on previous NAD^+ assays performed that NAD^+ levels should be high initially coming out of media with NA, but that those levels would rapidly drop in response to NA starvation and remain at a consistently low level for the remainder of starvation. Upon the addition of NA back to the starved culture after 10 hours we

expected cellular NAD^+ levels to rise back to normal homeostatic levels. Indeed our predictions about cellular NAD^+ levels were correct. In wild type *C. glabrata* after just two hours in media lacking NA, NAD^+ drops to about 20% of log phase plus NA level. For the remainder of the experiment NAD^+ remains at around 1% of homeostatic levels. NAD+ levels rebound to normal homeostatic levels 20-40 minutes after addition of NAD^+ back to the starved culture.

With the confidence we gained from the accuracy of the NAD^+ levels in the metabolic analysis we moved forward to look at additional metabolites that were impacted by NA starvation. There was a striking accumulation of the breakdown products of IMP, inosine and hypoxanthine (Figure 4B). Relative to the log phase plus NA reference, inosine levels within four hours in minus NA media jumped nearly 50 fold. The cellular inosine levels remained remarkably high through the entirety of starvation (approximately 40 fold higher than the + NA control), and upon addition of NA after 10 hours of starvation cellular inosine levels show a trend of diminishing back towards homeostatic levels. Moreover, intracellular hypoxanthine also accumulated to massive levels. After four hours in minus NA media, hypoxanthine accumulates more than 200 fold higher than the plus NA reference. The addition of NA back to the culture at 10 hours quickly resets hypoxanthine back to homeostatic levels. As it was described earlier, both inosine and hypoxanthine are breakdown metabolites of IMP. IMP is first broken down to inosine by the nucleotidase Isn1. Subsequently, inosine is further metabolized to hypoxanthine by Pnp1. It appears that under NA starvation conditions *C. glabrata* responds by quickly degrading IMP and accumulating massive levels of both inosine and hypoxanthine. It should also be noted that in our mouse model of The

suggests a model whereby if the cell is unable to metabolize IMP to inosine as is the case in an *isn1*Δ mutant virulence is tremendously impaired suggesting that IMP breakdown is an important process of the adaptation to NA limitation.

In addition to the accumulation of its breakdown products IMP itself actually accumulates in response to NA limitation (Figure 4C). When we examined NMPs in response to NA starvation there is an immediate marked increase in cellular IMP levels that peaks at the four hour time point. After four hours, IMP levels show a trend of diminishing slowly back to homeostatic levels and levels are fully restored to homeostasis 20 minutes after addition of NA to the culture. An additional interesting piece of data from this experiment is that in the in the first four hours in media lacking NA, cellular AMP levels increase approximately 3 fold relative to the plus NA time point. In contrast GMP levels in the cell never increase and stay remarkably consistent through the entire experiment. We were particularly interested in this result because in the first four hours in minus NA media cells are still actively growing and attempting to adapt to their NA starved environment properly. During this crucial time it appears that there is a clear imbalance between AMP and GMP. The data suggests that upon starvation IMP accumulates, and some portion of IMP is converted to AMP but GMP synthesis is not occurring. AMP is converted to XMP through the action of Imd1 in *C. glabrata.* Interestingly, in *S. cerevisiae,* IMD is a NAD^+-dependent enzyme. As it was mentioned previously, two additional NAD^+-dependent protein factors are Hst1 and Sir2, which become inactive when the cell is starved for NA. We reasoned that since IMD is also a NAD^+-dependent enzyme perhaps starvation for NA prevents full function of the enzyme which leads to the imbalance between AMP and GMP. It should also be noted

that C13 labeled glycine was used to monitor metabolic flux through the pathway after NAD^+ starvation. Glycine is utilized in the second step of *de novo* purine biosynthesis, thus labeled glycine can be used to monitor flux through the purine biosynthetic pathway[4]. After eight hours of starvation in media lacking NA the addition of C13 labeled glycine followed by a short incubation shows clear incorporation of C13 into IMP and downstream products, indicating new biosynthesis of metabolites even under starved conditions. Moreover, this new biosynthesis suggests that the purine pathway is not only transcriptionally induced in response to NA limitation but there are major fluxes in metabolites in response to NA limitation.

Figure 4A. Growth of *C. glabrata* in minus NA media and associated NAD^+ levels. After overnight growth to mid-log phase in media with NA, cells were washed and inoculated into minus NA media and allowed to grow for 10 hours. After the 10 hour time point NA is added back to the starved culture at a final concentration of 3.25uM. Cells were collected from + NA media at the beginning of the experiment, and then every

two hours for the next 10 hours of NA starvation. Additional collections were made 20, 40 and 60 minutes after the addition of NA to the starved culture after 10 hours. NAD^+ levels were analyzed over the course of the experiment. The growth curve shown and NAD^+ levels shown below are averages of a biological duplicate performed on two separate days. The error bars represent the standard deviation between the two experiments.

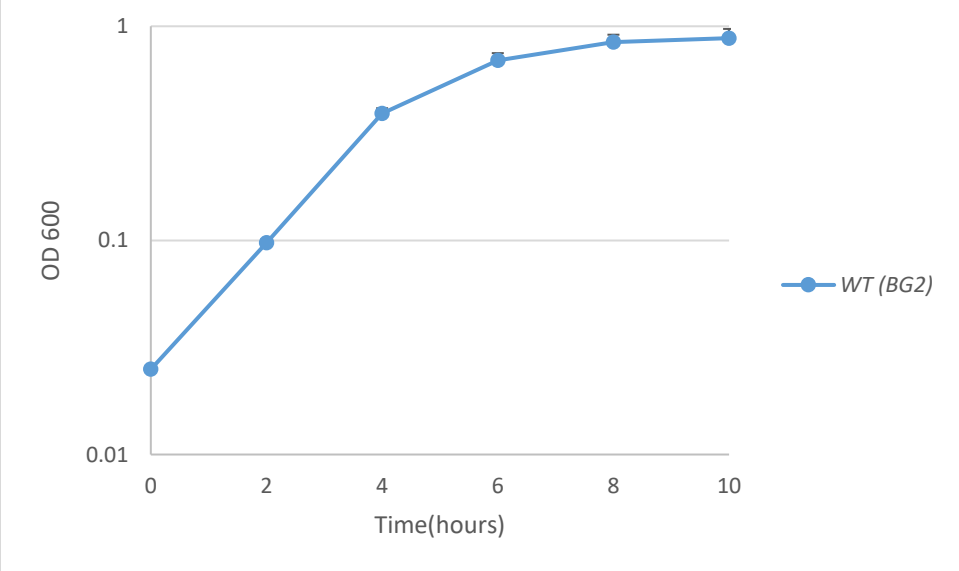

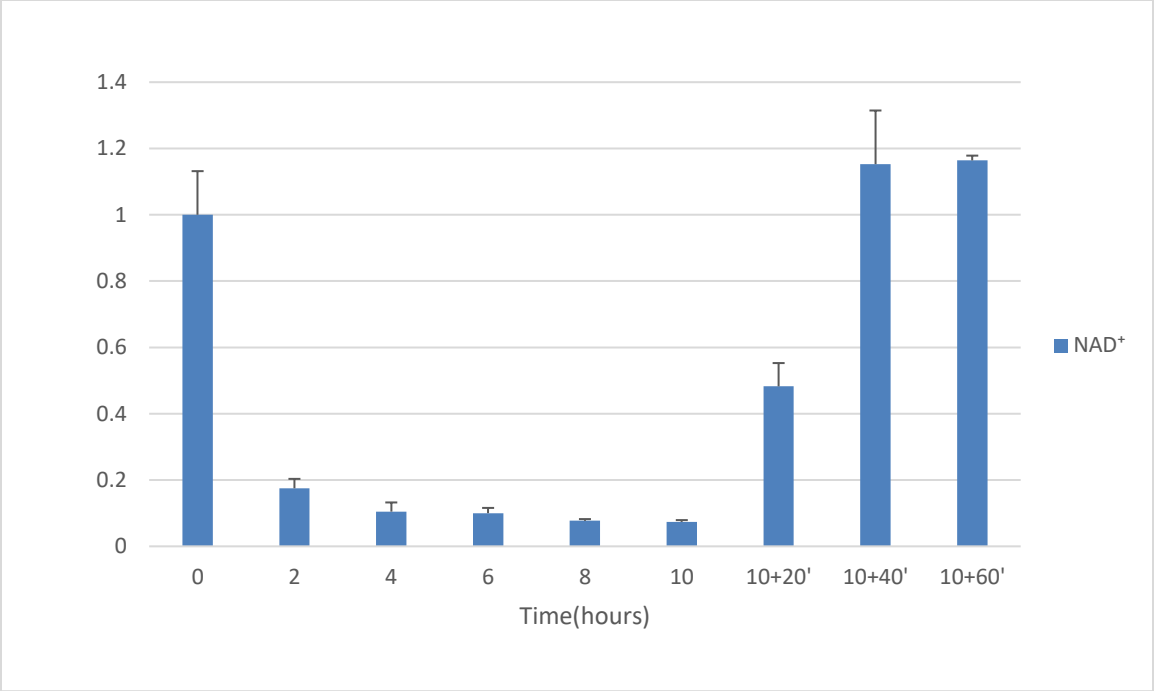
1.4
1.2
1
0.8
0.6
0.4
0.2
0
0
2
4
6
8
10
10+20'
10+40'
10+60'
Time(hours)
NAD+

Figure 4B. Cellular NAD^+ inosine and hypoxanthine levels in wild type *C. glabrata.*

Inosine and hypoxanthine levels in wild type *C. glabrata* were monitored over the course of 10 hours in media lacking NA. After the 10 hour time point NA is added back to the starved culture at a final concentration of 3.25uM. Error bars represent the standard deviation from a biological duplicate.

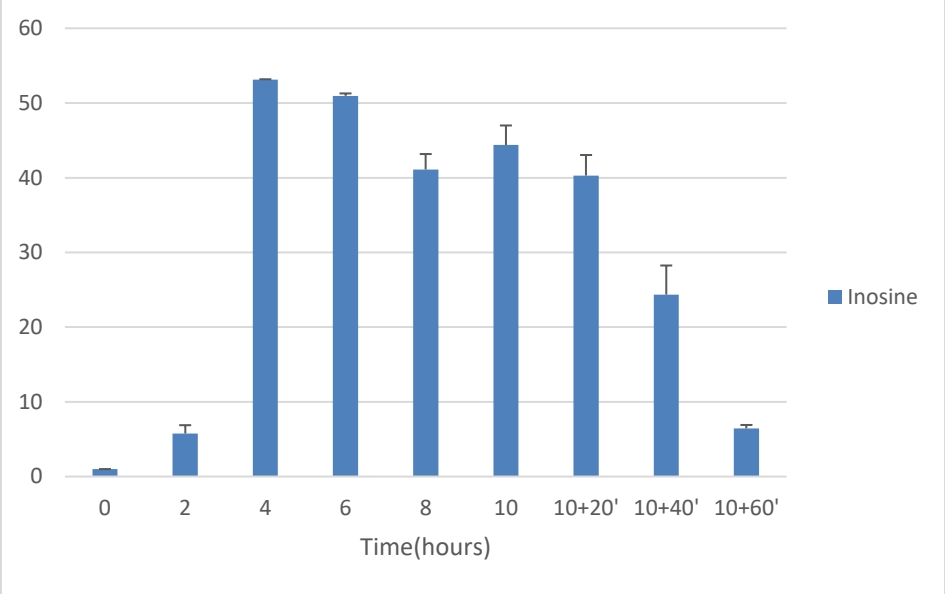

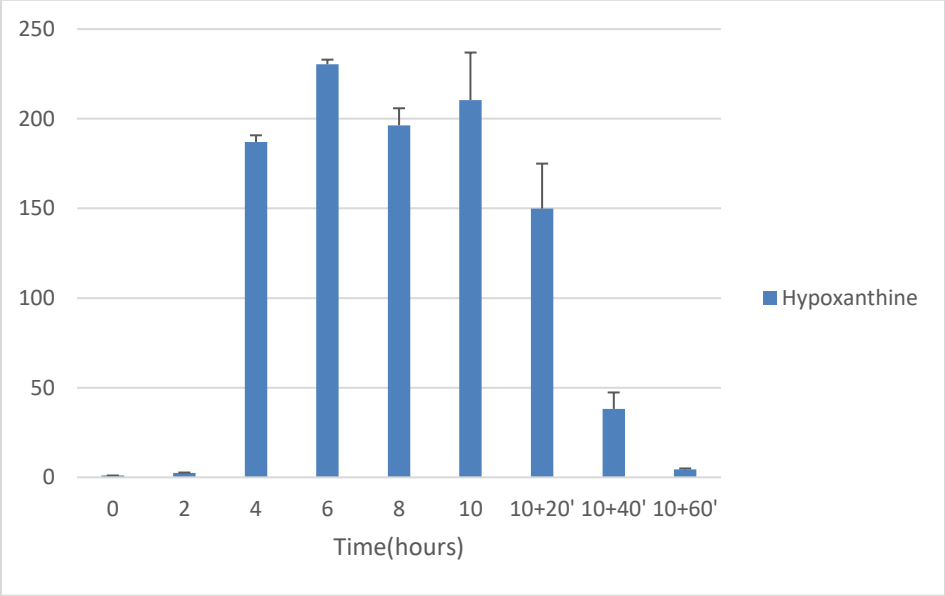

Figure 4C. Cellular NMP levels in wild type *C. glabrata.*

NMP and NTP levels in wild type *C. glabrata* were monitored over the course of 10 hours in media lacking NA. After the 10 hour time point NA is added back to the starved culture at a final concentration of 3.25uM. Error bars represent the standard deviation from a biological duplicate.

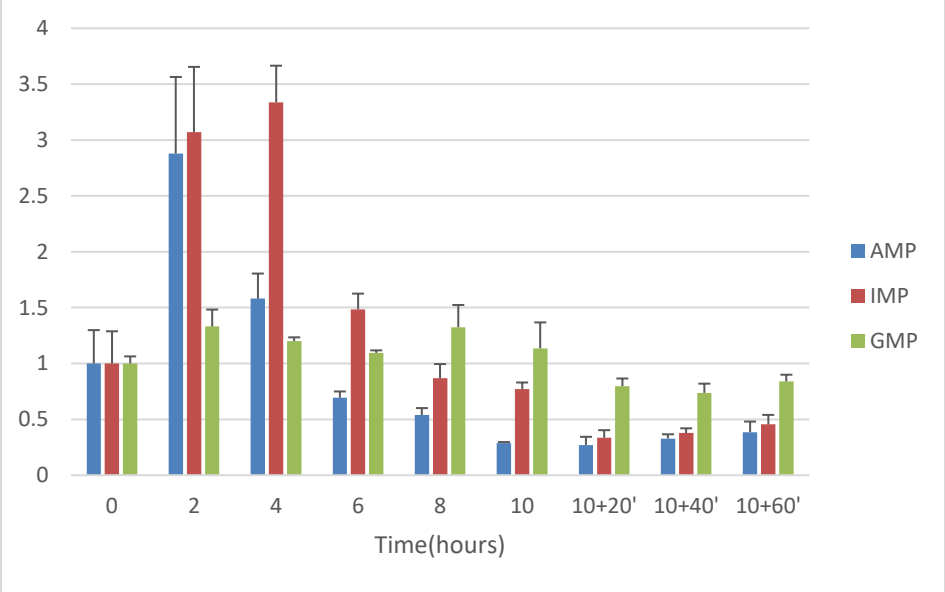

Guanine nucleotide pool depletion leads to hyper colonization of the mouse kidney

We found the apparent imbalance between AMP and GMP and the fact that IMD is a NAD^+-dependent enzyme particularly interesting. Based on this result, we hypothesized that in response to NAD^+ starvation what the cell may actually be sensing is a nucleotide imbalance between AMP and GMP which is mediated by the inactivity of Imd1 due to poor NAD^+ availability. To test this possibility we utilized two drugs, mycophenolic acid (MPA) and 6- azauracil (6AU), which specifically inhibit the activity of IMP dehydrogenase (IMD). IMD is responsible for *de novo* guanine nucleotide biosynthesis and converts IMP to XMP which subsequently gets converted to GMP. It has previously been documented that treatment of cells with both of these drugs inhibits the activity of IMD and results in a corresponding decrease in the cellular GTP pool [21, 22]. We wanted to use these drugs to set up a situation where even in the presence of NAD^+ we could manipulate *C. glabrata* into creating a nucleotide imbalance by depleting the cellular GTP pool with MPA and 6AU treatment, and then evaluate virulence in our mouse model of infection. To perform this experiment we treated independent cultures of wild type *C. glabrata* grown in the presence of NA with inhibitory concentrations of MPA and 6AU. As controls, we grew up *C. glabrata* in media that lacked NA and media that possessed NA both of which were not treated with drug. All strains were injected into mice and after 7 days kidneys were harvested, homogenized, and plated and CFUs were counted (Figure 5). Strikingly, strains grown in the presence of NA, but treated with either MPA or 6AU had kidney hyper colonization phenotypes very similar to wild type *glabrata* grown in media lacking NA. This result indicates that the cellular response to NA starvation is phenocopied by depletion guanine nucleotide pools via treatment with

MPA and 6AU, suggesting the possibility that NA starvation is actually sensed in the cell and a purine nucleotide imbalance between AMP and GMP.

Figure 5. The effect of virulence in *C. glabrata* due to treatment with MPA and 6AU. *C. glabrata* grown in the presence of NA was treated with MPA and 6AU. As a control untreated *C. glabrata* grown in media with NA was used. Also as a positive control for the hyper colonization phenotype *C. glabrata* was grown untreated but in media lacking NA. Each dot represents a single mouse. The horizontal bar represents the average CFUs for each cohort of mice.

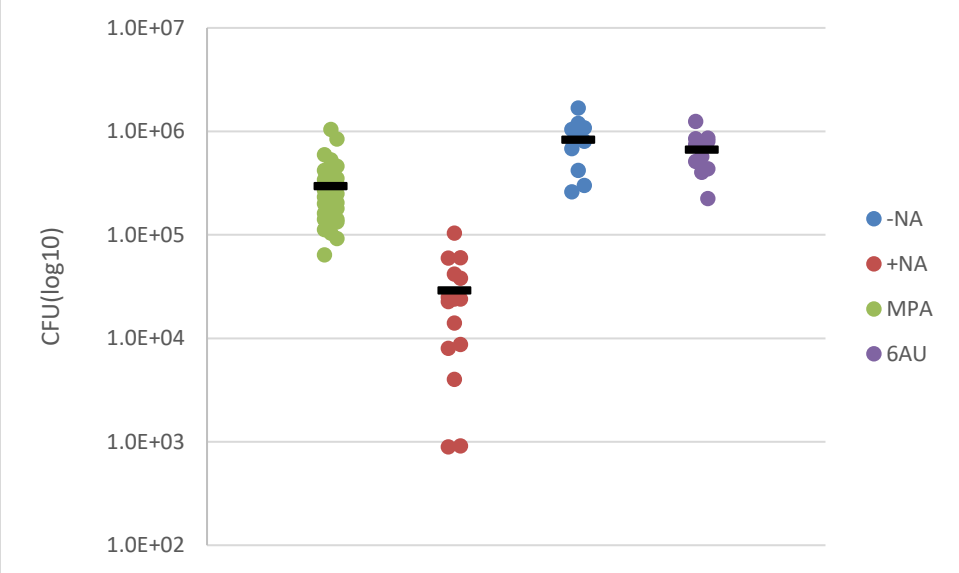

Discussion

Sir2 and Hst1 have previously been described as key regulators in response to NA starvation [1]. Sir2 has been shown to regulate the *EPA* family of adhesins, while Hst1 regulates expression of the high-affinity NAD^+ transporters *TNA1, TNR1* and *TNR2* [1, 3]. Interestingly, both Sir2 and Hst1 rely on NAD^+ as a co-factor to function properly. The dependence of these enzymes on NAD^+ links their activity directly to cellular NAD^+ levels. Thus, under conditions where cells are starved for NA Sir2 and Hst1 activity is impaired due to the lack of NAD^+ available in the environment, resulting in de-repression of the *EPA* adhesins and activation of the high-affinity NAD^+ transporters. In a mouse model of systemic infection wild type *C. glabrata* starved for NAD^+ leads to a dramatic hyper colonization of the kidney. Microarray analysis demonstrates that the response to NA limitation is mediated primarily by Hst1 and Sir2. Presumably these two factors work together to regulate *C. glabrata* virulence. However, mice infected with *hst1*Δ*, sir2*Δ*,* or *hst1*Δ *sir2*Δ strains fail to fully recapitulate the kidney hyper colonization phenotype of wild type *C. glabrata* and remain NA responsive*,* suggesting the involvement of additional factors in *C. glabrata* virulence.

We identified an additional set of genes that that were induced in response to NAD^+ starvation, which were regulated independently of Hst1 and Sir2. Surprisingly, this set of genes all functioned in purine nucleotide metabolism. We sought to understand how purine nucleotide metabolism was impacted by NAD^+ starvation, and how purine nucleotide metabolism could play a role in the virulence of *C. glabrata.* To address these questions we constructed a comprehensive set of mutants in key genes involved in purine nucleotide metabolism. The mutants we generated allowed us to interrogate the

contributions of the *de novo* pathway of IMP biosynthesis, the interconversion of IMP to AMP and GMP, and recycling and salvaging of metabolites for IMP biosynthesis, to the virulence of wild type *C. glabrata.* The entire set of purine metabolism mutants was injected into mice to determine their effect on the kidney hyper colonization phenotype. Four mutant strains had remarkably diminished colonization of the kidney: *ade4*Δ*, ade4*Δ *his1*Δ*, isn1*Δ*,* and *imd1*Δ. The *ade4*Δ*,* and *ade4*Δ *his1*Δ strains highlighted the importance of *de novo* IMP biosynthesis to *C. glabrata* virulence. Based on this result, we concluded that in the host exogenous adenine must not be readily available, and that the *de novo* pathway is the only method by which IMP can be synthesized. If exogenous adenine was available IMP could be synthesized through alternative pathways and the absence of the *de novo* pathway could be compensated for. Isn1 catalyzes the breakdown of IMP to inosine. The avirulence of an *isn1*Δ strain suggests that this process must be important. Furthermore, Pnp1 which converts inosine to hypoxanthine maintains its hyper colonization phenotype when deleted suggesting that inosine itself may potentially be important in virulence. In *S. cerevisiae* Imd1-4 function to convert IMP to XMP which leads to production of guanine nucleotides. We have shown in *C. glabrata* there is only one *IMD* gene responsible for *de novo* guanine nucleotide biosynthesis, and we renamed the previously uncharacterized ORF CAGL0K10780g as *IMD1*. The failure of the *imd1*Δ strain to hyper colonize the kidney illustrates the importance of *de novo* guanine nucleotide biosynthesis to virulence.

In an effort to understand how purine metabolism was impacted by NA starvation we conducted metabolomic analysis of wild type *C. glabrata* cells grown in media lacking NA over the course of 10 hours. When cells are starved for NAD^+ their intracellular

NAD^+ levels diminish rapidly. The cell responds by inducing the adenine biosynthetic pathway and accumulating high levels of cellular IMP. Additionally, there is a massive accumulation of inosine in the cell which is maintained throughout starvation and is only cleared when NA is added back to the starved culture after 10 hours. This suggests that when *C. glabrata* is starved for NAD^+ there is a massive flux through the purine nucleotide pathway where metabolites are funneled to produce inosine. The increase in cellular IMP levels corresponds to an increase in cellular AMP levels, but GMP remains consistently low through the entire experiment. Like Hst1 and Sir2, Imd1 is a NAD^+ dependent enzyme. We hypothesized that under conditions where NAD^+ is scarce the activity of Imd1 would be negatively impacted, resulting in a failure to produce guanine nucleotides. This failure to produce guanine nucleotides results in a purine nucleotide imbalance between AMP and GMP, and perhaps when cells are starved for NA they are sensing this nucleotide imbalance. To test this hypothesis we used two drugs which specifically inhibit the activity of Imd, MPA and 6AU. Wild type *C. glabrata* treated with either MPA or 6AU, even when grown in the presence of NA, phenocopied the kidney hyper colonization phenotype of *C. glabrata* starved for NAD^+. We took this data as evidence for our hypothesis that when cells are starved for NAD^+ the actual signal sensed by the cell is a purine nucleotide imbalance. Together this data suggest a potential model which connects NAD^+ status and purine metabolism. Moreover, this data provides an initial analysis of a novel pathway relevant to virulence regulation by NAD^+ depletion.

One additional possibility that we were unable to exclude is that the cell isn't actually sensing a purine nucleotide imbalance, but instead may directly be sensing the accumulation of intracellular IMP or inosine which appear to be hallmarks of the

response to NAD^+ starvation. However, we favor the model of NA starvation being sensed as a purine nucleotide imbalance between AMP and GMP because a model in which IMP and/or inosine accumulation serves as signal being sensed fails to explain why treatment with the Imd inhibitors MPA and 6AU would phenocopy the kidney hyper colonization phenotype of wild type *C. glabrata* starved for NAD^+. Moving forward, if the proximal signal being sensed in response to NA starvation is actually a nucleotide imbalance then we hypothesize that there must be a guanine nucleotide regulated protein which is activated in response to the nucleotide imbalance. We are currently in the process of preparing samples for RNA-seq from a *sir2*Δ *hst1*Δ strain as well as MPA and 6AU treated cells wild type *C. glabrata.* We hope to that analysis of this future dataset may identify genes involved in sensing and responding to NAD^+ starvation.

Materials and methods

Strains and media

All *Candida glabrata* deletion strains were derived from our wild type lab strain BG2 or from an *ura3* derivative of BG2, BG14. For routine culturing of *C. glabrata* strains, we used synthetic complete medium supplemented with 2% dextrose (SCD).

Gene deletion in *Candida glabrata*

Gene deletion in *C. glabrata* was done via a split-marker transformation. The ORF of the gene was replaced with a nourseothricin (NAT) cassette. The sequence information for generating gene deletion constructs came from the Candida Genome Database website (http://www.candidagenome.org) combined with the Cormack laboratory *C. glabrata* genome sequence. For deletion with NAT cassette, we utilized a split marker replacement method. Briefly, approximately 500 bp of both the 5' and 3' untranslated regions (UTR) of each gene to be deleted were amplified. The anti-sense primer for the 5' UTR amplification and the sense primer for the 3' UTR amplification contained 20 additional nucleotides found specifically in our NAT deletion cassette. The NAT cassette was then amplified as two distinct portions. The 5' portion of the NAT cassette is amplified with a 20 nt primer that is the reverse complement of the tailed anti-sense primer used to amplify the 5' UTR. The 3' portion of the Nat cassette is amplified with a 20 nt primer that is the reverse complement of the tailed sense primer used to amplify the 3' UTR. For a total of 4 PCR amplified fragments. All 4 of those reactions were cleaned up with the QIAquick PCR Purification Kit.

The 5' UTR fragment and the 5' portion of the NAT cassette are fused together in a Splicing by Overlap Extension (SOEing) PCR reaction. The 3' UTR fragment and 3'

portion of the NAT cassette are fused together in the same manner. The two fused fragments were purified with the Qiaquick PCR Purification Kit, and then transformed into *C. glabrata* via the lithium acetate method and selected on YPD plates supplemented with 200 µg/ml NAT. Homologous recombination and allele replacement of each locus was verified by PCR analysis using a primer that anneals in the sequences external to the cloned fragments and a primer annealing within the NAT cassette. We also verified the absence of a gene by inability to PCR amplify an internal fragment from each deleted gene.

Systemic infection in mice

C. glabrata strains were grown overnight in either SCD supplemented with 10 µM niacin or SCD without niacin to mid-log phase (OD_{600} ~0.5). This was done to ensure cells were not unintentionally deprived of any nutrients. The cells were washed three times with PBS and re-suspended in PBS for injection. Ten to twelve -week-old female BALB/C mice (Taconic) were infected with approximately 2×10^7 CFUs of *C. glabrata* cells in a volume of 100 µl via tail vein injection. Mice were sacrificed via CO_2 asphyxiation seven days post infection. Spleen, kidney and liver were harvested and homogenized in 1 ml of PBS. Appropriate dilutions were plated on YPD plates supplemented with 100 U/ml penicillin and 0.1 mg/ml streptomycin. Colonies were counted after 40 h of growth at 30°C. For MPA and 6AU treated cells the strains were grown overnight to mid-log phase in standard SCD media with 25 µg/mL MPA or 50 µg/mL 6AU.

Sample preparation for metabolomics

Cells were collected and processed as described by Francois, Pedersen, and Loret with minor adaptations. Briefly, *C. glabrata* was grown overnight in SCD media to mid-log

phase (OD_{600} ~0.5). This was done to ensure cells were not unintentionally deprived of any nutrients. 10 OD units of cells were collected out of the log phase + NA culture. Cells were then collected on Corning 250 mL filter units and washed 4 times with 50 mL of SCD-NA media and re-suspended in the same media in media. Cultures were inoculated into 400mL of SCD-NA media to an OD_{600} of 0.025 and allowed go grow in minus NA media for 10 hours. Cells were collected over two hour increments during the starvation. After the 10 hour collection NA was spiked into the culture and cells were collected at 20, 40, and 60 minutes after the addition of NA. The cells were then processed and analyzed for metabolites through mass spectrometry. At each time point 10 OD units of cells were collected by adding the appropriate volume to a collection tube filled with four times the volume of cells being added of 60% methanol/10mM Tricine, pH 7.4 that was maintained at -40 ºC to stop metabolism. Cells were then spun at 3,000 XG for 5 min at -10 ºC. The supernatant was poured off and the pellet was washed in 60% methanol/10mM Tricine, pH 7.4 that was maintained at -40 ºC. Samples were spun down at 3,000 XG for 5 min at -10 ºC and re-suspended in 1mL of 75% ethanol/0.5mM Tricine, pH 7.4. Tubes were incubated at 80 ºC for 3 minutes, followed by incubation at 4 ºC. Samples were spun at 13,000 RPM for 1 minute and the supernatant was transferred to a fresh tube which was lyophilized overnight in a speed-vac.

AMP/ATP analysis by LC-MS/MS

AMP and ATP analysis were performed on an Agilent 6490 triple quadropole LC-MS/MS system with iFunnel and Jet-Stream® technology (AgilentTechnologies, Santa Clara, CA) equipped with an Agilent 1260 infinity pump and autosampler. Chromatographic separation was performed on a Diamond Hydride column (150mm x 2.1 mm i.d., 4µm

particle size, Microsolv, Eatontown, NJ). The LC parameters were as follows: autosampler temperature, 4°C; injection volume, 4 µl; column temperature, 35°C; and flow rate, 0.4 ml/min. The solvents and optimized gradient conditions for LC were: Solvent A, water with 5mM ammonium acetate, pH=7.2; Solvent B, 90% acetonitrile with 10mM ammonium acetate, pH=6.5; elution gradient: 0 min 95% B; 15–20 min 25% B; post-run time for equilibration, 5 min in 95% B. MS was operated in positive-ion electrospray mode (unit resolution) with all analytes monitored by SRM. Compound identity was confirmed by comparison to the retention times of pure standards. The optimized operating ESI conditions were: gas temperature 230°C (nitrogen); gas flow 15 L/min; nebulizer pressure 40 psi; sheath gas temperature 350°C and sheath gas flow 12 L/min. Capillary voltages were optimized to 4000V in positive mode with nozzle voltages of 2000 V. The iFunnel parameters were: 130V for high pressure RF and 80V for low pressure RF. All data processing was performed with Mass Hunter Quantitative Analysis software package.

References

1. Ma, B., et al., *Assimilation of NAD(+) precursors in Candida glabrata.* Mol Microbiol, 2007. **66**(1): p. 14-25.
2. Froyd, C.A. and L.N. Rusche, *The duplicated deacetylases Sir2 and Hst1 subfunctionalized by acquiring complementary inactivating mutations.* Mol Cell Biol, 2011. **31**(16): p. 3351-65.

3. Ma, B., et al., *High-affinity transporters for NAD+ precursors in Candida glabrata are regulated by Hst1 and induced in response to niacin limitation.* Mol Cell Biol, 2009. **29**(15): p. 4067-79.

4. Ljungdahl, P.O. and B. Daignan-Fornier, *Regulation of amino acid, nucleotide, and phosphate metabolism in Saccharomyces cerevisiae.* Genetics, 2012. **190**(3): p. 885-929.

5. Saint-Marc, C., et al., *Phenotypic consequences of purine nucleotide imbalance in Saccharomyces cerevisiae.* Genetics, 2009. **183**(2): p. 529-38, 1SI-7SI.

6. Smolina, V.S. and M.L. Bekker, *[Properties of 5-phosphoryl-1-pyrophosphate amidotransferase from the yeast Saccharomyces cerevisiae wild type and mutant with altered purine biosynthesis regulation].* Biokhimiia, 1982. **47**(1): p. 162-7.

7. Woods, R.A., et al., *Hypoxanthine: guanine phosphoribosyltransferase mutants in Saccharomyces cerevisiae.* Mol Gen Genet, 1983. **191**(3): p. 407-12.

8. Alifano, P., et al., *Histidine biosynthetic pathway and genes: structure, regulation, and evolution.* Microbiol Rev, 1996. **60**(1): p. 44-69.

9. Byrne, K.P. and K.H. Wolfe, *The Yeast Gene Order Browser: combining curated homology and syntenic context reveals gene fate in polyploid species.* Genome Res, 2005. **15**(10): p. 1456-61.

10. Hyle, J.W., R.J. Shaw, and D. Reines, *Functional distinctions between IMP dehydrogenase genes in providing mycophenolate resistance and guanine prototrophy to yeast.* J Biol Chem, 2003. **278**(31): p. 28470-8.

11. Dorfman, B.Z., *The isolation of adenylosuccinate synthetase mutants in yeast by selection for constitutive behavior in pigmented strains.* Genetics, 1969. **61**(2): p. 377-89.

12. Lipps, G. and G. Krauss, *Adenylosuccinate synthase from Saccharomyces cerevisiae: homologous overexpression, purification and characterization of the recombinant protein.* Biochem J, 1999. **341 (Pt 3)**: p. 537-43.

13. Bogan, K.L., et al., *Identification of Isn1 and Sdt1 as glucose- and vitamin-regulated nicotinamide mononucleotide and nicotinic acid mononucleotide [corrected] 5'-nucleotidases responsible for production of nicotinamide riboside and nicotinic acid riboside.* J Biol Chem, 2009. **284**(50): p. 34861-9.

14. Itoh, R., et al., *The yeast ISN1 (YOR155c) gene encodes a new type of IMP-specific 5'-nucleotidase.* BMC Biochem, 2003. **4**: p. 4.

15. Lecoq, K., et al., *YLR209c encodes Saccharomyces cerevisiae purine nucleoside phosphorylase.* J Bacteriol, 2001. **183**(16): p. 4910-3.

16. Ali, L.Z. and D.L. Sloan, *Studies of the kinetic mechanism of hypoxanthine-guanine phosphoribosyltransferase from yeast.* J Biol Chem, 1982. **257**(3): p. 1149-55.

17. Woods, R.A., et al., *Adenine phosphoribosyltransferase mutants in Saccharomyces cerevisiae.* J Gen Microbiol, 1984. **130**(10): p. 2629-37.

18. Schmidt, R., M.F. Manolson, and M.R. Chevallier, *Photoaffinity labeling and characterization of the cloned purine-cytosine transport system in Saccharomyces cerevisiae.* Proc Natl Acad Sci U S A, 1984. **81**(20): p. 6276-80.

19. Weber, E., et al., *The purine-cytosine permease gene of Saccharomyces cerevisiae: primary structure and deduced protein sequence of the FCY2 gene product.* Mol Microbiol, 1990. **4**(4): p. 585-96.

20. Meyer, S.L., K.L. Kvalnes-Krick, and V.L. Schramm, *Characterization of AMD, the AMP deaminase gene in yeast. Production of amd strain, cloning, nucleotide sequence, and properties of the protein.* Biochemistry, 1989. **28**(22): p. 8734-43.

21. Exinger, F. and F. Lacroute, *6-Azauracil inhibition of GTP biosynthesis in Saccharomyces cerevisiae.* Curr Genet, 1992. **22**(1): p. 9-11.

22. Hupe, D.J., B.A. Azzolina, and N.D. Behrens, *IMP dehydrogenase from the intracellular parasitic protozoan Eimeria tenella and its inhibition by mycophenolic acid.* J Biol Chem, 1986. **261**(18): p. 8363-9.

THE JOHNS HOPKINS UNIVERSITY SCHOOL OF MEDICINE

BASIL HUSSAIN **OCTOBER 7, 2016**

15 Charles Plaza Apt 1105
Baltimore, MD 21201
bhussai3@jhmi.edu
630-306-0956

EDUCATIONAL HISTORY

Ph.D. expected	2016	BCMB Program Mentor: Brendan Cormack, PhD Department of Molecular Biology and Genetics	Johns Hopkins School of Medicine
B.S.	2007	Molecular and Cellular Biology	University of Illinois

AWARDS AND HONORS

Molecular Biology and Genetics Journal Club Outstanding Presentation Prize (2012-13 and 2014-15)

1st place 2015 Wake Forest/Boston Scientific Healthcare Case Competition (1st place out of 10 teams)

1st place 2015 Johns Hopkins Venture Capital and Investment Competition (1st place out of 20 teams)

PUBLICATIONS, PEER REVIEWED

Kim, J.J., Rajagopalan, K, **Hussain, B,** Williams, B.H., Kulkarni, P, and Mooney, S.M., *CETN1 is a cancer testis antigen with expression in prostate and pancreatic cancers.* Biomark Res, 2013. **1**(1): p. 22. PMCID:PMC4177615

SERVICE AND LEADERSHIP

Co-President Johns Hopkins Graduate Consulting Club (JHGCC) **April 2015-May 2016**

Awarded $10,000 from JHU Idea Lab for creation of a Business Essentials program for all students at JHU

Co-Director Case Competition Committee (JHGCC) **June 2014-April 2015**

Worked with a team to design and promote 2 business cases for the JHGCC Case Competition series
Led bi-weekly case study sections for approximately 50 members of the JHGCC

Pro-Bono Consultant (JHGCC and Carey School of Business)

Led a team to identify and implement new training strategies for a private corporate security company
Worked with a team to identify and remedy organizational inefficiencies for a national museum association